SLAC-PUB-9981
hep-ph/9503479

FSU-HEP-950401
LBL-37016
UH-511-822-95

LOW ENERGY SUPERSYMMETRY PHENOMENOLOGY*†

H. Baer*[a], A. Bartl[b], C.H. Chen[a], H. Eberl[h], J. Feng[c], K. Fujii[d], J. Gunion[e], T. Kamon[f], C. Kao[g], J. L. Lopez[f], W. Majerotto[h], P. McIntyre[f], R. Munroe[a], H. Murayama*[i], F. Paige[j],W. Porod[b], J. Sender[k],A. Sopczak[l], X. Tata*[k], T. Tsukamoto[d] and J. White[f]

* Sub-group leaders

[a] *Department of Physics, Florida State University, Tallahassee, FL 32306 USA*
[b] *Institut für Theoretische Physik, Universität Wien, Austria*
[c] *SLAC, Stanford University, Stanford, CA 94309 USA*
[d] *National Laboratory for High Energy Physics (KEK), Tsukuba, 305 Japan*
[e] *Department of Physics, University of California, Davis, CA USA*
[f] *Department of Physics, Texas A&M University, College Station, TX 77843 USA*
[g] *Dep't of Physics and Astronomy, Univ. of Rochester, Rochester, NY 14627 USA*
[h] *Institut für Hochenergiephysik,*
d. Österreichischen Akademie der Wissenschaften, Wien, Austria
[i] *Theoretical Physics Group, Lawrence Berkeley Laboratory*
Berkeley, CA 94720 USA
[j] *Brookhaven National Laboratory, Upton, NY 11973 USA*
[k] *Dep't of Physics and Astronomy, University of Hawaii*
Honolulu, HI 96822 USA
[l] *PPE Division, CERN, CH-1211 Geneva 23, Switzerland*

ABSTRACT

We summarize the current status and future prospects for low energy (weak scale) supersymmetry. In particular, we evaluate the capabilities of various e^+e^-, $p\bar{p}$ and pp colliders to discover evidence for supersymmetric particles. Furthermore, assuming supersymmetry is discovered, we discuss capabilities of future facilities to dis-entangle the anticipated spectrum of super-particles, and, via precision measurements, to test mass and coupling parameters for comparison with various theoretical expectations. We comment upon the complementarity of proposed hadron and e^+e^- machines for a comprehensive study of low energy supersymmetry.

*Manuscript prepared by H. Baer, H. Murayama and X. Tata.

†This work was supported by the Director, Office of Energy Research, Office of High Energy and Nuclear Physics, Division of High Energy Physics of the U.S. Department of Energy under Contract DE-FG05-87ER40319, DE-AC03-76SF00098 and DE-FG-03-94ER40833.

Work supported in part by Department of Energy Contract DE-AC03-76SF00515
Stanford Linear Accelerator Center, Stanford University, Stanford, CA 94309, USA

Disclaimer

1 Goal of this study and outline

The recent demise of the Superconducting Supercollider project in the United States has led to the need for a re-evaluation of directions for not only the U.S., but indeed for the world High Energy physics community. The goal of this report is to evaluate the capabilities of current and future experimental facilities with respect to the search for weak scale supersymmetric particles. To this end, we only review analyses that attempt to make a more or less detailed study of experimental signatures and backgrounds in e^+e^-, $p\bar{p}$, and pp interactions. Other aspects of supersymmetry model building and phenomenology are discussed in the accompanying review by Drees and Martin[1]. It is hoped that the information reviewed in this report will serve as an aid to the decision making process of how to most wisely allocate limited resources such that progress in supersymmetry phenomenology (in particular) and high energy physics (in general) can be maximized.

This report is organized into the following sections.

1. Goal and outline
2. Introduction (theoretical framework and experimental facilities)
3. Production, decay and simulation of super-particles
4. Current status of sparticle searches
5. The reach of LEP II
6. Search for SUSY at the Tevatron and upgrades
7. Search for SUSY at CERN LHC
8. Supersymmetry at future linear e^+e^- colliders
9. Overview and complementarity of facilities
10. Conclusions

2 Introduction

2.1 Theoretical Framework

Supersymmetry (SUSY)[2] is a novel type of symmetry that relates properties of bosons to those of fermions. It is the largest known symmetry[3] of the S-matrix. Locally supersymmetric theories necessarily incorporate gravity[4]. SUSY is also an essential ingredient of superstring theories[5] which, today, offer the best hope for a consistent quantum theory of gravitation. Although no compelling supersymmetric model has yet emerged, and despite the fact that there is no direct experimental evidence for SUSY, the remarkable theoretical properties of SUSY theories have

provided ample motivation for their study. Of importance to us is the fact that SUSY leads to an amelioration of divergences in quantum field theory. This, in turn, protects the electroweak scale from large quantum corrections, and stabilizes the ratio $\frac{M_W}{M_X}$, when the Standard Model (SM) is embedded into a larger theory, involving an ultra-high energy scale M_X (*e.g.* M_{GUT} or M_{Planck}). In other words, SUSY models do not require[6] the incredible fine-tuning endemic to the Higgs sector of the SM, provided only that the super-partners exist at or below the TeV energy scale. On the experimental side, while the measurements of the three SM gauge couplings at LEP[7] are incompatible with unification in the minimal SU(5) model, they unify[8] remarkably well in the simplest supersymmetric SU(5) GUT, with SUSY broken at the desired scale $\sim$ 1 TeV. The last two arguments are especially important in that they bound the SUSY breaking scale and strongly suggest that supersymmetric partners of ordinary particles should be accessible at colliders designed to probe the TeV energy scale[9].

To evaluate the experimental consequences of low energy supersymmetry, one must set up a Lagrangian including the various particles and partner sparticles, and their interactions. Such a theory should reduce to the well-tested SM when the supersymmetric degrees of freedom are integrated over. The simplest possibility[1], the Minimal Supersymmetric Standard Model (MSSM), is a direct supersymmetrization of the SM[9]. It is a Yang-Mills type gauge theory based on the SM gauge group, with electroweak symmetry spontaneously broken via vacuum expectation values (VEVs) of two different Higgs superfields that respectively couple to $T_3 = \frac{1}{2}$ and $T_3 = -\frac{1}{2}$ fermions. The (renormalizable) superpotential that determines the Yukawa interactions of quarks and leptons is required to conserve baryon and lepton numbers; it is then possible to define a multiplicatively conserved R-parity quantum number which is +1 for ordinary particles and -1 for supersymmetric partners. The MSSM is thus minimal in that it contains the smallest number of new particles and new interactions to be compatible with phenomenology. An important consequence of R-parity conservation is that the lightest supersymmetric particle (LSP) is stable. The LSP, which would have been abundantly produced in the early universe, is unlikely[10] to be colored or electrically charged since it would then be able to bind to nuclei or atoms to make heavy isotopes, for which searches[11] have yielded negative results. The LSP, which is the end product of every sparticle decay, thus escapes experimental detection, resulting in apparent non-conservation of energy/momentum in SUSY events.

Supersymmetry must, of course, be a broken symmetry. In the absence of fundamental understanding of the origin of supersymmetry breaking, supersymmetry breaking is parametrized by incorporating all soft supersymmetry breaking terms (defined to be those that do not destabilize the ratio $\frac{M_W}{M_X}$ introduced above) consistent with the SM symmetries. These terms have been classified by Girardello and Grisaru[12]. For the MSSM, they consist of

- gaugino masses (M_1, M_2 and M_3 for each of the $U(1)$, $SU(2)$ and $SU(3)$ gauge groups),
- mass terms for various left- and right- spin-0 (squark, slepton, Higgs) fields,

- trilinear (A-term) interactions amongst the scalars, and
- analogous bilinear (B-term) interactions.

In addition to these soft-breaking terms, the ratio $\tan\beta$ of the two Higgs field VEVs and a supersymmetric Higgsino mixing parameter μ must be specified. Aside from the particles of the Standard Model, the physical spectrum of the MSSM consists of the following additional states.

- squarks (spin-0): $\tilde{d}_L$,$\tilde{u}_L$,$\tilde{s}_L$, $\tilde{c}_L$,$\tilde{b}_1$,$\tilde{t}_1$, $\tilde{d}_R$,$\tilde{u}_R$,$\tilde{s}_R$, $\tilde{c}_R$,$\tilde{b}_2$,$\tilde{t}_2$;
- sleptons (spin-0): $\tilde{e}_L$,$\tilde{\nu}_{eL}$, $\tilde{\mu}_L$,$\tilde{\nu}_{\mu L}$, $\tilde{\tau}_1$,$\tilde{\nu}_{\tau L}$, $\tilde{e}_R$,$\tilde{\mu}_R$,$\tilde{\tau}_2$;
- charginos (spin-$\frac{1}{2}$): $\widetilde{\chi}_1^{\pm}$, $\widetilde{\chi}_2^{\pm}$;
- neutralinos (spin-$\frac{1}{2}$): $\widetilde{\chi}_1^0$, $\widetilde{\chi}_2^0$, $\widetilde{\chi}_3^0$, $\widetilde{\chi}_4^0$
- gluino (spin-$\frac{1}{2}$): $\tilde{g}$;
- Higgs bosons: (spin-0): h, H, A, $H^{\pm}$.

Here, $\tilde{t}_i, \tilde{b}_i$, and $\tilde{\tau}_i$ ($i = 1, 2$) are mixtures of the corresponding left- and right-chiral scalar fields, charginos are mixtures of charged higgsino and wino, and neutralinos are mixtures of two neutral higgsinos, bino and the neutral wino. In our analysis, we neglect any inter-generational sfermion mixing. The intra-generational mixing (being proportional to the corresponding *fermion* mass) is negligible for the first two generations of sfermions.

An independent value for each one of the above masses and couplings leads to a proliferation of new parameters, making phenomenological analyses intractable. It is customary to assume that higher symmetries, which are broken at some ultra-high scale, relate these parameters. An especially appealing and economic class of models is based on minimal supergravity (SUGRA) GUTs, where it is assumed the three gauge couplings unify at some ultra-high energy scale M_X. It is also assumed that SUSY breaking in the effective theory defined at M_X arises due to gravitational interactions which, being universal, allow[9, 1] only a *few* independent soft SUSY breaking parameters, renormalized at M_X: these are

- a common gaugino mass ($m_{1/2}$),
- a common scalar mass (m_0),
- a common trilinear interaction (A_0), and
- the bilinear coupling (B_0).

The various MSSM masses and couplings have to be evolved[13] from the common value at M_X to the electroweak scale to sum the large logarithms arising from the disparity between the two scales. This generally involves solving 26 coupled

differential equations, with the values of the four GUT-scale parameters as boundary conditions. A bonus of this framework is that the same radiative corrections that give rise to these large logs also yield a mechanism for the breakdown of electroweak gauge symmetry, leaving colour and electromagnetic gauge symmetries unbroken[13, 14]. The electroweak symmetry breaking constraint allows one to eliminate B_0 in favour of $\tan\beta$, and also to adjust the magnitude (but not the sign) of the μ parameter to get the measured Z boson mass. Thus, the Renormalization Group (RG) evolution of these four parameters, renormalized at the GUT scale where the physics is simple, results in a rich pattern of sparticle masses and couplings at the weak scale relevant for phenomenology. The various SUSY parameters, masses and mixings are then determined in terms of the four plus a sign parameter set

$$m_0,\ m_{1/2},\ \tan\beta,\ A_0 \text{ and } sign(\mu). \tag{1}$$

In addition, as with the SM, the top mass m_t must be specified. The simplest supergravity model (with minimal kinetic energy terms[15]) leads to (approximate) degeneracy of the first two generations of squarks, and so, is automatically consistent with constraints[16] from flavour changing neutral currents in the K-meson sector[17]. The masses of third generation squarks can be significantly different[18]: this can lead to interesting phenomenology[19, 20] as discussed below. When these supergravity constraints are incorporated, one finds (approximately) $m_{\tilde{q}}^2 \simeq m_{\tilde{\ell}}^2 + (0.7-0.8)m_{\tilde{g}}^2$; thus sleptons may be significantly lighter than the first two generations of squarks. Furthermore, the value of $|\mu|$ is generally large compared to the electroweak gaugino masses, so that the lighter neutralinos ($\widetilde{\chi}_{1,2}^0$) and the lighter chargino ($\widetilde{\chi}_1^\pm$) are gaugino-like, while the heavy chargino and the heavier neutralinos are dominantly Higgsinos. If $m_{\tilde{q}} \simeq m_{\tilde{g}}$ so that sleptons are significantly lighter than squarks, the leptonic decays of $\widetilde{\chi}_2^0$, and sometimes also of $\widetilde{\chi}_1^\pm$ can be significantly enhanced relative to those of Z and W bosons, respectively; this has important implications[21] for detection of sparticles at hadron colliders. Within the SUGRA framework, the lightest SUSY particle is a viable candidate for dark matter[22], provided that the sfermions are not too heavy (the LSP, being mostly a hypercharge gaugino, mainly annihilates via sfermion exchange, so that the annihilation rate is proportional to $\frac{1}{m_{\tilde{f}}^4}$).

While minimal supergravity models indeed provide an economic and elegant framework, it should be recognized that the assumptions (about the physics at an ultra-high energy scale) on which they are based may ultimately prove to be incorrect. The point, however, is that these models lead to rather definite correlations between various sparticle masses[23] as well as between the cross-sections[24, 25, 26] for numerous signals. We will see that these predictions, which serve as tests of the underlying assumptions, can be directly tested at future accelerator facilities. Thus the discovery of sparticles and a determination of their properties[24] may provide a window to the nature of physics at an ultra-high energy scale.

It is also worth considering various extensions of the minimal framework that we have been describing. On the one hand, in some string-inspired models[27], the

four SUGRA input parameters are not all independent so that these models are even more tightly constrained. On the other hand, there has been some recent interest in non-universal SUSY-breaking terms[28], so that the correlations would be modified from their expectations within the minimal framework. In addition, there is no reason why the grand unification scale should exactly coincide with the scale at which the boundary conditions for the RGEs are specified. Furthermore, some models prefer unification at the string scale ($\sim 0.5 \times 10^{18}$ GeV), so that the apparent unification at $\sim 10^{16}$ GeV is only coincidence[29]. It may also be that the particle content of the low energy theory goes beyond that of the MSSM[30] (*e.g.* there might be additional Higgs singlets or gauge bosons), or R-parity might not be conserved by superpotential interactions[31]. In this latter case, there would be additional unknown parameters and the phenomenology might differ substantially from what is expected in minimal supergravity. However, in the absence of large R-violating interactions, many of the gross features of minimal supergravity seem likely to be manifest if low energy supersymmetry exists. But practically speaking, minimal supergravity is a simple and phenomenologically viable framework that offers distinctly testable consequences from a small parameter set. It serves as the paradigm for most phenomenological investigations, although one must bear in mind the consequences of possible modifications to this scheme.

In the early literature[32], it is common to see analyses based upon a more general supersymmetry parameter set, but frequently with various SUGRA GUT inspired assumptions built in. For instance, assuming all gaugino masses evolve as in a SUSY GUT allows the correlation of the various gaugino masses, which are frequently parametrized in terms of $m_{\tilde{g}}$ ($m_{\tilde{g}} \simeq |M_3|$, modulo the distinction[33] between the $\overline{DR}$ and pole mass[1]), or M_2. In addition, the various squarks or sleptons are assumed approximately degenerate, as predicted by minimal SUGRA with its common GUT scale m_0 mass. A common but more general parameter set (which we will loosely refer to as the MSSM parameter set to distinguish it from the SUGRA set (2.1)) is frequently specified by

$$m_{\tilde{g}},\ m_{\tilde{q}},\ m_{\tilde{\ell}},\ A_t,\ A_b,\ \mu,\ m_A,\ \tan\beta, \tag{2}$$

where the supersymmetric Higgsino mass μ and the pseudoscalar Higgs boson mass determine (at tree level) all the other parameters of the Higgs sector, and the weak scale soft SUSY-breaking trilinear couplings A_t and A_b mainly only influence the phenomenology of third generation sfermions. As in the SM, m_t must be input as well. We caution the reader that the SUGRA model specified by the parameter set (2.1) is referred to as the MSSM by some authors[1]. Here, we will reserve the term MSSM for the broader framework specified by the set (2.2) above, and refer to the more constrained framework as minimal SUGRA. The parameter set (2.2) yields much of what is expected in minimal SUGRA, but (with some modification) can also accommodate other models with non-universal soft-breaking terms, which can yield substantially different Higgs masses (m_A) and μ values (leading to Higgsino-like LSP's) than the usual SUGRA prediction (for an example, see Ref. [28]).

[1]See discussions on Fig. 14

2.2 Experimental facilities

The formalism of supersymmetry was developed in the 1970's, and viable phenomenological (low energy) models (*e.g.* the MSSM) were formulated in the early 1980's. A reasonable picture of how supersymmetry might manifest itself has emerged, and now the urgent need is to either discover supersymmetry, or experimentally rule out the existence of weak scale sparticles. It is possible that the first evidence for supersymmetry could arise in a number of experiments: *e.g.* dark matter detectors, study of rare B or K decays, proton decay. However, it is usually expected that unambiguous evidence for supersymmetry must be obtained at colliding beam experiments, where super-particles can be directly produced, and their decay products detected and analyzed. Hence, in this report, we focus on future colliding beam facilities, and their ability to cover regions of the supersymmetric parameter space. For e^+e^- colliders, we consider, along with current constraints from LEP and SLC, future searches at LEP II and at hypothetical linear colliders [34] operating at $\sqrt{s} = 500 - 1000$ GeV. For $p\bar{p}$ colliders, we consider current constraints from the Tevatron collider ($\sqrt{s} = 1.8$ TeV), and its possible high luminosity (TeV*) and high energy (DiTevatron ($\sqrt{s} = 4$ TeV)) upgrades[35]. Finally, we also examine the capability of the CERN LHC pp collider, at $\sqrt{s} = 14$ TeV, approved at CERN Council Meeting in December 1994.

3 Production, decay and simulation of sparticles

If R-parity is conserved, then sparticles ought to be pair-produced at colliders with sufficiently high energy, and furthermore, sparticles ought always to decay into other sparticles, until the decay cascade terminates in the stable LSP. Within the minimal framework, the only viable candidates are the sneutrino and the lightest neutralino $\widetilde{\chi}_1^0$. If we further assume that the LSP is the dominant component of galactic dark matter, the sneutrino is heavily disfavoured[36] when the negative results of experiments searching for double beta decay are combined with LEP constraints discussed below. In what follows, we will assume that $\widetilde{\chi}_1^0$ is the LSP.

3.1 Hadron colliders

At hadron colliders, sparticles can be produced via the following lowest order reactions (particles/anti-particles not distinguished):

- $qq,\ gg,\ qg \to \tilde{g}\tilde{g},\ \tilde{g}\tilde{q},\ \tilde{q}\tilde{q}$, (strong production)
- $qq,\ qg \to \tilde{g}\widetilde{\chi}_i^0,\ \tilde{g}\widetilde{\chi}_i^\pm,\ \tilde{q}\widetilde{\chi}_i^0,\ \tilde{q}\widetilde{\chi}_i^\pm$ (associated production)
- $qq \to \widetilde{\chi}_i^\pm\widetilde{\chi}_j^\mp,\ \widetilde{\chi}_i^\pm\widetilde{\chi}_j^0,\ \widetilde{\chi}_i^0\widetilde{\chi}_j^0$ ($\tilde{\chi}$ pair production)
- $qq \to \tilde{\ell}\tilde{\nu},\ \tilde{\ell}\tilde{\ell},\ \tilde{\nu}\tilde{\nu}$ (slepton pair production)

In addition, the Higgs bosons of the MSSM can be produced via direct s-channel subprocess,

- $qq,\ gg \to h,\ H,\ A,\ H^{\pm}H^{\mp}$,

in addition to production in association with other heavy quarks and vector bosons, and in some cases, production via vector boson fusion.

Once produced, sparticles rapidly decay to other sparticles through a cascade ending in the LSP[37]. The decay modes and branching fractions of sparticles are too numerous to be listed here. However, a number of groups have generated computer programs to calculate some or all of the sparticle decays. Perhaps the most complete listing is available as a public access program called ISASUSY, and can be extracted from the ISAJET program[38] described below. Given a point in MSSM parameter space, ISASUSY lists all sparticle and Higgs masses, decay modes, decay widths and branching fractions.

The crucial link between the theoretical framework of supersymmetry (discussed above), and the detection of long lived particles such as π's, K's, γ's, e's, μ's, *etc.* at colliding beam experiments, lies with event generator programs. Many groups have combined sparticle production and decay programs, to create parton level Monte Carlo programs. Some have added in as well parton showers and hadronization. ISAJET 7.13 is currently the most comprehensive of the supersymmetry event generators available for hadron colliders.

To simulate sparticle production and decay at a hadron collider, the following steps are taken using ISAJET:

- input the parameter set ($m_0, m_{1/2}, A_0, \tan\beta, sign(\mu)$), (or the less constrained MSSM set (2.2)),
- all sparticle and Higgs masses and couplings are computed,
- all sparticle, top and Higgs decay modes and branching fractions are calculated,
- all lowest order $2 \to 2$ sparticle production processes are calculated (if desired, subsets of the reactions can be selected),
- the hard scattering is convoluted with CTEQ2L PDF's[39],
- initial and final state QCD radiation is calculated with the parton shower model,
- particles and sparticles decay through their various cascades,
- quarks and gluons are hadronized, and heavy hadrons are decayed,
- the underlying soft scattering of beam remnants is modelled,
- the resulting event and event history is generated for interface with detector simulations, or for direct analysis.

There are a variety of shortcomings to (the current) ISAJET supersymmetry simulation. Some of these include:

- direct Higgs production mechanisms for hadron colliders are currently absent,
- large $\tan\beta$ solution, (currently, ISAJET is only valid for $\tan\beta \lesssim 10$, primarily because the mixing between b-squarks and third generation sleptons, due to the corresponding Yukawa interactions has not yet been incorporated—this can be very important if *e.g.* the resulting mass splitting opens up new gluino, chargino or neutralino decay channels).
- first two generations of squarks are assumed mass degenerate,
- lack of spin correlation between initial and final state sparticles,
- although decay branching fractions are calculated with full matrix elements, decays in event generation are modelled using only phase space.

Some of these deficiencies should be corrected in the near future.

Separate programs can be extracted from ISAJET 7.13 which generate just the SUGRA mass solution plus decay table (ISASUGRA), and also the sparticle decay table with MSSM input (ISASUSY). ISAJET is maintained in PATCHY format. The complete card image PAM file for ISAJET 7.13 can be copied across HEPNET, the high energy physics DECNET, from `bnlcl6::$2$dua14:[isajet.isalibrary]isajet.car`. A Unix makefile `makefile.unix` and a VMS `isamake.com` are available in the same directory. The same files can be obtained by anonymous ftp from `bnlux1.bnl.gov:pub/isajet`.

3.2 e^+e^- colliders

At e^+e^- colliders, the following production mechanisms can be important:

- $e^+e^- \to \tilde{q}\bar{\tilde{q}}$ (squark pair production)
- $e^+e^- \to \tilde{\ell}\bar{\tilde{\ell}}$ (slepton pair production)
- $e^+e^- \to \widetilde{\chi}_i^{\pm}\widetilde{\chi}_j^{\mp},\ \widetilde{\chi}_i^0\widetilde{\chi}_j^0$ ($\tilde{\chi}$ pair production)
- $e^+e^- \to hZ,\ HZ, hA,\ HA,\ H^+H^-$ (Higgs production),

in addition to vector boson annihilation to Higgs particles. After production, the sparticles and Higgs bosons decay through the usual cascades.

ISAJET 7.13 includes all lowest order $e^+e^- \to SUSY$ and Higgs particle production processes[40], so that cascade decays and minimal SUGRA can be simulated for electron machines as well. However, ISAJET does not include initial state photon radiation, spin correlations, decay matrix elements or polarizable beams. All these effects are expected to be more important in the environment of e^+e^- colliders.

An event generator for $e^+e^- \to SUSY$ particles, containing the above first three sets of reactions, has been released by Katsanevas, under the name SUSYGEN[41].

SUSYGEN also includes cascade decays as calculated by Bartl *et. al.*[42]. SUSYGEN includes initial state photon radiation, and is interfaced to the LUND JETSET string hadronization program. Like ISAJET, SUSYGEN currently lacks spin correlations, final state decay matrix elements, and beam polarizability.

Various groups have created generators that correct some or all of the deficiencies in the SUSYGEN or ISAJET e^+e^- generators, but these are limited to specific production and decay configurations[43]. The problem then becomes that it is difficult to simulate all reactions and decays simultaneously, so a separate program is needed for each possible configuration. However, it is desirable to incorporate the angular correlation in the decay for the studies at an e^+e^- collider since it affects the detection efficiencies and background contaminations which are important especially for precision studies. The helicity amplitude technique is better suited for this purpose. A set of FORTRAN subroutines HELAS [44] can be used to calculate helicity amplitudes numerically, where each of the subroutine calls correspond to each of the vertices in the Feynman diagrams. A repeated use of HELAS calls computes helicity amplitudes rather easily. It can be obtained via anonymous ftp at `tuhep.phys.tohoku.ac.jp`.

4 Current status of supersymmetry searches

The most direct limits on sparticle masses come from the non-observation of any SUSY signals at high energy colliders, and from the precision measurements of the properties of Z bosons in experiments at LEP (for a compilation of constraints, see [45]). The agreement[7] of the measured value of Γ_Z with its expectation in the SM gives model-independent constraints on decays of the Z-boson into any new particles with known $SU(2) \times U(1)$ quantum numbers[36, 46]. This translates to a lower limit $\sim 30 - 45$ GeV on the masses of the sneutrinos, squarks and charginos of the MSSM, independent of the decay patterns of these sparticles. Likewise, the measurement of the invisible width of the Z-boson which leads to the well-known bound on the number of light neutrino species, leads the lower bound of $m_{\tilde{\nu}} > 43$ GeV, even when the sneutrinos decay invisibly via $\tilde{\nu} \to \nu\tilde{\chi}_1^0$[36, 46]. These bounds are relatively insensitive to the details of the model. In contrast, even within the MSSM framework, the corresponding bounds on neutralino masses are sensitive to model parameters. This is because in the limit $\mu \gg M_1, M_2$, the lighter neutralinos are dominantly gaugino-like, so that their couplings to the Z-boson are strongly suppressed by electroweak gauge invariance[36, 46]. The LEP experiments[47] have also directly searched for charginos, sleptons and squarks in Z decays. These searches assume that the charginos and sfermions decay directly to the LSP which is assumed to be the lightest neutralino. The typical signature of SUSY events is a pair of acollinear leptons, acollinear jets or a lepton-jet pair recoiling against $\not{E}_T$ (missing transverse energy). The non-observation of such spectacular event topologies have led to lower bounds very close to $\frac{M_Z}{2}$ on the masses of these sparticles. Finally, LEP experiments have also searched[48] for neutralino production via $Z \to \tilde{\chi}_1^0\tilde{\chi}_2^0$ and $Z \to \tilde{\chi}_2^0\tilde{\chi}_2^0$ decays, assuming that $\tilde{\chi}_2^0 \to$

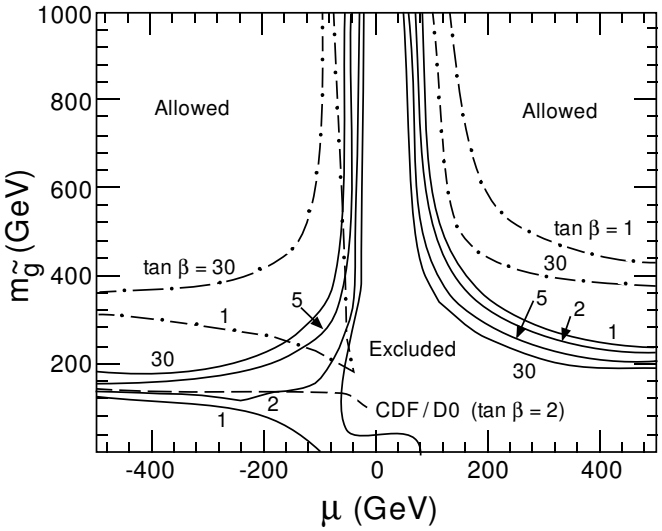

Figure 1: Regions in the μ *vs.* $m_{\tilde{g}}$ plane excluded by various constraints from LEP experiments described in the text, for $\tan\beta = 1$, 2, 5 and 30. We also show the approximate reach of LEP II via the dot-dashed curves ($m_{\widetilde{\chi}_1^\pm} = 90$ GeV), and the region excluded by CDF and D0 gluino and squark searches at the Tevatron.

$\widetilde{\chi}_1^0 f\bar{f}$ ($f = q$ or ℓ). The non-observation of acollinear jet or lepton pairs from this process excludes certain regions of the parameter space, but does not (for reasons already explained) lead to an unambiguous lower bound on $m_{\widetilde{\chi}_2^0}$. The region of the $\mu - m_{\tilde{g}}$ plane excluded by LEP searches for charginos and neutralinos is illustrated in Fig. 1 for various values of $\tan\beta$. Also shown in this figure are corresponding contours of $m_{\widetilde{\chi}_1^\pm} = 90$ GeV, which roughly denote the reach of LEP II, discussed in the next Section.

Although LEP experiments have yielded a limit of $m_{\tilde{q}} \gtrsim \frac{M_Z}{2}$, the search for the strongly interacting squarks and gluinos is best carried out at high energy hadron colliders such as the Tevatron via $\tilde{q}\tilde{q}, \tilde{g}\tilde{q}$ and $\tilde{g}\tilde{g}$ production as discussed in Sec. 3. The final state from the subsequent cascade decays[37] of squarks and gluinos consists of several jets plus (possibly) isolated leptons (from $\widetilde{\chi}_1^\pm$ and $\widetilde{\chi}_2^0$ production via their primary decays) and $\not{E}_T$ from the two LSPs in each final state. For an integrated luminosity of $\sim 20\ pb^{-1}$ that has been accumulated by the CDF and D0 experiments at Tevatron run IA, the classic $\not{E}_T$ channel offers the best hope for detecting SUSY. The non-observation of an excess of $\not{E}_T$ events above SM background expectation has enabled the D0 collaboration[49] to infer a lower limit of ~ 150 GeV on their masses, improving on the published CDF limit[50] of ~ 100 GeV. The region of the $m_{\tilde{g}} - m_{\tilde{q}}$ plane excluded by these anlyses depends weakly on other SUSY parameters, and is shown in Fig. 2 for $\mu = -250$ GeV and $\tan\beta = 2$. We see that the lower bound on the mass improves to about 205 GeV if $m_{\tilde{q}} = m_{\tilde{g}}$. As the experiments at the Tevatron continue to accumulate more data, they will also become sensitive to leptonic signals from cascade decays of squarks and gluinos. Although the single lepton signals are overwhelmed by the background

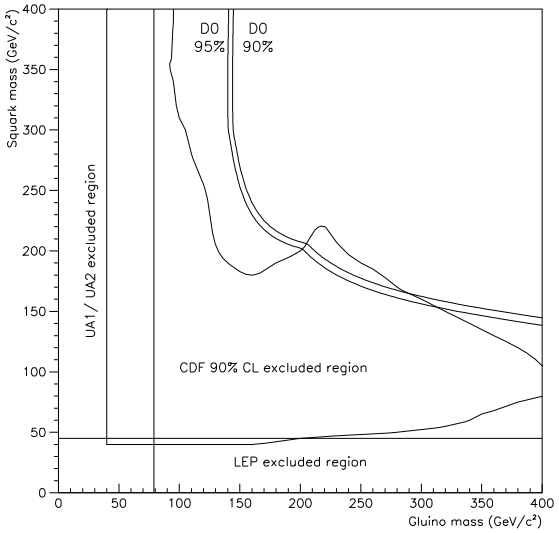

Figure 2: Regions in the $m_{\tilde{g}}\ vs. m_{\tilde{q}}$ plane excluded by searches for $\not\!\!E_T + jets$ events at various colliders, for $\tan\beta = 2$ and $\mu = -250$ GeV. The curves labeled D0 exclude the regions below the curves at 90 and 95 % confidence levels, respectively. The figure is taken from Ref. [49].

from $(W \to \ell\nu) + jet$ events, we will see in Sec. 6 that the multilepton signals offer new ways of searching for supersymmetry at various Tevatron upgrades[51, 52].

Before closing this Section, we briefly remark upon some constraints from "low energy" experiments and from cosmology. Some judgement must be exercised in evaluating these constraints which, unlike the direct constraints from collider experiments, can frequently be evaded by relatively minor modifications of the model framework. For instance, an overabundance of LSPs produced in the early universe leads to significant restrictions on SUGRA parameters[22]. This bound can, however, be simply evaded by allowing a small amount of R-parity violation that causes the LSP to decay, although at a rate that has no other impact on particle physics phenomenology. Likewise, constraints from proton decay[53] are sensitive to assumptions about physics at the GUT scale. Supersymmetry also allows for new sources of CP violation[54] in the form of new phases in gaugino masses or SUSY breaking trilinear scalar interactions. Indeed, for sparticle masses ~ 100 GeV, these phases (which are usually set to zero in the MSSM) are limited[54, 55] to be $\sim 10^{-3}$ in order that the induced electric dipole moment of the neutron or electron not exceed its experimental upper limit. If, however, these phases are zero at some ultra-high unification scale, it has been checked that their values at the weak scale induced via renormalization group evolution do not lead to phenomenological problems. This only pushes the problem to the unification scale where the physics is as yet speculative[56]. There are also constraints from the universality

of the charged-current and neutral-current weak interactions. The Cabbibo universality between the μ-decay and β-decays put constraints only on rather light sparticles $\lesssim$ 20 GeV [57]. Z-decay partial widths into different species of light fermion are more sensitive than the low-energy experiments. However most of the decoupling effects do not put constraints better than that from the direct search [58]. Non-decoupling effects in ρ-parameter [59] or $\Gamma(Z \to b\bar{b})$ [60] are relatively sensitive to the virtual exchange of sparticles. Indeed, it has been claimed that the experimental value of $R_b = \Gamma(Z \to b\bar{b})/\Gamma(Z \to \text{hadrons})$ prefers a light top squark and chargino[61]. Even so, it is hard to obtain a large enough effect to explain the "anomaly" [62]. These measurements do not currently lead to any significant restrictions on sparticle masses.

Finally, we turn to the flavour violating inclusive decay $b \to s\gamma$ recently measured by the CLEO collaboration[63]. Even within the minimal SUSY framework, there are several additional contributions to this amplitude. Of course, the agreement of the SM computations with the experimental data lead to an interesting limit (within theoretical and experimental errors) on the *sum* of various new physics contributions. Since it is possible[64] for these new contributions to (partially) cancel over a significant range of model parameters, these measurements do not lead to unambiguous bounds on the masses of various sparticles. Like the neutralino search at LEP, they do, however, exclude significant regions of parameter space. It should, however, be mentioned that complete calculations of QCD corrections (which are known to be significant within the SM[65]) to these amplitudes[66] are not yet available, so that there is still considerable uncertainty[67] in the theoretical estimates of the $b \to s\gamma$ decay rate.

To summarize: a wide variety of empirical constraints have served to restrict the parameter ranges of supersymmetric models. It is, however, interesting that even the simplest, highly constrained supergravity GUT model, is consistent with *all* experimental data including those from cosmology.

5 Search for SUSY at LEP II

For LEP-II, the second phase of the LEP program, the center-of-mass energy will be raised to about 175 GeV in 1996 and could reach about 200 GeV at a later stage. The reach of LEP II experiments on the search for sparticles has been discussed extensively in the literature. The basic result is that all sparticles close to the kinematic limit can be discovered except special cases of small visible energies or very low cross sections. The measurements of various SUSY parameters have also been discussed, and are shown to be possible for particular combinations of the parameters by studying the first chargino alone. These are the topics which will be described in this section.

5.1 Characteristics of LEP-II experiments

First of all, e^+e^- experiments gradually raise the center of mass energy,[2] so that one does not expect the production of many different sparticles at the same time. We expect the discovery of the lightest visible sparticle (LVSP) first, which does not decay in a (long) cascade as for squarks or gluinos at hadron colliders. This fact makes the search for LVSP at an e^+e^- collider very simple. We look for the production of just one new particle which leaves clear signatures.

In the MSSM framework, there are three candidates for LVSP: (1) slepton (mostly right-handed $\tilde{e}_R$, $\tilde{\mu}_R$, $\tilde{\tau}_R$), (2) chargino $\tilde{\chi}_1^{\pm}$, or (3) stop $\tilde{t}$ (or sbottom in some cases). When we relax the theoretical assumptions built in to the MSSM, one may also expect other sparticles to be LVSP. We will discuss each case separately below.

The following point is worth emphasizing. A search for a sparticle below m_W is relatively easy because one can set the center-of-mass energy below the W-pair threshold, so that most of the signatures are nearly background-free. This is a continuation of searches done at lower energy colliders PEP, PETRA and TRISTAN. Cuts on missing p_T and on the acoplanarity angle removes almost all the QED backgrounds. Above the W-pair threshold, W-pair production becomes the most severe background. Most of the time, we assume $\sqrt{s} = 190$ GeV, and an integrated luminosity of 100 to 500 pb^{-1}.

5.2 $\tilde{l}$-pair production

We assume that one of the sleptons is the LVSP in this subsection. We also assume that R-parity is conserved, and the LSP is the lightest neutralino. Then the only possible decay mode is $\tilde{l} \to l\tilde{\chi}_1^0$ further assuming lepton family number conservation.

Fig. 3 shows the total cross sections for right-handed and left-handed $\tilde{\mu}$ pair production. The threshold behavior is β^3 characteristic of scalar pair production. The experimental signature is a lepton pair with the same flavors with large missing energy or acoplanarity. Here we summarize the analysis of Ref. [68, 69] based on a rather conservative LEP detector simulation using the resolutions of $18\%/\sqrt{E}$ for ECAL at $5^\circ \le \theta \le 175^\circ$, $120\%/\sqrt{E}$ for HCAL at $10^\circ \le \theta \le 170^\circ$, and the angular resolutions $\Delta\phi = \Delta\theta = 0.01$ (ECAL) and 0.02 (HCAL). We made a slight modification: the level of the W-pair background is recalculated with $m_W = 80$ GeV and we discuss right-handed sleptons only without assuming the degeneracy with their left-handed counter parts.[3] The reach for the left-handed sleptons is the same because their production cross sections are almost the same with the right-handed ones. One standard set of cuts is

1. Two isolated muons well inside the detector $|\cos\theta_{\mu^\pm}| < 0.9$, and $E_{\mu^\pm} > 5$ GeV,

[2] Even if LEP-II immediately goes from $\sqrt{s} = m_Z$ to $\simeq 175$ GeV, this step is in a much smaller ratio compared to that of the Tevatron to the LHC.

[3] More detailed studies with the real detector simulations are ongoing in LEP-II workshop.

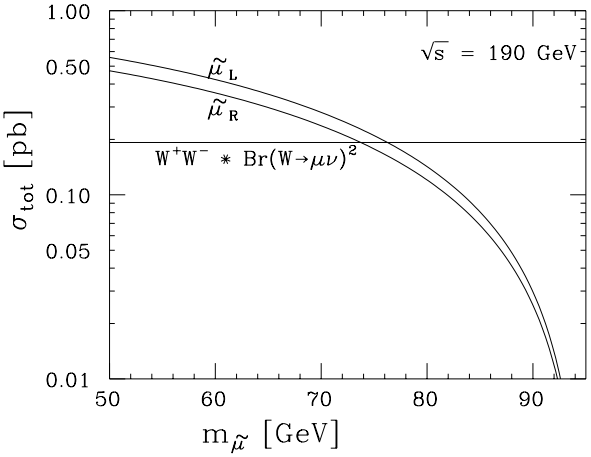

Figure 3: Total cross sections of $\tilde{\mu}_R$ and $\tilde{\mu}_L$ pair production at $\sqrt{s} = 190$ GeV.

Table 1: Cross sections for $\tilde{\mu}$-pair signals and standard model backgrounds at $\sqrt{s} = 190$ GeV, with $m_{LSP} = 20$ GeV.

process	σ_{tot} (pb)	σ_{acc} (pb)
$\tilde{\mu}_R(75)$-pair	0.18	0.058
$\tilde{\mu}_R(80)$-pair	0.11	0.0375
$\tilde{\mu}_R(85)$-pair	0.064	0.020
$\mu\mu(\gamma)$	7.8	0.0
$WW \to \mu\mu + \nu$'s	0.26	0.034

2. large acoplanarity angle[4] $\cos\theta_{acop} < 0.9$,

3. $\pm\cos\theta_{\mu^\pm} > 0$, where the polar angle θ is defined as an angle from the *electron* beam axis.

A typical efficiency for the signal is about 35% [68, 69]. Then the discovery reach (5 σ) extends to 65 GeV (80 GeV) with 100 pb^{-1} (500 pb^{-1}).

The production of $\tilde{e}$-pairs has a larger cross section than $\tilde{\mu}$-pairs due to the t-channel neutralino exchange diagram. The additional background specific to the $\tilde{e}$-pairs is $e\nu_e W$ final state, but it can be safely neglected at LEP-II energy. Therefore, the reach is in general higher than $\tilde{\mu}$-pair depending on the neutralino mass spectrum, and ranges between 85–90 GeV with 500 pb^{-1} [68, 69].

The study of $\tilde{\tau}$ requires a special treatment due to the decay of τ in the final state. There are purely hadronic final state, mixed hadronic-lepton final state, and

[4]We define the acoplanarity angle as $\theta_{acop} = \pi - \Delta\phi$ where $\Delta\phi$ is a difference between the azimuths of the two final-state momenta. Some people use $180^\circ - \theta_{acop}$ as the definition.

purely leptonic final state depending on the decay of each of the τ leptons. The purely leptonic mode suffers the most from the W-pair background, because the signal is reduced by the τ leptonic branching ratios $0.36^2 = 0.13$, while the W-pair background is four times as big as the $\tilde{\mu}$-pair case because both e and μ final states contribute (see Table 1). The hadronic decay of the τ leptons can be distinguished from that from $W \to q\bar{q}$ by requiring small invariant mass of the hadronic system. However, the mixed mode still suffers from W-pair where one W decays into $\tau\nu_\tau$ and the other into $e\nu_e$ or $\mu\nu_\mu$, whose level is twice as high as in the $\tilde{\mu}$-pair case, while the signal level is reduced by a factor of $0.36 \times 0.74 = 0.23$. The hadronic decay of both τ's is the most efficient mode to avoid the background from W-pair. The background level is the same as in $\tilde{\mu}$-pair case, while the signal is reduced only by a factor of $0.74^2 = 0.55$. If one uses the following selection criteria [69]:

1. topology of 1-1 or 1-3 charged particles (with an efficiency of 30%),
2. mass of each clusters to be less than m_τ,
3. $|\cos\theta| < 0.9$ for both clusters,
4. each clusters with $E > 2$ GeV,
5. total $E_{vis} > 10$ GeV,
6. no isolated γ,
7. acoplanarity $-0.8 < \cos\theta_{acop} < 0.87$,

a typical efficiency is about 10%. The discovery reach at 5 σ is estimated to be about 75 GeV with 500 pb^{-1}.

5.3 $\tilde{\chi}_1^\pm$-pair production

At the mass range explorable at LEP-II, $\tilde{\chi}_1^\pm$ decays into three-body states $\tilde{\chi}_1^0 f \bar{f}'$ where f and f' belong to the same weak isodoublet. We assume in this subsection that $\tilde{\chi}_1^\pm$ is the LVSP, and hence the decay $\tilde{\chi}_1^+ \to \tilde{l}^+\nu_l$ or $\tilde{\nu}_l l^+$ is not allowed.[5]

The production cross section is sensitive to the mass of $\tilde{\nu}_e$, which is exchanged in the t-channel. Fig. 4 shows the cross sections for varying $m_{\tilde{\nu}_e}$. The destructive interference between the s-channel γ, Z-exchange and the t-channel $\tilde{\nu}_e$ exchange can suppress the cross section by about an order of magnitude if $m_{\tilde{\nu}_e} \sim \sqrt{s}/2$.

The decay proceeds via virtual W-, $\tilde{l}$- and $\tilde{q}$-exchange. Then the leptonic and hadronic branching ratios vary as a function of $\tilde{l}$ mass. For a wide range of parameter space, W-exchange dominates [70] and the leptonic branching ratio is roughly

[5]Even when $\tilde{\chi}_1^\pm$ is the LVSP, there is a possibility that $\tilde{\nu}$ decays invisibly $\tilde{\nu} \to \nu\tilde{\chi}_1^0$ and has been missed experimentally, and $\tilde{\chi}_1^\pm$ decays mainly into $\tilde{\nu}_l l^+$. Then the search for $\tilde{\chi}_1^\pm$-pairs is similar to the search for slepton pairs, and the reach is expected to be higher than that for sleptons because of larger cross sections and sharper threshold behavior (β vs. β^3 for sleptons). We do not discuss this case below.

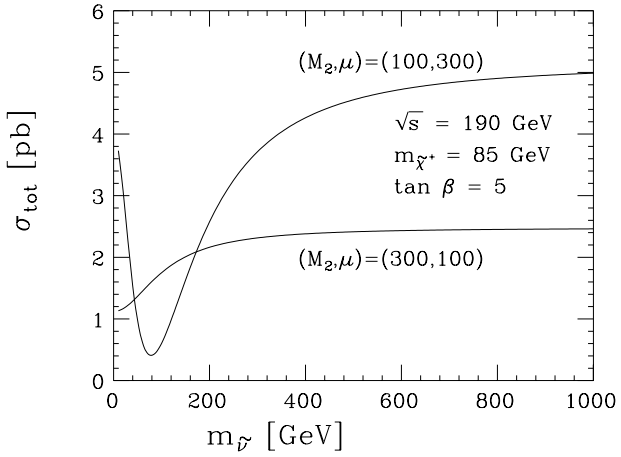

Figure 4: Total cross sections of $\tilde{\chi}_1^\pm$ pair production at $\sqrt{s} = 190$ GeV, as a function of $m_{\tilde{\nu}_e}$, for two representative cases of gaugino-rich and higgsino-rich $\tilde{\chi}_1^\pm$.

30%. The leptonic branching ratio is larger when the chargino is gaugino-dominant and the sleptons are light. The dependence of the leptonic branching ratio on the underlying parameters is shown in Fig. 5. Below, the dominance of W-exchange is assumed with a leptonic (hadronic) branching fraction of $\sim 30\%$ (70%). Even when one has different branching ratios, the efficiency of mixed leptonic-hadronic mode used below obviously does not change much (and could be even better).

The mixed leptonic-hadronic mode is the most efficient one for the search [71]. Even though the pure hadronic mode has the largest branching ratio, it suffers from the background of W-pair where one W decays hadronically and the other W into τ, with its subsequent hadronic decay.[6] The pure leptonic mode suffers the most from the W-pair production where both of them decay into leptonic final states.[7]

Here we summarize the analysis done in Ref. [71]. The detector simulation is based on the parameters of ALEPH detector at LEP. One possible set of cuts is

1. # charged particles > 5.

2. $\not{p}_T > 10$ GeV.

[6]This is not a problem if charginos are well within the threshold. Then the typical total cross section is of order > 3 pb, with roughly half of this in the hadronic final state, while the $jj\tau\nu_\tau$ final state from W-pair has a cross section of 3.5 pb, and it is not difficult to find the excess. The advantage of the mixed mode is that one can go very close to the kinematic reach. Indeed, we also use pure hadronic mode in studying the branching ratios and cross sections later in this section.

[7]This is indeed much more difficult than the other modes. Signal cross section is of order 0.06 pb, while the background from W-pair is 0.8 pb, assuming the dominance of the W-exchange in the chargino decay. However, the leptonic branching ratio of the chargino may be much larger if the slepton-exchange dominates in the chargino decay (see Fig. 5); in this case, the purely leptonic mode is also useful.

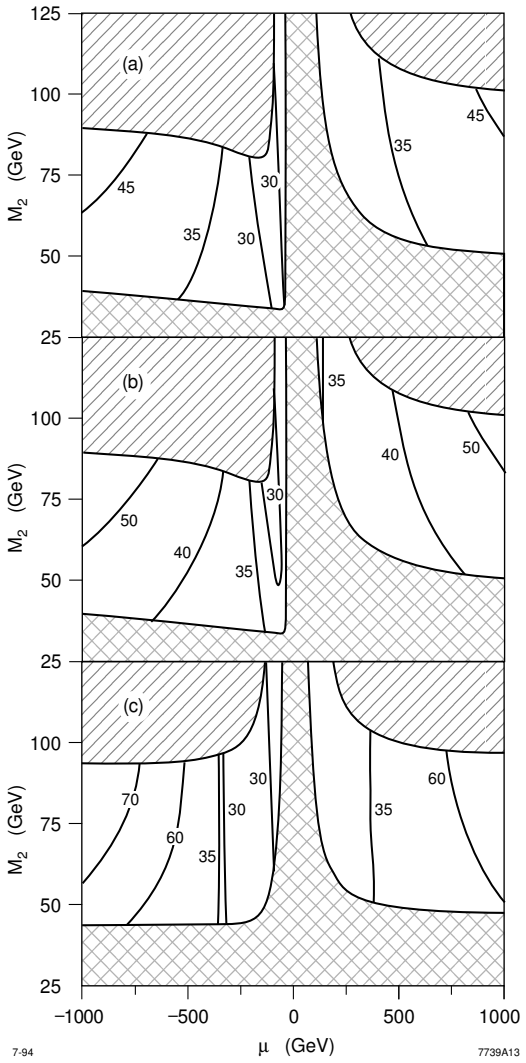

Figure 5: Contours of constant value of the leptonic branching fraction B_l (in %) in the (μ, M_2) plane for $M_1/M_2 = 0.5$ and three sets of parameters $(\tan\beta, m_{\tilde{l}}, m_{\tilde{q}})$: (a) (2, 200, 200), (b) (2, 200, 800), and (c) (10, 200, 200). Note that we used different scales for μ and M_2 to make the numbers visible and to expand the gaugino region. For all figures, the value of B_l is $\frac{1}{3}$ in the Higgsino region and grows as one approaches the gaugino region. The growth is faster for large $\tan\beta$ (c) than for low $\tan\beta$ (a). In (a) and (b) the B_l contours differ by approximately 5% in the far gaugino region. Note also the "pocket" in the $\mu < 0$ near gaugino region, where $B_l < \frac{1}{3}$. The exchange of the charged Higgs is neglected in the decay process. Taken from Ref. [70].

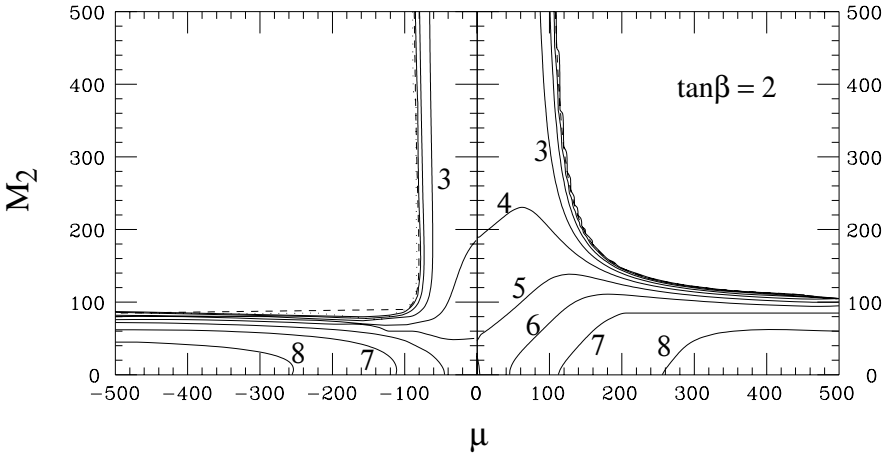

Figure 6: Contour of the total cross sections in pb of $\tilde{\chi}_1^{\pm}$ pair production at $\sqrt{s} =$ 190 GeV, for $m_{\tilde{\nu}_e} = 1$ TeV. The kinematic limit is shown in dashed line, while the discovery reach at 500 pb^{-1} is shown in dotted line. Units are in GeV.

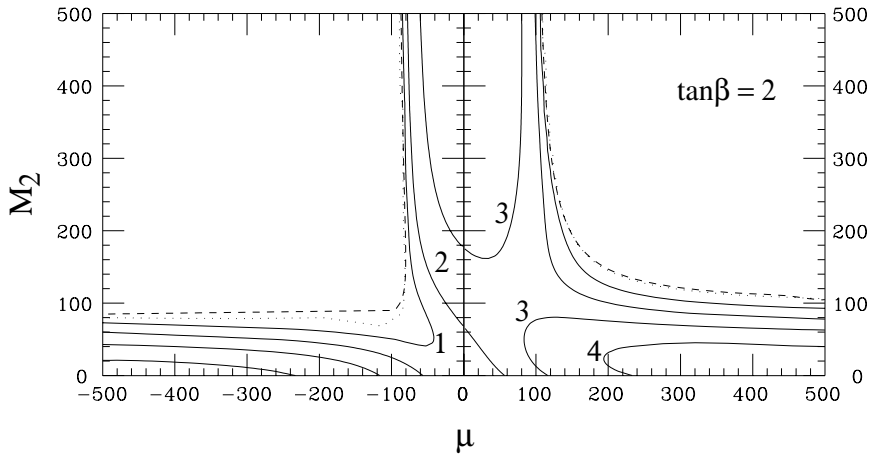

Figure 7: Contours of the total cross sections in pb of $\tilde{\chi}_1^{\pm}$ pair production at $\sqrt{s} = 190$ GeV, for $m_{\tilde{\nu}_e} = 100$ GeV. The kinematic limit is shown in dashed line, while the discovery reach at 500 pb^{-1} is shown in dotted line. Units are in GeV.

3. e or μ with $p_l > 5$ GeV and with a good isolation (no energy deposited larger than 1 GeV within a cone of 30° half-angle).

4. squared missing mass > 4000 GeV^2.

5. mass of the hadronic system < 45 GeV.

6. $m_{l\nu} < 70$ GeV with W-pair hypothesis.

The efficiency of the signal is $\gtrsim 12\%$ including the branching ratio, while the W-pair background after the cuts is 7 pb; other standard model backgrounds are 2 pb. Given 100 (500) pb^{-1}, a 5 σ signal can be found if the $\tilde{\chi}_1^{\pm}$-pair cross section exceeds 0.40 (0.17) pb assuming 12% efficiency.

The coverage on the parameter space (μ, M_2) is shown in Figs. 6,7. For a typical choice of MSSM parameters, $\mu = -100$ GeV and $\tan\beta = 2$, charginos up to 94 GeV can be discovered at 5 σ level even with 100 pb^{-1} if $m_{\tilde{\nu}_e}$ is large enough. If $m_{\tilde{\nu}_e} \sim 100$ GeV, the discovery reach reduces to 81 GeV, but can be pushed up to 90 GeV if 500 pb^{-1} is accumulated.

Once the chargino-pair is found, one can determine the masses of $\tilde{\chi}_1^{\pm}$ and $\tilde{\chi}_1^0$, and decay branching ratios. Here we use both mixed and purely hadronic modes to determine the branching ratios. This is possible if the chargino does not lie too close to the kinematic limit. For a sample parameter set[8]

$$(\mu, M_2, \tan\beta, M_1/M_2, m_{\tilde{l}}, m_{\tilde{q}}) = (-400, 75, 4, 0.5, 200, 300) \tag{3}$$

in units of GeV for dimensionful parameters, a parton-level analysis was performed with the same selection criteria as above [70]. The quark parton and lepton energies are smeared with the resolutions of ALEPH detector. It is assumed that the jet energy measurement can be improved by 25% by matching the tracks with the hits in HCAL and use momentum measurements by the tracking detector for charged particles [72]. The di-jet invariant mass and energy distributions are shown in Fig. 8. For an integrated luminosity of 1 fb^{-1}, the resolutions for the mass determination from the end points of the di-jet energy distribution are estimated to be,

$$\Delta m_{\tilde{\chi}_1^{\pm}} = 2.5 \text{ GeV} \qquad \text{and} \qquad \Delta m_{\tilde{\chi}_1^0} = 2.2 \text{ GeV}. \tag{4}$$

Similarly, the total production cross section and the leptonic branching ratio can be determined as

$$\Delta\sigma_{tot}/\sigma_{tot} = 5.0\% \qquad \text{and} \qquad \Delta B_l/B_l = 4.8\%. \tag{5}$$

The important point is that we can often determine some of the original SUSY parameters even though we have six parameters (the rough degeneracy of all sleptons and all squarks is assumed) while there are only four observables. This is because one cannot reproduce observed masses, cross section and branching ratios

[8]Here, we take the value M_1/M_2 as predicted from GUT, but try to reproduce the number by taking it as a free parameter in the analysis.

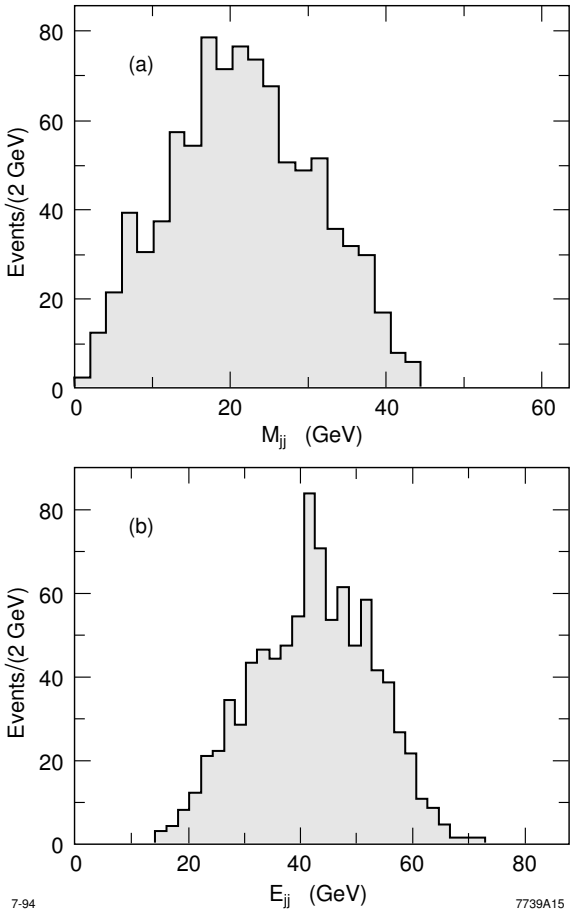

Figure 8: The dijet (a) mass spectrum and (b) energy spectrum, after cuts, for the gaugino case $(\mu, M_2, \tan\beta, M_1/M_2, m_{\tilde{l}}, m_{\tilde{q}}) = (-400, 75, 4, 0.5, 200, 300)$ with integrated luminosity 1 fb^{-1}. In these distributions, hadrons from τ lepton decays have not been included. The finite detector resolution effects cause the spectra to have tails that exceed the theoretical limits, but despite this, the endpoints are fairly sharp. We estimate that the 1σ uncertainty of m_{jj} is 2 GeV, and that for E_{jj} is 3 GeV. Note that very few events have dijets with low invariant mass, and it is therefore possible to distinguish hadrons that result from τ decays and those that result from hadronic chargino decays.

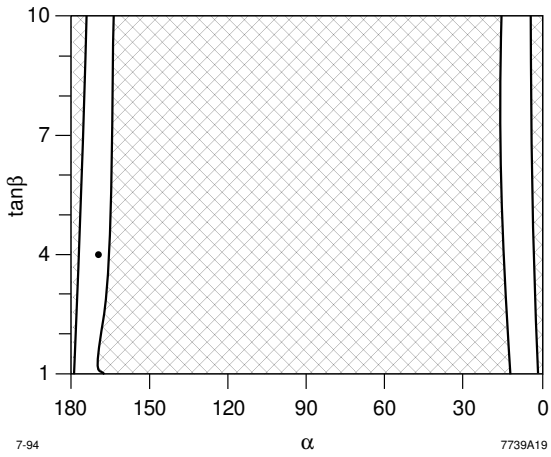

Figure 9: The allowed region in the $(\alpha, \tan\beta)$ plane for the gaugino case study with both signs of M_1 allowed, where $\alpha = \arctan \mu/M_2$. The hatched regions are excluded by the measurements of $m_{\tilde{\chi}_1^\pm}$, $m_{\tilde{\chi}_1^0}$, σ_{tot}, and B_l, which confine the allowed region to narrow strips in the gaugino region. The dot indicates the underlying value of $(\alpha, \tan\beta)$ for the gaugino case study.

by choosing the parameters arbitrarily. For instance, see the strong dependence of the leptonic branching ratio on the underlying slepton mass and chargino parameters in Fig. 5. Also the parameter space is cut off by boundary conditions (*e.g.*, lower bound on sparticle masses). For the above sample parameter set, the ratio $|\mu|/M_2$ can be determined rather well. The result is shown in Fig. 9, on the two-dimensional parameter space $(\alpha, \tan\beta)$ where $\alpha \equiv \arctan \mu/M_2$. Other parameters are determined as

$$\begin{aligned}
0.97 &< \rho_{\tilde{\chi}_1^\pm} < 1.00 \\
0.97 &< \rho_{\tilde{\chi}_1^0} < 1.00 \\
180\ \text{GeV} &< m_{\tilde{l}} < 225\ \text{GeV} \\
0.43 &< \tfrac{M_1}{M_2} < 0.58 \\
-1\ \text{TeV} < \mu < -290\ \text{GeV} &\quad \text{or} \quad 300\ \text{GeV} < \mu < 1\ \text{TeV} \\
63\ \text{GeV} &< M_2 < 93\ \text{GeV}\ ,
\end{aligned} \tag{6}$$

assuming the positive relative sign for M_1 and M_2. Here, $\rho_{\tilde{\chi}_1^\pm}$, $\rho_{\tilde{\chi}_1^0}$ are "gauginoness" of the chargino and LSP, respectively; they are defined as the squared sum of the coefficients of the gaugino fields in the linear expansion of the mass eigenstates in terms of the interaction eigenstates. Note that one could obtain an upper bound on the slepton mass. It is also interesting to note that one can verify the GUT relation $M_1/M_2 = 0.5$, illustrating the ability of precision measurements to shed light on physics at the very high energy scale.

5.4 Other sparticles and Higher Order Processes

The associated $\tilde{\chi}_1^0\tilde{\chi}_2^0$ production is kinematically allowed for a larger range than $\tilde{\chi}_1^\pm$-pair production in the gaugino-region $M_2 < |\mu|$[69]. The total cross section for this process is typically quite small since the gaugino components of the neutralinos don't couple to the Z. However, if $m_{\tilde{\ell}}$ is small enough, a detectable rate is possible. An analysis has been performed in the framework of the minimal SUGRA model[73]. They find that the dilepton channel from $\tilde{\chi}_2^0 \to l\bar{l}\tilde{\chi}_1^0$ is plagued by background from WW production, but suitable cuts can allow a region of observability. The dijet channel, which occurs when $\tilde{\chi}_2^0 \to q\bar{q}\tilde{\chi}_1^0$, is also observable, but only in a small region of SUGRA space, when chargino pair production is not allowed.

If squarks are within the reach of LEP-II, but the chargino $\tilde{\chi}_1^\pm$ is not, they decay directly into $\tilde{q} \to q\tilde{\chi}_1^0$. This case was studied in Ref. [68], with the same detector parameters shown in the case for $\tilde{\mu}$-pair study. The selection criteria are:

1. 85 GeV $< \not{E} <$ 160 GeV,
2. 40 GeV $< \not{p}_T <$ 100 GeV,
3. no isolated leptons, where an isolated lepton is defined as one with $E_l >$ 10 GeV and with hadronic energy smaller than 2 GeV inside the 20° cone around the lepton momentum.

Requirements (2) and (3) completely eliminates Z-pair and most of the W-pair and $q\bar{q}\gamma$ backgrounds. The efficiency of the signal is found to be 51% for $m_{\tilde{q}} = 85$ GeV and $m_{\tilde{\chi}_1^0} = 20$ GeV. The background levels are 0.05 pb from $q\bar{q}\gamma$, 0.15 pb from W-pair and none from Z-pair. A 5 σ signal can be obtained up to $m_{\tilde{q}_L} = 85$ GeV with 100 pb^{-1} at $\sqrt{s} = 190$ GeV [68], with 10 degenerate flavors assumed, which is a common assumption made at a hadron collider.

If one does not assume the degeneracy between squark flavors, the reaches are very different for each of the quantum numbers. The production cross sections are very different for $\tilde{u}_L$, $\tilde{u}_R$, $\tilde{d}_L$, $\tilde{d}_R$, with a ratio of roughly 7.3:4.0:6.0:1. Assuming the same efficiencies as above, the 5 σ discovery reach for individual squarks is about 72 GeV, 59 GeV, 70 GeV, and none at 100 pb^{-1}, and 83 GeV, 76 GeV, 80 GeV and 31 GeV at 500 pb^{-1}. It is noteworthy that one can have better discovery reach for $\tilde{d}_R$ below the W-pair threshold: 35 GeV with 100 pb^{-1} and 54 GeV with 500 pb^{-1} at $\sqrt{s} = 150$ GeV.

An interesting possibility is that the scalar top $\tilde{t}_1$ is light. When $\tilde{t}_1$ is lighter than $\tilde{\chi}_1^\pm$, it mostly decays[74] into $c\tilde{\chi}_1^0$. The signature is the same as $\tilde{q}$ discussed above, acoplanar $c\bar{c}$. Therefore a discovery reach of about 76–83 GeV is expected with 500 pb^{-1} depending on the mixing angle $\tilde{t}_1 = \tilde{t}_L \cos\theta_t + \tilde{t}_R \sin\theta_t$.

If the "visible" sparticles do not lie within the kinematic reach of their pair productions, we can still look for three-body final states such as

$$e^+e^- \to \tilde{\chi}_i^0\tilde{\chi}_j^0\gamma, \tag{7}$$

$$\to \tilde{\nu}\tilde{\nu}^*\gamma, \tag{8}$$

$$\to e^\pm\tilde{e}^\mp\tilde{\chi}_i^0, \tag{9}$$

$$\rightarrow e^{\pm}\tilde{\chi}_i^{\mp}\tilde{\nu}_e^{(*)}, \tag{10}$$
$$\rightarrow \mu^{\pm}\tilde{\mu}^{\mp}\tilde{\chi}_i^0, \tag{11}$$
$$\rightarrow q\tilde{q}\tilde{\chi}_i^0. \tag{12}$$

However, their cross sections are usually suppressed due to the small phase space and because they are higher order in coupling constants than the pair production. The first four processes above were studied in detail in Ref. [69]. However, the cross sections are $\lesssim 0.1$ pb for $\tilde{\nu}\tilde{\nu}^*\gamma$, and even smaller for the other three processes given the current LEP constraint on $\tilde{\nu}$ mass and the assumption that either $\tilde{e}$ or $\tilde{\chi}_1^{\pm}$ are beyond the threshold of their pair productions. The standard model background from the $\nu\bar{\nu}\gamma$ final state was studied in [75] with a similar cut and found to be $\simeq 0.36$ pb. Therefore, the discovery potential of these signals via the observation of an excess of single photon events over SM expectations is marginal. Other signals have not yet been fully studied.

6 Search for SUSY at the Tevatron and its upgrades

Various sparticle pair production cross sections are shown in Fig. 10 for $\sqrt{s} = 2$ TeV $p\bar{p}$ collisions at the Tevatron collider. In this plot, we take (a) $m_{\tilde{q}} = m_{\tilde{g}}$ and (b) $m_{\tilde{q}} = 2m_{\tilde{g}}$, with $\tan\beta = 2$ and $\mu = -m_{\tilde{g}}$.[9] We convolute with CTEQ2L parton distribution functions. From (a), we see that strong production of $\tilde{g}\tilde{g}$, $\tilde{g}\tilde{q}$ and $\tilde{q}\tilde{q}$ is the dominant production cross section for $m_{\tilde{g}} \lesssim 325$ GeV. As one goes to higher gluino masses, the gluino and squark cross sections become kinematically suppressed. However, the charginos and neutralinos are still relatively light ($m_{\widetilde{\chi}_1^{\pm}} \sim m_{\widetilde{\chi}_2^0} \sim \frac{1}{4} - \frac{1}{3}m_{\tilde{g}}$); then, when μ is large compared to M_1 and M_2, $\widetilde{\chi}_1^{\pm}\widetilde{\chi}_2^0$ and $\widetilde{\chi}_1^{\pm}\widetilde{\chi}_1^{\mp}$ become the dominant cross sections. It is instructive to see that if $m_{\tilde{q}} = 2m_{\tilde{g}}$, $\widetilde{\chi}_1^{\pm}\widetilde{\chi}_2^0$ production begins to be the dominant source of SUSY events for gluinos heavier than just 200 GeV. The sum of all associated production mechanisms remains below these other cross sections, and never dominates. This gives a good idea of what to search for, depending on $m_{\tilde{g}}$: as long as one is probing $m_{\tilde{g}} \lesssim 200$ GeV, one should focus on $\tilde{g}$ and $\tilde{q}$ production, with their subsequent cascade decays; for gluinos with masses between 200-325 GeV, this is still the best channel to search for SUSY if $m_{\tilde{q}} = m_{\tilde{g}}$, but for heavier squarks, $\widetilde{\chi}_1^{\pm}\widetilde{\chi}_2^0$ production dominates even if gluinos are as light as ~ 200 GeV. Note, however, that given sufficient integrated luminosity, the highest reach in $m_{\tilde{g}}$ will ultimately be reached by exploring the $p\bar{p} \rightarrow \widetilde{\chi}_1^{\pm}\widetilde{\chi}_2^0$ and $\widetilde{\chi}_1^{\pm}\widetilde{\chi}_1^{\mp}$ reactions.

[9] This is motivated by supergravity models.

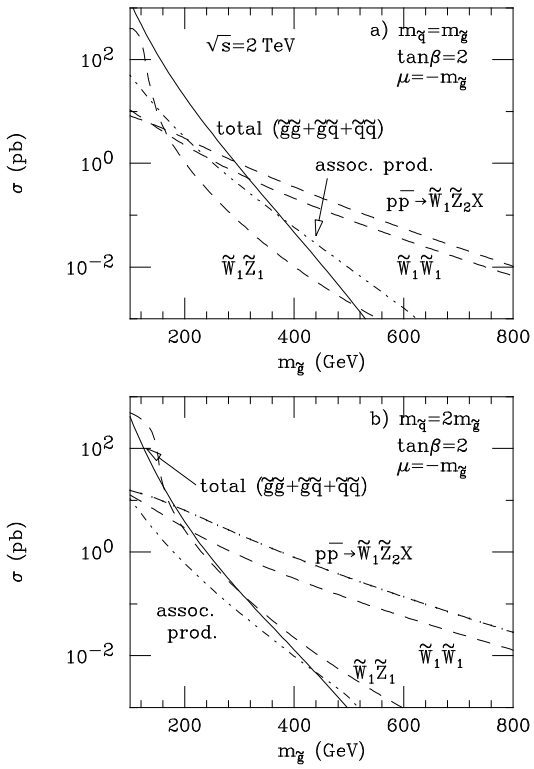

Figure 10: Total cross sections for various sparticle pair reactions for $p\bar{p}$ collisions at $\sqrt{s} = 2$ TeV.

6.1 Sparticle cascade decay signatures at the Tevatron

In general, sparticle pair production at the Tevatron collider is followed by sparticle decays through a cascade until the LSP ($\widetilde{\chi}_1^0$) state is reached[37]. Hence, sparticle production is signalled by events with n-jets plus m-isolated leptons plus $\not\!\!E_T$ (n, m non-negative integers). These events can be broken down into various distinct classes:

- $multi - jet + \not\!\!E_T$ events (veto isolated leptons);
- $1\ell + jets + \not\!\!E_T$ events (these have huge backgrounds from direct W production);
- $2\ell + jets + \not\!\!E_T$ events (these can further be broken down into opposite-sign (OS) isolated dileptons, which have substantial backgrounds from $t\bar{t}$, WW and $\tau^+\tau^-$ production, and same-sign (SS) isolated dileptons, for which the SM backgrounds are expected to be much smaller);
- $3\ell + jets + \not\!\!E_T$ events (these further sub-divide into those containing jets, which usually come from gluino and squark cascade decays, or events with

three isolated leptons, plus little or no jet activity, which usually come from $\widetilde{\chi}_1^{\pm}\widetilde{\chi}_2^0$ production, followed by their leptonic decays. Assuming that leptonic decays of the Z can be identified with high efficiency, SM backgrounds to these events are expected to be small);

- $4\ell + jets + \not\!\!E_T$ events (these events usually come from the presence of two $\widetilde{\chi}_2^0$'s in an event; they have low cross section, but tiny backgrounds as well).

- $\geq 5\ell + jets + \not\!\!E_T$ events (these can only be produced by multi-step cascades of very heavy sparticles, or, in R-parity violating models where the LSP decays into leptons via lepton number violating interactions).

In Ref. [52], ISAJET 7.13 was used to generate *all* lowest order $2 \to 2$ subprocesses, with a complete event simulation. Experimental conditions were simulated using a toy calorimeter with segmentation $\Delta\eta \times \Delta\phi = 0.1 \times 0.09$ and extending to $|\eta| = 4$. An energy resolution of $\frac{0.7}{\sqrt{E}}$ ($\frac{0.15}{\sqrt{E}}$) for the hadronic (electromagnetic) calorimeter was assumed. Jets were defined to be hadron clusters with $E_T > 15$ GeV in a cone with $\Delta R = \sqrt{\Delta\eta^2 + \Delta\phi^2} = 0.7$. Leptons with $p_T > 8$ GeV and within $|\eta_\ell| < 3$ were considered to be isolated if the hadronic scalar E_T in a cone with $\Delta R = 0.4$ about the lepton was smaller than $\frac{E_T(\ell)}{4}$. Finally, $\not\!\!E_T > 20$ GeV was required in all events. For each of the event topologies introduced above, we impose the following additional requirements:

1. $\not\!\!E_T$ events, are required to have $n_{jet} \geq 4$ with at least one of the jets in the central region, $|\eta| < 1$, and following the recent analysis by the D0 collaboration[49], $\not\!\!E_T \geq 75$ GeV. We veto events with either isolated leptons with $E_T \geq 15$ GeV (to reduce W backgrounds), or a jet within 30^o of $\not\!\!\vec{p}_T$.

2. Single lepton events were defined to have exactly one isolated lepton with $E_T \geq 15$ GeV. We reject events with 60 GeV $\leq m_T(\ell, \not\!\!E_T) \leq 100$ GeV which have large backgrounds from W production.

3. The OS dilepton sample was defined to have two opposite sign isolated leptons with $p_T \geq 15$ GeV and $30^o \leq \Delta\phi_{\ell^+\ell'^-} \leq 150^o$ and no other isolated leptons. To eliminate backgrounds from Z production, events with 80 GeV $\leq m(\ell^+\ell^-) \leq 100$ GeV were rejected.

4. The SS dilepton sample was required to have exactly two isolated leptons, each with $p_T \geq 15$ GeV, and no other isolated leptons. At least two jets are also required.

5. The $n_\ell \geq 3$ event sample was defined to have exactly n_ℓ isolated leptons, with $p_T(\ell_1) \geq 15$ GeV and $p_T(\ell_2) \geq 10$ GeV.

The cross sections for the various SUSY signals calculated within the SUGRA-inspired MSSM framework are shown in Fig. 11, for (a) $m_{\tilde{q}} = m_{\tilde{g}} + 10$ GeV, (b) $m_{\tilde{q}} = m_{\tilde{g}} - 10$ GeV, and (c) $m_{\tilde{q}} = 2m_{\tilde{g}}$. Here, $\tan\beta = 2$, $\mu = -m_{\tilde{g}}$, $m_t = 170$ GeV,

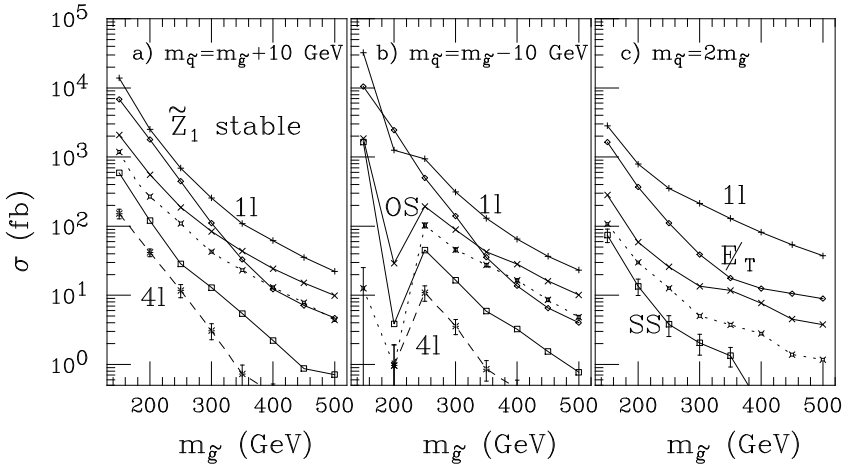

Figure 11: Cross sections at the Tevatron ($\sqrt{s} = 1.8$ TeV) in *fb* for various event topologies after cuts given in the text for the MSSM, for three choices of squark mass. We take $\mu = -m_{\tilde{g}}$, $\tan\beta = 2$, $A_t = A_b = -m_{\tilde{q}}$ and $m_A = 500$ GeV. The $\not\!\!E_T$ events are labelled with diamonds, the 1-ℓ events with crosses, the $\ell^+\ell^-$ events with x's and the SS with squares. The dotted curves are for 3-ℓ signals, while dashes label the 4-ℓ signals. For clarity, error bars are shown only on the lowest lying curve; on the other curves the error bars are considerably smaller. We note that the $m_{\tilde{g}} = 150$ GeV case in *b* is already excluded by LEP constraints on the Z width, since this implies $m_{\tilde{\nu}} = 26$ GeV.

and the pseudoscalar Higgs boson mass is taken to be 500 GeV. The slepton masses are determined in terms of $m_{\tilde{g}}$ and $m_{\tilde{q}}$ using renormalization group equations to evolve from a common sfermion mass at the GUT scale.

The *physics* backgrounds to these event topologies within the SM framework are shown in Table 2 for a top quark mass of 150 GeV and 175 GeV. Detector-dependent backgrounds to multilepton signals from misidentification of jets as isolated leptons[76] or to the $\not\!\!E_T > 75$ GeV signal from mismeasurement of QCD jets should be small.

We see that while SUSY signals and SM backgrounds are of comparable magnitude in the $\not\!\!E_T$ and OS dilepton channels, the signal cross sections substantially exceed backgrounds in the SS and $n_\ell = 3$, and in some cases, $n_\ell \geq 4$ isolated lepton channels. The reach of the Tevatron is estimated by requiring that the SUSY signal (in any channel) exceed the background by 5σ; *i.e.* $N_{sig} > 5\sqrt{N_{back}}$, where N_{sig} (N_{back}) are the expected number of signal (background) events in a collider run, and where the $m_t = 150$ GeV background numbers have been used. In addition, to incorporate systematic uncertainties inherent to these calculations, it is further required[52] (somewhat arbitrarily) that $N_{sig} > 0.25N_{back}$. For further discussion of this point, see Sec. 9. The reach of the Tevatron is illustrated in Table 3, both

Table 2: Standard Model background cross sections in fb for various event topologies after cuts described in the text, for $p\bar{p}$ collisions at $\sqrt{s} = 1.8$ TeV. The $W + jet$ and $Z + jet$ results include decays to τ leptons.

case	$\not\!\!E_T$	$1\ \ell$	OS	SS	$3\ \ell$	$\geq 4\ \ell$
$t\bar{t}(150)$	270	1200	190	0.8	0.7	–
$t\bar{t}(175)$	145	590	90	0.3	0.3	–
$W + jet$	710	1.2×10^6	–	–	–	–
$Z + jet$	320	2200	69	–	–	–
WW	0.4	110	130	–	–	–
WZ	0.04	4.3	1.2	2.1	0.4	–
total $BG(150)$	1300	1.2×10^6	390	2.9	1.1	–
total $BG(175)$	1175	1.2×10^6	290	2.4	0.7	–

Table 3: Reach in $m_{\tilde{g}}$ via various event topologies for the SUGRA-inspired MSSM, assuming an integrated luminosity of 0.1 fb^{-1} (1 fb^{-1}), at the Tevatron collider. The reach has been conservatively calculated using $m_t = 150$ GeV, and will be slightly larger since the top quark mass has recently been measured to be $m_t \simeq 175$ GeV.

case	$\not\!\!E_T$	$1\ \ell$	OS	SS	$3\ \ell$	$\geq 4\ \ell$
$m_{\tilde{q}} = m_{\tilde{g}} + 10$ GeV	240 (260)	— (—)	225 (290)	230 (320)	290 (425)	190 (260)
$m_{\tilde{q}} = m_{\tilde{g}} - 10$ GeV	245 (265)	— (—)	160 (235)	180 (325)	240 (440)	— (—)
$m_{\tilde{q}} = 2m_{\tilde{g}}$	185 (200)	— (—)	— (180)	160 (210)	180 (260)	— (—)

for an integrated luminosity of 0.1 fb^{-1} that is expected to be accumulated by the end of Tevatron run IB, and, in parenthesis, for an integrated luminosity of 1 fb^{-1} that should be accumulated after one year of Main Injector (MI) operation. The multi-lepton signals have only been evaluated for negative values of μ. For $\mu > 0$ and somewhat heavy squarks, the leptonic decay of $\tilde{\chi}_2^0$ is strongly suppressed by complicated interference effects. This could lead to a substantial reduction of the 3ℓ signal. In Table 3, a minimum of five signal events (ten for the MI reach) are required in each channel. For the SS and 3ℓ samples where the expected background is very small (so that the 5σ criterion is not meaningful), we have checked that the Poisson probability for the background to fluctuate to this minimum event level is $\leq 2 \times 10^{-4}$ and $< 10^{-5}$, respectively.

Several conclusions can be drawn from Table 3. We have checked that in run IA of the Tevatron collider (integrated luminosity $\sim 0.02\ fb^{-1}$), the greatest reach in $m_{\tilde{g}}$ is achieved in the $\not\!\!E_T + jets$ channel, with essentially no reach via multi-lepton signals. However, for run IB (integrated luminosity $\sim 0.1\ fb^{-1}$), there is now a comparable reach also in each of the OS and SS dilepton channels, and for $\mu < 0$, especially in the 3ℓ channel. In the main injector era (integrated

luminosity $\sim$ 1 fb^{-1}), the reach in the $\not\!\!E_T + jets$ channel will be background limited. However, in the SS dilepton and 3ℓ channels, a much larger range of masses can be explored. In the 3ℓ channel, for $m_{\tilde{q}} \sim 2m_{\tilde{g}}$, $m_{\tilde{g}} \sim 260$ GeV can be explored, while for $m_{\tilde{q}} \sim m_{\tilde{g}}$, squarks and gluinos as heavy as 425-440 GeV might be detectable!

The reach in $m_{\tilde{g}}$ has also been evaluated in Ref. [76] for the TeV* and the DiTevatron. At the DiTevatron, the strong production of SUSY particles is greatly enhanced relative to the $\not\!\!E_T$ background, which is mainly electroweak. In the $\not\!\!E_T + jets$ channel, it is estimated the DiTevatron has a reach of $m_{\tilde{g}} \sim 500 - 600$ GeV.

6.2 $\widetilde{\chi}_1^{\pm}\widetilde{\chi}_2^0 \to 3\ell$ signal

The usefulness of the reaction $p\bar{p} \to W \to \widetilde{\chi}_1^{\pm}\widetilde{\chi}_2^0 \to 3\ell + \not\!\!E_T$ was suggested long ago in Ref. [77], while complete calculations for *on-shell* W's were carried out in Ref. [78]. Arnowitt and Nath pointed out that with an integrated luminosity of 100 pb^{-1}, signals from the $p\bar{p} \to \widetilde{\chi}_1^{\pm}\widetilde{\chi}_2^0$ reaction remains substantial even when the intermediate W is *off-shell*[79]. Even so, subsequent full calculations of the 3ℓ signature reached rather pessimistic conclusions for Tevatron energies[80], although these assumed $\widetilde{\chi}_2^0$ and $\widetilde{\chi}_1^{\pm}$ decays only via virtual W and Z bosons. Ultimately, it was pointed out that, in SUGRA models, where $m_{\tilde{\ell}}$ is frequently much lighter than $m_{\tilde{q}}$, the $\widetilde{\chi}_2^0$ and sometimes also $\widetilde{\chi}_1^{\pm}$ leptonic branching ratios enjoy a large enhancement (for $\mu < 0$), if all decay diagrams are included[21]. This allows Tevatron collider experiments to probe much deeper into the SUGRA parameter space than previously expected. Further calculations, some using the SUGRA framework with particular choices of string-motivated soft-breaking boundary conditions[81, 76], others performed within the minimal SUGRA framework[82], confirmed these expectations.

In Ref. [83], simulations of clean trilepton signal and background were performed using the minimal SUGRA framework. We show in Fig. 12a and Fig. 13a (taken from Ref. [83]) the regions in the m_0 *vs.* $m_{1/2}$ plane where the clean trilepton signal ought to be observable (after cuts) at the Tevatron Main Injector with an integrated luminosity of 1 fb^{-1} (black squares), and at a luminosity upgraded (25 fb^{-1}) Tevatron, TeV*, at the 10σ (squares with x's) and 5σ level (open squares). In Fig. 12b and Fig. 13b, we show corresponding mass contours for $\tilde{g}$, $\widetilde{\chi}_1^{\pm}$ and $\tilde{\ell}_R$, for comparison.

We see that the reach of the MI and TeV* are variable in parameter space, but that the largest reach is attained when m_0 is small, so that $\widetilde{\chi}_2^0 \to \tilde{\ell}\ell$ two body decay dominates the branching fractions. In this case, for both signs of μ, TeV* can probe to $m_{\tilde{g}} \sim 600 - 700$ GeV. As m_0 increases, $\widetilde{\chi}_2^0 \to \tilde{\ell}_L\ell$ closes, and decays are dominated by $\widetilde{\chi}_2^0 \to \tilde{\nu}\nu$, and there is a gap in trilepton reach, even though $\widetilde{\chi}_2^0 \to \tilde{\ell}_R\ell$ is accessible. For even higher values of m_0, $\widetilde{\chi}_2^0$ decays via 3-body decays, unless the $\widetilde{\chi}_2^0 \to \widetilde{\chi}_1^0 h$ or $\widetilde{\chi}_2^0 \to \widetilde{\chi}_1^0 Z$ decay modes are kinematically allowed. For $\mu < 0$ and large m_0, the MI (TeV*) can see to $m_{\tilde{g}} \sim 300$ GeV (500 GeV). However,

for $\mu > 0$, we see that for large m_0 there is *no reach*[10] via trileptons for either MI or TeV*. For large values of $m_{1/2}$, the $\widetilde{\chi}_2^0 \to \widetilde{\chi}_1^0 h$ or $\widetilde{\chi}_2^0 \to \widetilde{\chi}_1^0 Z$ decay modes turn on, dominating the branching fractions, and spoiling the signal. Thus, the onset of these "spoiler modes" provides a natural limit beyond which the 3ℓ signal is no longer viable, (for large m_0).

In Ref. [76], the reach in the 3ℓ channel for the proposed DiTevatron upgrade is calculated, with $\sqrt{s} = 4$ TeV. Their results show that the reach via trileptons of the DiTevatron is not enhanced much beyond what a 2 TeV Tevatron can do. This is easy to understand. $\widetilde{\chi}_1^{\pm}\widetilde{\chi}_2^0$ production takes place mainly via valence quark annihilation, and hence doubling the Tevatron energy only increases the cross section in this channel by a factor of ~ 3. Meanwhile, a very significant SM background comes from $t\bar{t}$ production, which takes place via gg as well as $q\bar{q}$ fusion. The $t\bar{t}$ background increases by a factor of ~ 20 when going from 2 to 4 TeV collisions[11].

It has also been pointed out that observation of a sufficient number of 3ℓ events can allow for a relatively precise $m_{\widetilde{\chi}_2^0} - m_{\widetilde{\chi}_1^0}$ mass measurement, by measuring the $m(\ell\bar{\ell})$ distribution in *e.g.* $e\bar{e}\mu$ events[21]. Such a measurement requires a significant trilepton sample that is devoid of contamination from SM backgrounds or from other SUSY sources. While this measurement may turn out to be possible at the Tevatron (for some ranges of parameters), it will require the highest attainable luminosity, and will be contingent upon how well the detectors function in the high luminosity environment. In the next section, we will also see that this measurement should be relatively easy at the LHC, unless the leptonic decay of the neutralino is strongly suppressed. A measurement of $m_{\widetilde{\chi}_2^0} - m_{\widetilde{\chi}_1^0}$ may thus be a starting point for disentangling the various sparticle masses.

6.3 Top squark search

In minimal SUGRA, the soft-breaking masses $m^2_{\tilde{t}_L}$ and $m^2_{\tilde{t}_R}$ are driven to lower values than for the other squarks, due to the large top quark Yukawa coupling. The $\tilde{t}_L - \tilde{t}_R$ mixing induced by Yukawa interactions reduces the light top squark mass $m_{\tilde{t}_1}$ even further. Hence, the light top squark is frequently much lighter than the other squark species; in this case, Tevatron limits on $m_{\tilde{q}}$, which are derived assuming ten degenerate squark types, are not applicable to the top squark. Top squarks require an independent search effort at Tevatron experiments. For identical top and stop masses, the stop pair total cross section is typically $\sim \frac{1}{5} - \frac{1}{10}$ of the top pair cross section[19].

[10]This is due to a strong suppression of the leptonic branching fraction of $\widetilde{\chi}_2^0$ which mainly occurs due to negative interference between Z and $\tilde{\ell}_L$ exchange diagrams in the $\widetilde{\chi}_2^0$ leptonic width. The result presented here is at variance with results presented in Ref. [81, 76, 82], where the authors suggest that trilepton searches will significantly extend the reach in $\widetilde{\chi}_1^{\pm}$ independently of the sign of μ. Of course, for very large values of m_0, the sfermion mediated amplitudes become suppressed, and the neutralino branching ratios are those of the Z boson.

[11]It may, however, be possible to suppress the $t\bar{t}$ background with about a 50% loss of signal using a cut described in Sec. 7.2 where we discuss the extraction of this signal at the LHC.

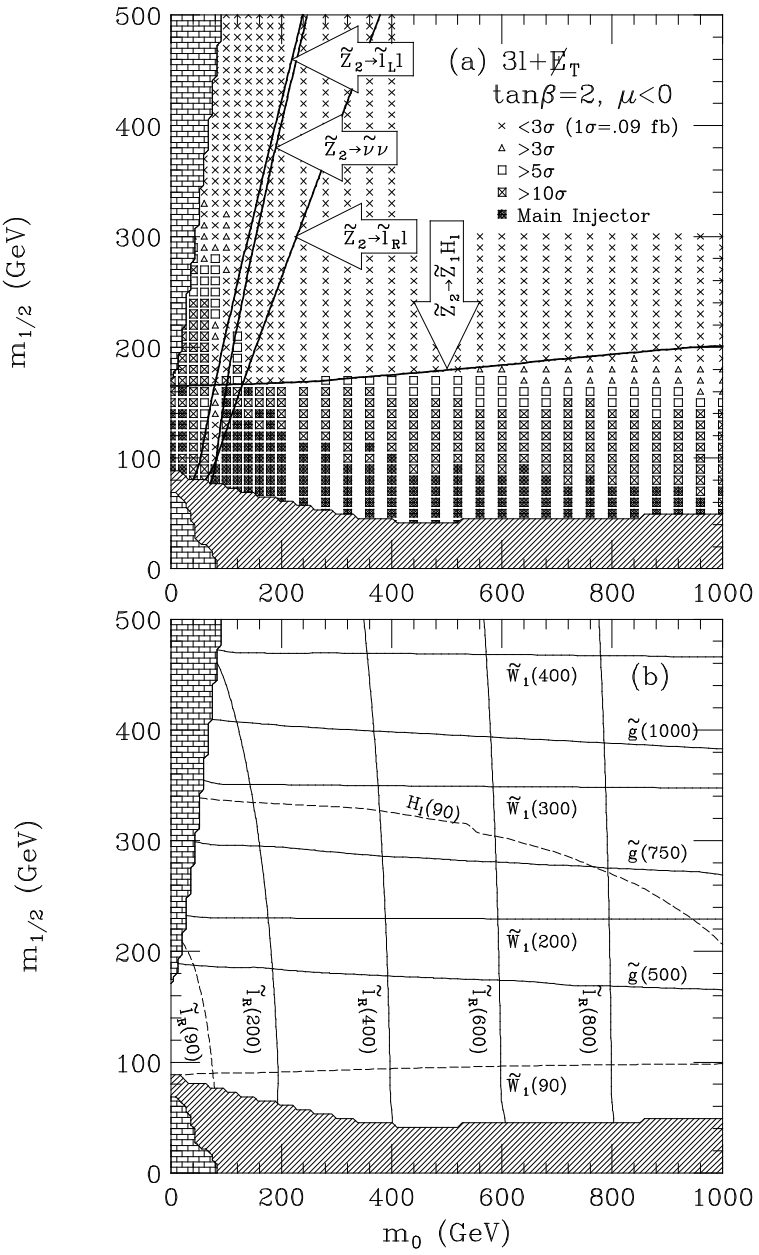

Figure 12: Regions of m_0 *vs.* $m_{1/2}$ plane where clean trilepton signal is observable over background, for Tevatron MI project ($1\ fb^{-1}$) and TeV* ($25\ fb^{-1}$). We take $A_0 = 0$ and $\mu < 0$. The decay $\widetilde{\chi}_2^0 \to \widetilde{\chi}_1^0 h$ is allowed above the indicated contour, while the decays $\widetilde{\chi}_2^0 \to \tilde{\nu}\nu$ and $\widetilde{\chi}_2^0 \to \tilde{\ell}_R \ell$ are allowed to the left of the labelled contours.

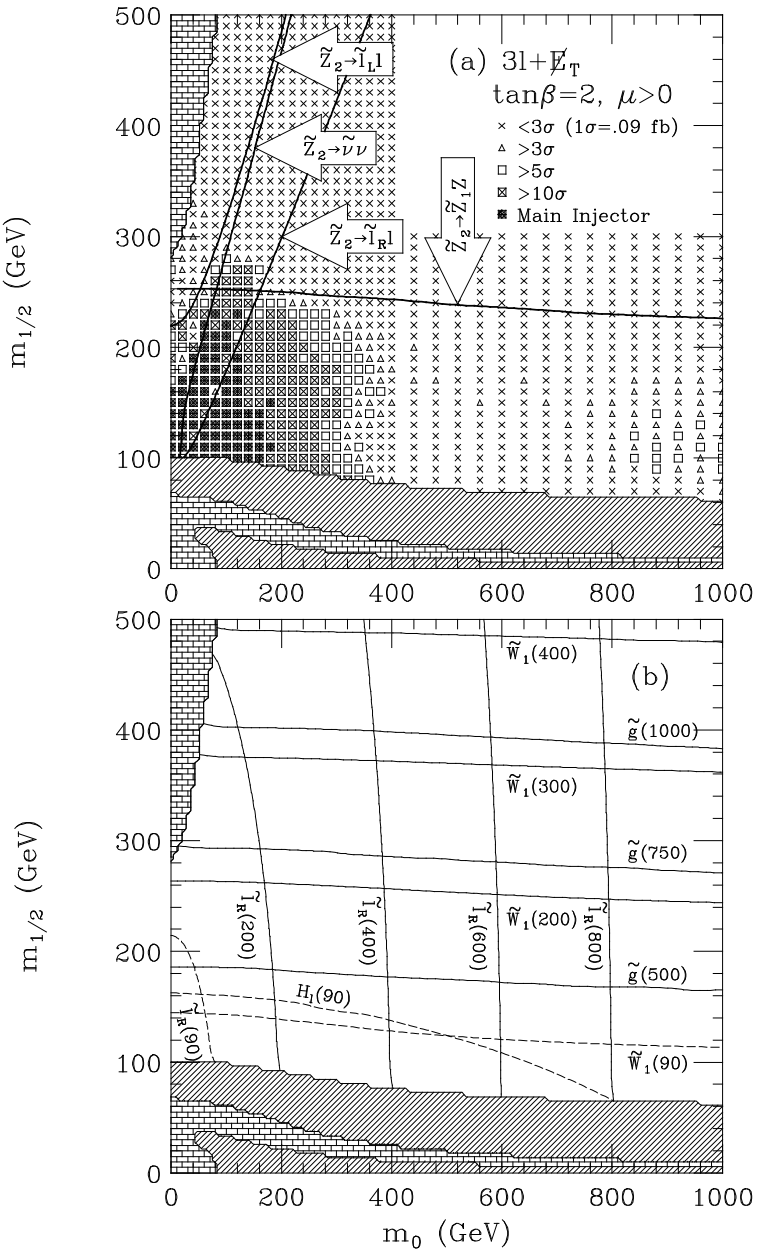

Figure 13: Regions of m_0 *vs.* $m_{1/2}$ plane where clean trilepton signal is observable over background, for Tevatron MI project ($1\ fb^{-1}$) and TeV* ($25\ fb^{-1}$). We take $A_0 = 0$, and $\mu > 0$. The decay $\widetilde{\chi}_2^0 \to \widetilde{\chi}_1^0 h$ is allowed above the indicated contour, while the decays $\widetilde{\chi}_2^0 \to \tilde{\nu}\nu$ and $\widetilde{\chi}_2^0 \to \ell_R \ell$ are allowed to the left of the labelled contours.

If $m_{\tilde{t}_1} > m_b + m_{\widetilde{\chi}_1^\pm}$, then $\tilde{t}_1 \to b\widetilde{\chi}_1^\pm$ decays are expected to dominate for the stop masses $m_{\tilde{t}_1} \sim 50 - 125$ GeV accessible to Tevatron experiments. In the case where other squarks and sleptons are all relatively heavy, the lighter chargino decays dominantly via virtual W exchange so that the branching fractions for the leptonic decay $\widetilde{\chi}_1^\pm \to \ell\nu\widetilde{\chi}_1^0$ is $\sim$11% per lepton family. Then, top squark pair signatures are identical to top quark pair signatures, except that the decay products are softer. In the $p\bar{p} \to \tilde{t}_1\bar{\tilde{t}}_1 \to b\bar{b}\ell\nu q\bar{q}'\widetilde{\chi}_1^0\widetilde{\chi}_1^0$ channel, it has been shown that[20] given a data set of 0.1 fb^{-1}, a signal may be detectable for $m_{\tilde{t}_1} \lesssim 100$ GeV, but only if adequate B micro-vertex tagging is available. In the $p\bar{p} \to \tilde{t}_1\bar{\tilde{t}}_1 \to b\bar{b}\ell\bar{\ell}'\nu'\bar{\nu}\widetilde{\chi}_1^0\widetilde{\chi}_1^0$ channel, the t-squark signal can be separated from the top quark background by searching for *soft* dilepton events: one cuts, for instance, on the sum $|p_T(\ell_1)| + |p_T(\ell_2)| + |\not{E}_T| < 100$ GeV to remove harder dilepton events from top quark pairs. This cut works well if $m_t \geq 150$ GeV, which now appears to be the case. We also note that scalar top signals may be significantly enhanced if the sleptons are significantly lighter than squarks and $|\mu|$ is large, in which case the branching fractions for the leptonic decays of chargino may be considerably larger than those for W.

If the decay $\tilde{t}_1 \to b\widetilde{\chi}_1^\pm$ is kinematically closed, then the $\tilde{t}_1$ will decay[74] dominantly via a flavor changing loop to $c\widetilde{\chi}_1^0$. In this case $\tilde{t}_1\bar{\tilde{t}}_1$ production is signalled by $\not{E}_T$ events, exactly as for squark production (but without any cascade decays). Hence, the relevant reaction is $p\bar{p} \to \tilde{t}_1\bar{\tilde{t}}_1 \to c\bar{c}\widetilde{\chi}_1^0\widetilde{\chi}_1^0$, and one looks for two jets plus $\not{E}_T$. Again, suitable cuts will allow Tevatron experiments to probe $m_{\tilde{t}_1} \lesssim 100$ GeV with 0.1 fb^{-1} of data, even if the LSP is rather heavy[20].

6.4 Slepton search

The search for sleptons at the Tevatron collider was addressed in Ref.[84]. In that work, all channels of slepton production and decay were simulated using ISAJET. The best bet for observing slepton signals appeared to be in the OS $2\ell + \not{E}_T$ channel. Even here, there were large irreducible backgrounds from WW production (as well as possible contamination from other SUSY souces such as $\widetilde{\chi}_1^\pm\widetilde{\chi}_1^\mp$ production) which precludes clear identification of the slepton signal. The conclusions were that, even using the Tevatron main injector, a signal would be very difficult to see for slepton production via off-shell Z bosons– *i.e.*, if $m_{\tilde{\ell}} > 45 - 50$ GeV.

6.5 Multichannel search for minimal SUGRA

How do the various search strategies outlined above correlate to each other? Which SUSY searches are complementary, and which overlap? How do searches for SUSY at the Tevatron compare to SUSY searches at LEP, or LEP-II? These questions can most sensibly be addressed by working within the relatively constrained framework of minimal supergravity with radiative electroweak symmetry breaking, and universal soft-breaking terms at the unification scale. In this framework, all sparticle masses and couplings are determined by specifying the parameter set

$m_0, m_{1/2}, A_0, \tan\beta, sign(\mu)$, introduced in Sec. 2. The parameter A_0 mainly affects the 3rd generation sparticle masses, and the spectrum changes slowly with variation in $\tan\beta$ (of course, the phenomenology may be significantly altered if new decays, *e.g.* $\widetilde{\chi}_1^{\pm} \to \tilde{t}_1 b$ become allowed). Hence, the m_0 *vs.* $m_{1/2}$ plane seems to provide a convenient panorama in which to plot results. In Fig. 14, we take $A_0 = 0$, $\tan\beta = 2$ and $m_t = 170$ GeV, and show results for both signs of μ. We note the following features:

- the gray regions are excluded on theoretical grounds, since in the lower left region, electroweak symmetry breaking does not occur, or cannot attain the proper Z-boson mass. Other parts of the gray regions are excluded because sparticles other than the $\widetilde{\chi}_1^0$ become the LSP.

- In Fig. 14*a*, the currently experimentally excluded region is below the hatch marks, and is due to four separate limits: the LEP limits that $m_{\widetilde{\chi}_1^{\pm}} > 47$ GeV, $m_h \gtrsim 60$ GeV, and $m_{\tilde{\nu}} > 43$ GeV, and also the Tevatron $\not\!\!E_T + jets$ search. In Fig. 14*b*, the experimentally excluded region is made up entirely of the LEP chargino mass bound.

- Future searches at LEP II should probe $m_{\widetilde{\chi}_1^{\pm}}$, $m_{\tilde{\ell}}$ and m_h up to nearly 90 GeV. These regions are denoted by dot-dashed lines.

- The corresponding value of $m_{\tilde{g}}$ is plotted on the right axis, for comparison with reaches calculated in the summary Table in Sec. 10, or Ref. [76]. These values vary only slightly with m_0 due to inclusion of differences between the $\overline{DR}$ and pole values of $m_{\tilde{g}}$[33].

- The total $\widetilde{\chi}_1^{\pm}\widetilde{\chi}_2^0 \to 3\ell + \not\!\!E_T$ cross section is plotted for 200 fb (roughly attainable by Tevatron run IB), and for 20 fb (roughly attainable by the Tevatron MI run with 1 fb^{-1} of data). Since no simulation has been performed, these must be regarded as maximal regions, because in some areas, lepton p_T values may be too soft for detection. We remind the reader that the results of the complete simulation of the trilepton signal are shown in Fig. 12 and Fig. 13.

- We also show with the dotted lines the regions where the $\widetilde{\chi}_2^0$ spoiler modes turn on. These regions show the limit beyond which no Tevatron upgrade is likely to probe. We also show regions where $\widetilde{\chi}_2^0$ can decay via two-body modes into real sleptons or sneutrinos. In these regions, there can be large fluctuations of signal due to branching fraction and kinematical effects. Again, these regions may be compared with the corresponding regions in Fig. 12 and Fig. 13.

It is easy to see from Fig. 14 that the regions explorable by Tevatron $\not\!\!E_T$ searches (across all m_0 values) are complementary to the regions explorable via $3\ell + \not\!\!E_T$ searches (which favor small m_0). Also, the complementarity of searches at LEP and Tevatron, and LEP II and Tevatron Main Injector, is also easily seen. Similar plots for a different A_0 value (where the $\tilde{t}_1$ search also enters), and $\tan\beta = 10$ are

shown in Ref. [26]. Since this constrained SUGRA framework has been embedded into ISAJET, various experimental search efforts should be able to combine results within the GUT scale SUGRA parameter space.

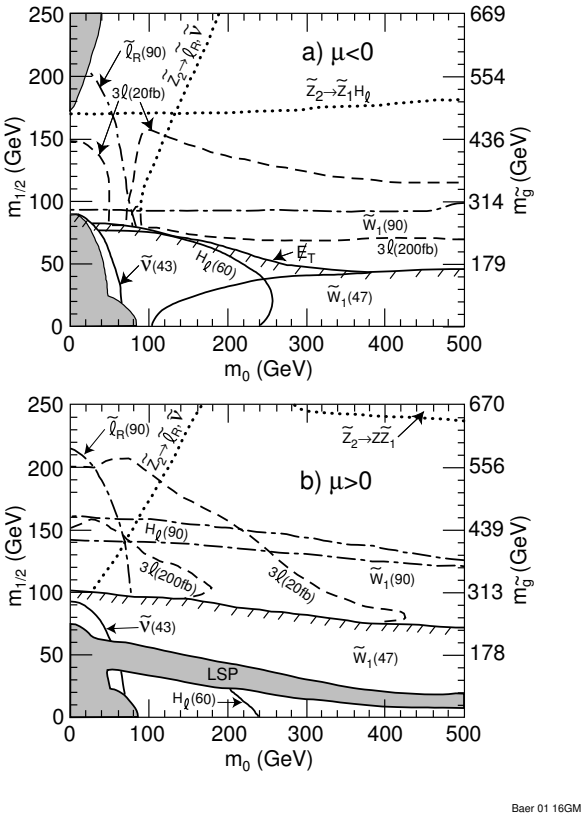

Figure 14: Regions in the m_0 $vs.m_{1/2}$ plane explorable by Tevatron and LEP II experiments.

Additional assumptions from theories at the GUT or Planck scale can further reduce the parameter space of supersymmetric models. For example, in superstring models with supersymmetry breaking in the dilaton sector, the universal soft breaking parameters are related such that

$$m_{1/2} = -A_0 = \sqrt{3}m_0. \tag{13}$$

In models with supersymmetry breaking in the moduli sector, one expects the "extreme" (sometimes called "no-scale") boundary conditions

$$m_0 = A_0 = 0, \tag{14}$$

although quantum corrections can distort these simplified values. Implementation of such boundary conditions can reduce the parameter space to just one or two

dimensions (depending on whether one further specifies the soft-breaking B parameter), plus the usual sign of μ ambiguity. Various analyses have been performed within these contexts, assuming gauge unification at the GUT scale, or sometimes at the string scale, where extra heavy particles ($m \sim 10^7 - 10^{12}$ GeV) must be added to maintain unification[85]. In Ref. [86], these various classes of models have been examined, and rather complete parameter space scans have been carried out for Tevatron energies. ISAJET was used to simulate all sparticle subprocesses and decay mechanisms. In general, the low values of m_0 in these models lead to slepton masses much smaller than squark masses. Consequently, one generates a large number of leptons in the final state. In the best cases, one can probe to $m_{\tilde{g}} \sim 500$ GeV using the Tevatron MI, by searching for trilepton and SS dilepton events. In the worst case (Dilaton models with GUT scale unification and negative μ), the light chargino and neutralino dominantly decay to real sneutrinos, so that only $m_{\tilde{g}} \lesssim 300$ GeV can be explored at the MI. Further details regarding the features of these models may be found in Ref. [81] and Ref. [76].

We emphasize, finally, that the various GUT or string scale assumptions made in this section are just that– assumptions. Whenever possible, search efforts should be performed using the most general, and encompassing, framework available.

6.6 What if R-parity is violated?

Additional interactions which respect gauge symmetry, but violate baryon (B) and/or lepton (L) number conservation, can be added to the superpotential of the MSSM. In this case, R-parity is violated. Simultaneous presence of both B and L violating interactions can lead to catastrophic proton decay, so usually one or the other (or both!) of the interactions is assumed absent. In general, a large number of different R-violating interactions can be introduced, which can lead to very complicated (and intractable) phenomenology[31]. If the R-violating interactions are large, sparticle production and decay patterns are altered, and in particular, single production of sparticles is possible. In addition, these interactions can also affect the renormalization group flow of various masses and couplings. If the R-violating interactions are sufficiently small, then gauge interactions still dominate sparticle production and decay rates but the LSP $\widetilde{\chi}_1^0$ becomes unstable so that the classic $\not{E}_T$ signature may be destroyed.

This latter case of R-violation has been examined for Tevatron experiments in Ref. [52], for a "worst case" and "best case" situation. The worst case is where $\widetilde{\chi}_1^0 \to qqq$ (B-violating), in which case the $\not{E}_T$ signature might be lost, and additional hadronic activity would cause leptons from cascade decays to fail the isolation requirements causing the SUSY signal to be lost beneath SM backgrounds. The best case might be where $\widetilde{\chi}_1^0 \to \ell\bar{\ell}\nu$, which may lead to a plethora of isolated leptons in the final state[87].

In Ref. [52], for the baryon number violating case it is assumed that the only effect of R-violation is to cause $\widetilde{\chi}_1^0 \to cds$ or $\bar{c}\bar{d}\bar{s}$. Then sparticle production and decay are simulated exactly as in Sec. 6.1, with the same detector characteristics. The resulting mass reach is listed in Table 4. We see that there is almost no reach

Table 4: Reach in $m_{\tilde{g}}$ via various event topologies for R-parity violating SUGRA-inspired MSSM, assuming an integrated luminosity of 0.1 fb^{-1} (1 fb^{-1}), at the Tevatron collider. We use $m_t = 150$ GeV for the background. In *a*), we show results for B-violating interactions, while in *b*) we show results for L-violating interactions.

case	$\not\!\!E_T$	$1\ \ell$	OS	SS	$3\ \ell$	$\geq 4\ \ell$
$a)BNV$						
$m_{\tilde{q}} = m_{\tilde{g}} + 10$ GeV	— (—)	— (—)	165 (210)	200 (280)	220 (350)	— (165)
$m_{\tilde{q}} = m_{\tilde{g}} - 10$ GeV	200 (210)	— (—)	150 (165)	165 (235)	— (360)	— (—)
$m_{\tilde{q}} = 2m_{\tilde{g}}$	— (—)	— (—)	— (—)	— (200)	— (190)	— (—)
$b)LNV$						
$m_{\tilde{q}} = m_{\tilde{g}} + 10$ GeV	— (150)	— (—)	240 (300)	330 (450)	480 (650)	540 (740)
$m_{\tilde{q}} = m_{\tilde{g}} - 10$ GeV	160 (180)	— (—)	250 (300)	330 (450)	460 (640)	520 (710)
$m_{\tilde{q}} = 2m_{\tilde{g}}$	— (—)	— (—)	190 (260)	340 (540)	540 (730)	600 (840)

in the $\not\!\!E_T$ channel, even given the Main Injector integrated luminosity of $\sim 1\ fb^{-1}$. However, the presence of cascade decays still allows hard leptons and neutrinos to be produced in the final state, although fewer leptons will be isolated due to the additional hadronic activity from LSP decays. We see that in the SS dilepton channel, and especially in the isolated $3\ell + jets + \not\!\!E_T$ channel, there remains enough signal to search for substantial ranges of $m_{\tilde{g}} \sim 200 - 350$ GeV with the Tevatron MI[12]. The reach of the Tevatron would be somewhat smaller if $\tan\beta$ is large since the MSSM SS and 3ℓ cross sections are known to be smaller for $\tan\beta = 10 - 20$.

For the "best case" scenario studied in Ref. [52] it is assumed that the LSP exclusively decays into (readily identifiable) muons and electrons via $\tilde{\chi}_1^0 \to \mu\bar{e}\nu_e$ (and related processes) which take place via L-violating interactions, with all other production and decay mechanisms remaining unaltered. In this case, four additional hard, potentially isolated leptons can exist in the final state. The reach is again listed in Table 4. We see that in the isolated multilepton channels, very large reaches in $m_{\tilde{g}}$ are possible. In particular, in the 4ℓ channel at the main injector, equivalent gluino masses of $\sim 700 - 800$ GeV can be probed!

7 Search for SUSY at the CERN LHC

The CERN Large Hadron Collider, a pp collider to operate at $\sqrt{s} = 14$ TeV, is frequently regarded as a machine capable of a thorough search for supersymmetric particles below the TeV scale. In Fig. 15, we show total cross sections for various sparticle pair production reactions as a function of $m_{\tilde{g}}$. We set $\tan\beta = 2$, and $\mu = -m_{\tilde{g}}$; the plots are insensitive to μ as long as μ is large so that the lighter -inos are mainly gaugino rather than higgsino. In *a*), we take $m_{\tilde{q}} = m_{\tilde{g}}$, while

[12]Again, it should be kept in mind that the reaches in Table 4 have been obtained with $\mu < 0$.

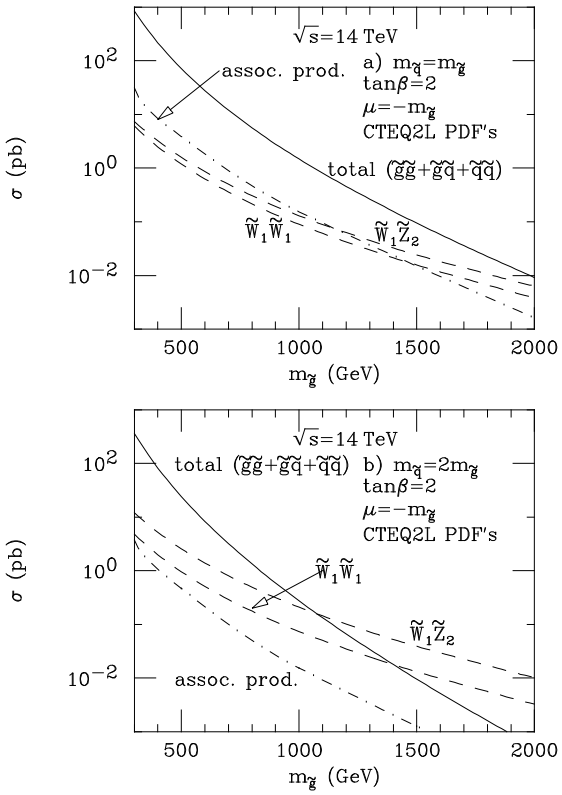

Figure 15: Total production cross sections for various reactions at the LHC.

in b) we take $m_{\tilde{q}} = 2m_{\tilde{g}}$. We see that in a), the summed strong production of $\tilde{g}\tilde{g} + \tilde{g}\tilde{q} + \tilde{q}\tilde{q}$ is the dominant cross section over the complete range of $m_{\tilde{g}}$ all the way up to 2 TeV. In case b), however, we see that the chargino/neutralino pair production reactions become the dominant SUSY particle production mechanism above $m_{\tilde{g}} \sim 1100$ GeV. In this mass range, $\widetilde{\chi}_1^{\pm}\widetilde{\chi}_2^0 \to (W\widetilde{\chi}_1^0) + (h\widetilde{\chi}_1^0) \to \ell b\bar{b} + \not{E}_T$ should have major background problems from $Wb\bar{b}$, Wh and $t\bar{t}$ production. In these figures, there is assumed five degenerate species of L- and R- squarks. If the light top squark is much lighter than other squarks, then its production mechanism may dominate other squark production mechanisms. Associated production is always a sub-dominant component of sparticle pair production for both cases a) and b).

7.1 Sparticle cascade decay signatures

As in the case of the Tevatron collider, sparticle pair signatures at LHC divide into the various $\not{E}_T$, 1ℓ, 2ℓ (SS and OS), 3ℓ and $\geq 4\ell$ classes. In addition, the rate for events containing high p_T leptonically decaying Z bosons together with $\not{E}_T$ can be substantial at LHC. In Ref. [88], these various signals were plotted with a set of nominal cuts, and compared with the corresponding SM backgrounds.

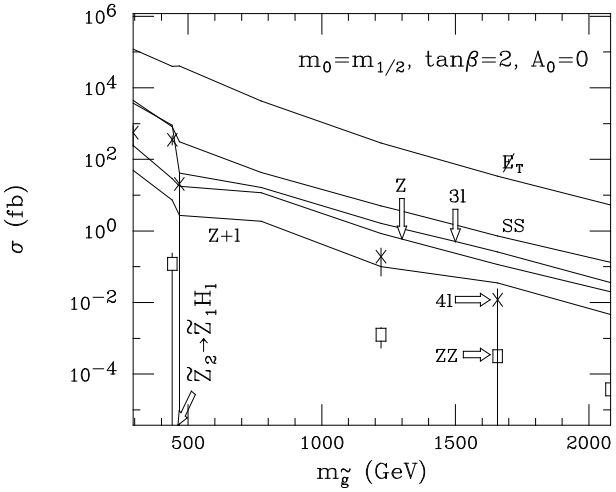

Figure 16: Cross sections after cuts for various event topologies at the CERN LHC pp collider.

We update[94] this plot in Fig. 16, using ISAJET 7.13, for the same set of cuts as in Ref.[88], except for now using a calorimeter out to $|\eta| < 5$, and requiring $|\eta_{jet}| < 3$. Error bars denote the statistical uncertainty in our simulation of the smallest cross sections. This sampling of a particular slice of SUGRA parameter space ($m_0 = m_{1/2}$, $A_0 = 0$ and $\tan\beta = 2$) illustrates several points:

- the $\not{E}_T + jets$ signal[90, 91], although dependent on the specific cuts, occurs at a significant rate for a large range of $m_{\tilde{g}}$ well beyond 1 TeV,
- the SS dilepton[92] and 3ℓ signal rates are also substantial over a large range of $m_{\tilde{g}}$. The kink just below $m_{\tilde{g}} = 500$ GeV marks where the previously mentioned $\widetilde{\chi}_2^0$ "spoiler modes" turn on. We see that while the trilepton signal drops by an order of magnitude, almost a hundred events are nevertheless expected annually at the LHC even if the gluino is as heavy as 1 TeV. This implies that a significant number of these events comes from other than $\widetilde{\chi}_2^0$ decays, *e.g.* $\tilde{g} \to t\tilde{t}_1$ decays. The other cross sections are less sensitive to the "spoiler mode".
- the signal from 4ℓ events is likely to be visible in only limited regions of parameter space, and
- there also exist regions of parameter space where signals from leptonically decaying high p_T Z bosons plus jets plus $\not{E}_T$ may be observable. Within the MSSM, this region is sensitive to the value of μ; within the SUGRA framework, μ is no longer a free parameter.

Table 5: 5σ discovery limits in $m_{\tilde{g}}$ (in TeV) via $\not{E}_T + jets$ events at LHC Atlas detector for various choices of squark and gluino mass ratios, and collider integrated luminosities. Variation of MSSM parameters can cause these limits to vary by ~ 150 GeV.

case	$10^3\ pb^{-1}$	$10^4\ pb^{-1}$	$10^5\ pb^{-1}$
$m_{\tilde{q}} = m_{\tilde{g}}$	1.8	2.0	2.3
$m_{\tilde{q}} = 2m_{\tilde{g}}$	1.0	1.3	1.6

7.1.1 $\not{E}_T + jets$ signature

Previous studies on $\not{E}_T + jets$ signal from gluinos and squarks by the GEM and SDC collaborations for the SSC concluded that $m_{\tilde{g}} \sim 0.3-$ 1-2 TeV should have been detectable[90]. Recently, the Atlas[91] collaboration has performed detailed studies on the $\not{E}_T + jets$ signal for the LHC. They found that gluinos as low as 300 GeV should easily be seen above SM backgrounds. Then, requiring rather stiff cuts

$$\not{E}_T > 600 \text{ GeV},\ p_T(jet_1, jet_2, jet_3) > 200 \text{ GeV},\ p_T(jet_4) > 100 \text{ GeV}, \quad (15)$$

and transverse sphericity $S_T > 0.2$, they found an upper reach for $m_{\tilde{g}}$ listed in Table 5, for various choices of integrated luminosity. We see that if squarks and gluinos have mass below ~ 1 TeV, and if the MSSM is a reasonable approximation of nature, then supersymmetry is unlikely to escape detection at the LHC.

A similar analysis has been performed in Ref. [89], where similar reach values were obtained. In addition, the regions of the minimal SUGRA model explorable via multi-jets $+\not{E}_T$ signature were mapped out. Sample results for $\mu < 0$, $A_0 = 0$ and $\tan\beta = 2$ are shown in Fig. 17*a*. Results differ only slightly for $\mu > 0$, or $\tan\beta = 10$. In Fig. 17*b*, contours of $m_{\tilde{g}}$ and $m_{\tilde{q}}$ are shown for comparison.

An interesting question to ask is: if a signal in the $\not{E}_T + jets$ channel is found at LHC, what information can be gleaned about sparticle properties? In general, many different subprocesses can be contributing to the SUSY signal, and the subsequent cascade decay channels can be numerous and complicated, especially for relatively heavy sparticles. Mapping out the size of the signal cross section, and the shapes of different jet distributions and $\not{E}_T$ distributions, and matching against Monte Carlo predictions, will significantly constrain the SUSY parameter space. Also, in first approximation, one expects $\tilde{g}\tilde{g}$ events to have higher jet multiplicity than $\tilde{q}\tilde{q}$ events. In practice, the cascade decays, along with substantial QCD radiation, distort this picture. Jet multiplicity distributions have been evaluated in Ref. [89], where it was found that mixed $\tilde{q}\tilde{q} + \tilde{g}\tilde{g} + \tilde{g}\tilde{q}$ subprocesses typically yield average jet multiplicities a half unit lower than pure $\tilde{g}\tilde{g}$ production if $m_{\tilde{q}} \simeq m_{\tilde{g}}$.

Can one measure $m_{\tilde{g}}$ or $m_{\tilde{q}}$ in the $\not{E}_T + jets$ channel? A rough mass determination can be made just based on the size of the total cross section, and the hardness of distributions such as $p_T(jet)$ and $\not{E}_T$. Direct measurement of $m_{\tilde{g}}$ is difficult. Even in the idealistic case of constructing a two-jet mass from $\tilde{g} \to q\bar{q}\widetilde{\chi}_1^0$,

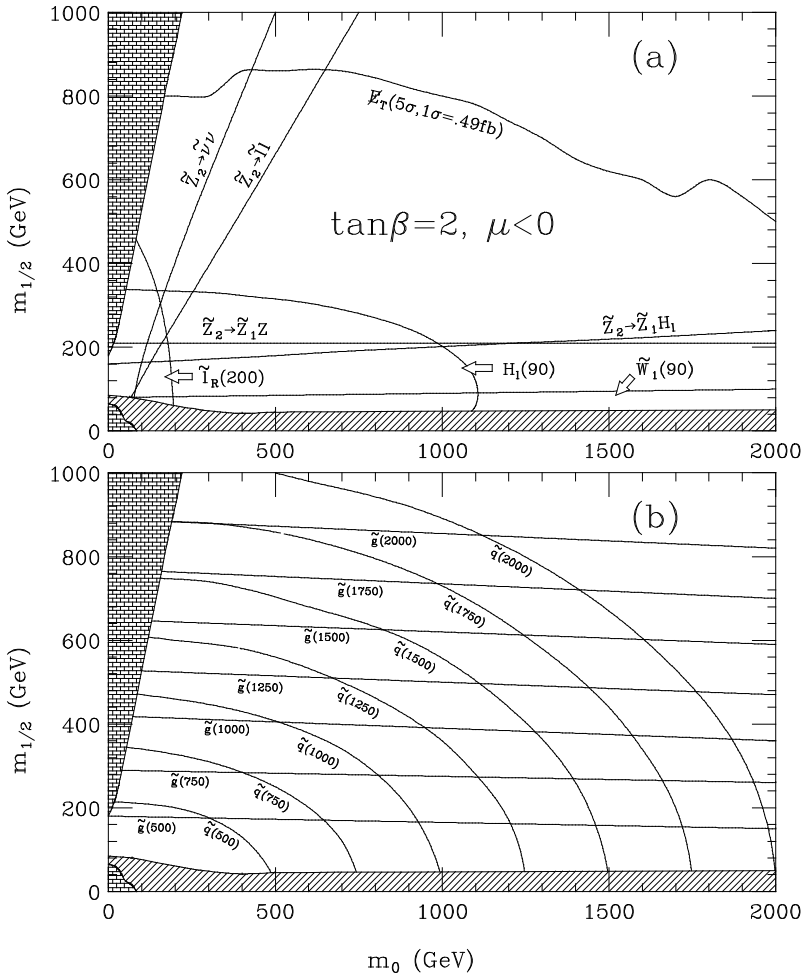

Figure 17: Contour in the m_0 *vs.* $m_{1/2}$ plane where the multi-jet $+\not{E}_T$ signal is observable above SM backgrounds.

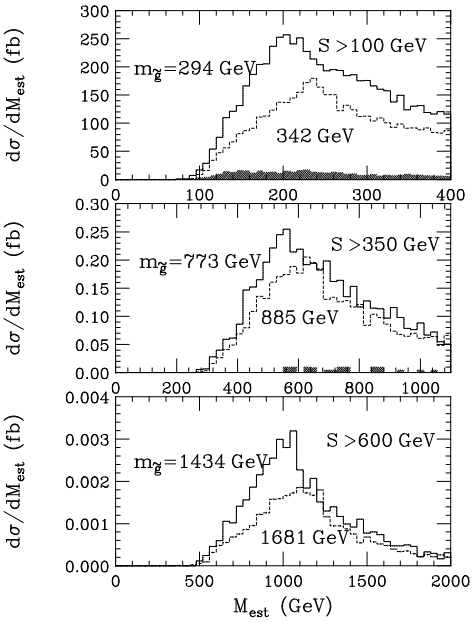

Figure 18: Distribution in M_{est} for various values of $m_{\tilde{g}}$ at the CERN LHC.

the mass distribution is a smear of values, with an end-point at $m_{\tilde{g}} - m_{\widetilde{\chi}_1^0}$. Realistic situations can only do worse. In Ref. [92], it was suggested to construct the mass value M_{est} (in the context of SS dilepton events) by a series of cuts designed to hemispherically separate the decay products of each gluino. This method suffers from the fact that it is difficult to obtain a reasonably pure sample of gluino dilepton events. Nonetheless, in Ref.[89] this technique has been pursued in the $\not{E}_T + jets$ channel, using ISAJET to simultaneously generate all sparticles. The procedure here is to divide the transverse plane into hemispheres using the transverse sphericity eigenvector, and then calculate the invariant mass of all hard jets in each hemisphere. The larger of the two values is taken to be M_{est}.

In Fig. 18, we show histograms of M_{est} for $\not{E}_T + jets$ events with the following cuts:

1. veto isolated leptons,
2. S_T (transverse sphericity) > 0.2,
3. $p_T(jet) > 100$ GeV,
4. $n(jets) \geq 2$,
5. $\not{E}_T > S$, and $p_T(jet_1, jet_2) > S$.

Then, M_{est} is calculated using only hard jets, with $p_T > S$. Events are rejected if there is only one qualifying jet in each hemisphere. In the figure, we take SUGRA

parameters $m_0 = m_{1/2}$, $A_0 = 0$, $\tan\beta = 2$, and $\mu < 0$. For these parameters, $m_{\tilde{q}} \sim m_{\tilde{g}}$. The corresponding values of $m_{\tilde{g}}$ are listed in the figure, as are background events from SM sources. We see that the distributions shown are able to distinguish $m_{\tilde{g}}$ to 15%. The resolution is somewhat worse if $m_0 = 4m_{1/2}$, but M_{est} distributions for gluino masses differing by 25% appear to be readily distinguishable. There is a wide spread of mass values in each plot, due to cascade decay effects, wrong jet assignments, QCD radiation, *etc.*. However, the overall trend is clear: heavier sparticles should give harder distributions of M_{est} values (or other measurable distributions), and so, may provide information on the underlying gluino and squark masses.

7.2 $\widetilde{\chi}_1^{\pm}\widetilde{\chi}_2^0 \to 3\ell$ signal

Can the clean tri-lepton signal from $pp \to \widetilde{\chi}_1^{\pm}\widetilde{\chi}_2^0 \to 3\ell + \not{E}_T$ be seen at the LHC as well as at the Tevatron? At first glance, this is unclear[80], since the signal cross section rises by typically a factor of ~ 10 in going from Tevatron to LHC, while background from $t\bar{t}$ production increases by a factor of ~ 160 (depending on m_t). Furthermore, there are additional sources of trilepton events from other SUSY reactions at LHC energy.

Detailed simulations of signal and background have been performed in Ref. [93]. In this work, a series of cuts were found that would allow for a clean extraction of the $\widetilde{\chi}_1^{\pm}\widetilde{\chi}_2^0 \to 3\ell + \not{E}_T$ signal. The procedure is to first establish the signal by requiring

- three isolated high p_T leptons.

After this requirement, the total event sample is dominated by *other* SUSY sources of trilepton events, which mainly come from gluino and squark cascade decays. To get rid of these, one requires

- no jets in the event, plus $\not{E}_T < 100$ GeV,

Then one is left with clean trilepton events, with large contamination from $WZ \to 3\ell + \not{E}_T$. After requiring a Z mass cut,

- for OS, same-flavor lepton pairs, $m(\ell\bar{\ell}) \neq M_Z \pm 8$ GeV,

the WZ contamination is reduces to tiny levels, but a significant background from $t\bar{t}$ may remain. Requiring either of the following conditions,

- two fastest leptons be SS and flavor of the slow lepton be the same (but anti-) the flavor of either of the two fast leptons, or
- two fastest leptons are OS if $p_T(slow\ lepton) > 20$ GeV,

leaves one with signals on the level of $10 - 40\ fb$, while SM background is below the fb level. Thus, at least for $\mu < 0$, the 3ℓ signal appears viable as long as the $\widetilde{\chi}_2^0$ spoiler modes are closed, *i.e.* $m_{\tilde{g}} \lesssim 550 - 650$ GeV. For positive values of

μ, a significant hole still remains in the $m_0 - m_{1/2}$ plane, even where the spoiler modes are not accessible[94]. The purity of the remaining event sample allows some detailed mass information to be extracted. For instance, in $\mu e\bar{e}$ events, the quantity $m(e\bar{e})$ is kinematically restricted to be less than $m_{\widetilde{\chi}_2^0} - m_{\widetilde{\chi}_1^0}$; thus a plot of the upper cutoff of this distribution can yield precise mass information on sparticles even in the difficult environment of an LHC detector. Other distributions can constrain different combinations of the chargino/neutralino masses[93].

7.3 Slepton search

The search for sleptons at the LHC has also been addressed in the literature[95, 84]. Detailed simulations of signals and backgrounds for *all* slepton production mechanisms including cascade decays were performed in Ref. [84]. There, it was shown that the only viable channel for observing a slepton pair signal was in the $2\ell + \not{E}_T$ channel, which usually comes from $\tilde{\ell}_R\bar{\tilde{\ell}}_R \to 2\ell + \not{E}_T$. By requiring events with two isolated leptons plus no jets, together with some additional angular cuts, a signal on the order of fb's could be seen for $m_{\tilde{\ell}} \lesssim 250$ GeV, against tiny backgrounds from SM and other SUSY sources. Extraction of any sort of detailed mass information from the small sample of remaining signal events appeared to be difficult.

8 Supersymmetry at future linear e^+e^- Colliders

A future linear e^+e^- collider will obviously have a higher discovery reach than LEP II, due to its higher center-of-mass energies, $\sqrt{s} = 0.5$–1 TeV. Furthermore, experimentation at a linear collider would be richer compared to that at LEP-II, due to the following characteristics: (1) flexible center-of-mass energies, (2) high beam polarization of 90% and beyond. It probably is not well known that the center-of-mass energy can be flexibly varied, for instance between 200 to 500 GeV within a single collider design. Upgrade to a higher energy machine (say up to 1 TeV) is possible either by making the accelerator longer or improving the acceleration gradient of the klystrons. Therefore, under most of the common designs, one single accelerator will be able to cover a wide range of center-of-mass energies. One can tune the center-of-mass energy for many different purposes. For instance, one can optimize the sensitivity on the slepton mass measurement by choosing the center-of-mass energy such that $\beta \simeq 0.5$ [24]; or one can avoid the complication due to simultaneous production of several sparticles by choosing the center-of-mass energy below one of the thresholds. The virtues of polarization are two-fold. (a) Use of polarization can suppress the background substantially even up to two orders of magnitudes. This allows us to obtain a very pure sample of signals appropriate for precision studies. (b) One basically doubles the number of experimental observables using both polarization states. This enables the efficient measurements of various parameters, which is proven already in the A_{LR} measurement at the SLD experiment.

In early days, beamstrahlung processes (emission of high intensity γ-rays due the interactions between beams at the collision point), which can smear the center-of-mass energy and produce large leptonic and hadronic underlying backgrounds from photon collision, had been a source of concern. This effect is negligible at LEP-II or SLC because of smaller energy and much larger beam size at the collision point. However, with improvements in accelerator designs and as well as in our understanding of photon structure function, it has been shown that beamstrahlung effects are not harmful for most of the interesting physics studies. One can achieve [96] (1) small beam energy spread even after including initial state radiation and beamstrahlung effects, and (2) a clean environment basically without underlying events even with photon induced hadronic processes.

Thus, all the virtues of lower energy e^+e^- colliders remain [97], while the high center-of-mass energy and beam polarization will give us additional tools to study physics. The goals of the e^+e^- linear collider experiment will be multiple: (1) discovery of sparticles, (2) measurement of SUSY parameters, (3) quantitative verification of supersymmetric invariance of the interactions.

It is also worth recalling here that an e^+e^- linear collider is also a Higgs discovery/study machine especially for supersymmetric models. As is well-known, the lightest neutral Higgs boson in MSSM is always lighter than $\lesssim 130$ GeV after including the radiative corrections due to the stop loop [98]. Even in models with additional singlets or extra families [99], an upper bound $\lesssim 160$ GeV persists under the assumption of perturbativity up to the GUT-scale. Furthermore, a reasonable size of production cross section is guaranteed for the lightest (or, sometimes, the second lightest if the lightest one is dominantly singlet) neutral Higgs boson even with the mixing to singlet states [100]. If we could further find other Higgs states via processes as $e^+e^- \to h^0Z^0$, H^0Z^0, h^0A^0, H^0A^0, or H^+H^-, it is a definite sign that the Higgs sector is beyond that in the minimal Standard Model. One can cover up to $m_A \simeq 200$ GeV with a 500 GeV collider [101].[13]

8.1 $\tilde{l}$-pair production

As before, we assume that one of the sleptons is LVSP in this subsection. We also assume R-parity is conserved, and LSP is the lightest neutralino. Then the only possible decay mode is $\tilde{l} \to l\tilde{\chi}_1^0$ assuming lepton family number conservation. The cross sections are shown in Fig. 19.

Here we summarize the analysis of Ref. [103]. One possible set of selection criteria is the following:[14]

1. $\theta_{acop} > 65^\circ$.

2. $\not{p}_T > 25$ GeV.

[13]Unfortunately, it is difficult to see the difference between the minimal Standard model and the MSSM if m_A is beyond the reach of the discovery at a given center-of-mass energy [102].

[14]See the footnote 4 for the definition of the acoplanarity.

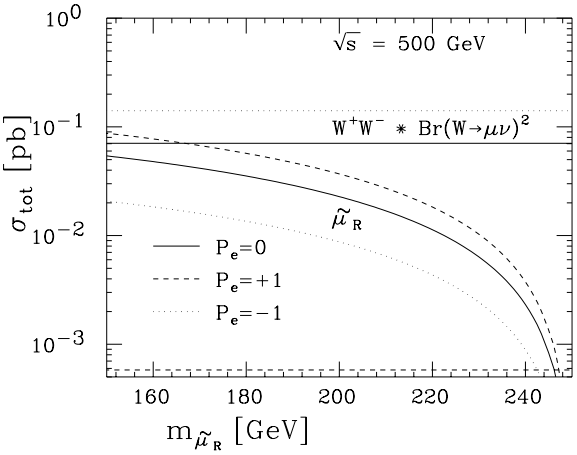

Figure 19: Total cross sections of $\tilde{\mu}_R$ pair production at $\sqrt{s} = 500$ GeV, for unpolarized $P_e = 0$ and polarized beams $P_e = \pm 1$. The backgrounds from W-pair is also shown.

3. The polar angle of one of the leptons should be larger than 46°, the other 26°.

4. $|m_{ll} - m_Z| > 10$ GeV.

5. $E_{l^\pm} < 150$ GeV.

The resulting signal and background cross sections, for $\sqrt{s} = 500$ GeV, are listed in Table 6. Here a relatively pessimistic (hard) beamstrahlung spectrum of the "Palmer-G" type is assumed. Conservative detector parameters are chosen: the tracking detector covers down to 15° with a momentum resolution $\Delta p_T/p_T = 1.5 \times 10^{-3} p_T(\text{GeV})$ and an angular resolution of 1 mrad. The EM calorimetry covers down to 11.5°, with $\Delta E/E = 0.17/\sqrt{E(\text{GeV})} + 0.03$.

Assuming a collider energy of $\sqrt{s} = 500$ GeV, and an integrated luminosity of 20 fb^{-1} (again conservative), a 5σ signal can be found up to 225 GeV, as long as the mass difference between the smuon and LSP is greater than 25 GeV.

For $\tilde{e}$, the production cross section is in general larger because of the additional diagram with t-channel exchange of neutralinos. The $e\nu_e W$ and eeZ final states are backgrounds to $\tilde{e}$-pair which are absent for $\tilde{\mu}$-pair. However with an additional cut $E_e > 15$ GeV, the backgrounds are reduced down to 2.0 fb (eeZ) and 1.7 fb ($e\nu_e W$). The discovery reach turns out to be even better than the $\tilde{\mu}$ case depending on the mass spectrum in the neutralino sector.

Even though the unpolarized beam is efficient enough for the discovery of sleptons, the background can be further suppressed to a negligible level using the polarized beam. This is useful for the precise measurements of the masses and cross sections. Since the right-handed electron does not couple to W, the diagram with t-channel neutrino exchange is absent, and hence the background from WW is greatly reduced. Then a slightly weaker set of cuts is sufficient [24]:

process	σ_{tot}(fb)	ϵ(%)	σ_{acc}(fb)
$\tilde{\mu}_R(150)$-pair	50	24	12
$\tilde{\mu}_R(200)$-pair	16	31	5
$\tilde{\mu}_R(230)$-pair	3	36	1
$\gamma\gamma \to \mu\mu$	7177.	0.0	0.0
$ee \to \gamma^*/Z^* \to \mu\mu$	608.	0.0	0.0
$\gamma\gamma \to \tau\tau \to \mu\mu + \nu$'s	215.	0.0	0.0
$ee \to \gamma^*/Z^* \to \mu\mu + \nu$'s	19.	0.0	0.0
$ee \to WW \to \mu\mu + \nu$'s	131	0.7	1.0
$\gamma\gamma \to WW \to \mu\mu + \nu$'s	3.4	17.6	0.6
total	8363.	0.02	1.8

Table 6: Cross sections and efficiencies for $\tilde{\mu}$-pair signals and standard model backgrounds [103] with an unpolarized beam. Relatively pessimistic bremsstrahlung spectrum is assumed. The LSP mass is $m_{\tilde{\chi}_1^0} = 100$ GeV.

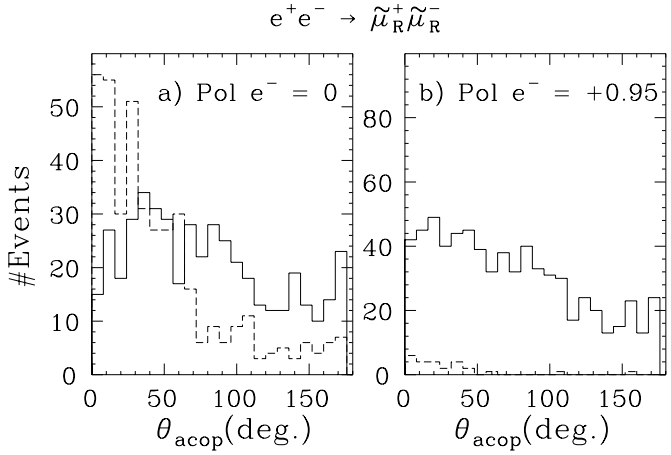

Figure 20: Acoplanarity distribution of lepton pair for $\sqrt{s} = 350$ GeV, $m_{\tilde{l}} = 142$ GeV, $\int \mathcal{L}dt = 20\,\mathrm{fb}^{-1}$. Fig. b) shows the dramatic reduction of the backgrounds using the right-handed electron beam.

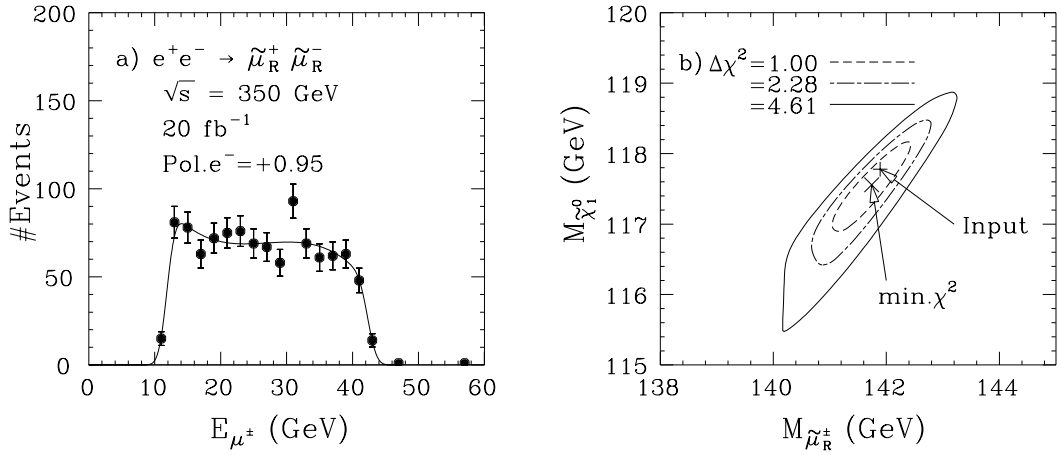

Figure 21: (a) Energy distribution of the final muon from $\tilde{\mu}_R$-pair production, including standard model backgrounds. (b) Two-parameter fit to the energy distribution on $(m_{\tilde{\mu}}, m_{\tilde{\chi}_1^0})$ plane.

1. 5 GeV $< E_\mu <$ ($\sqrt{s} - 100$ GeV)/2.
2. 20 GeV $< E_{vis} < \sqrt{s} - 100$ GeV.
3. $|m_{ll} - m_Z| > 10$ GeV.
4. $|\cos\theta_{l^\pm}| < 0.9$.
5. $-Q_l \cos\theta_l < 0.75$ where Q_l is the charge of the lepton and the polar angle is measured from the electron beam direction.
6. $\theta_{acop} > 30°$.

For a sample parameter $m_{\tilde{\mu}_R} = 142$ GeV, $m_{\tilde{\chi}_1^0} = 118$ GeV, $\sqrt{s} = 350$ GeV, and $\int dt\mathcal{L} = 20$ fb^{-1}, $P_e = 95\%$, one could obtain an event sample with signal purity at 99% and efficiency of 54.2% (Fig. 20). Given this pure signal samples, one can fit the energy distribution of the final leptons to measure masses of $\tilde{\mu}$ and $\tilde{\chi}_1^0$. The resolutions of mass determinations are better than 1% (Fig. 21).

It is worth noting that one can put an upper bound on the mass of charginos once one knows the mass of the LSP, assuming the GUT-relation for gauino masses [24]. Therefore, precision measurement on the masses will give us a useful clue to the next target center-of-mass energy. Comparing the cross sections from both right-handed and left-handed beams, one can test that the gauge quantum numbers of the observed $\tilde{\mu}_R$ is indeed the same as μ_R, which is a quantitative support that it is a superpartner of μ_R. Also, the angular distribution could tell us that the newly discovered particle is a scalar particle.

Another interesting study can be done once $\tilde{\tau}$-pairs are found [104]. Let us suppose for the moment that $\tilde{\tau}$ decays mainly into $\tau\tilde{\chi}_1^0$ to simplify discussions.

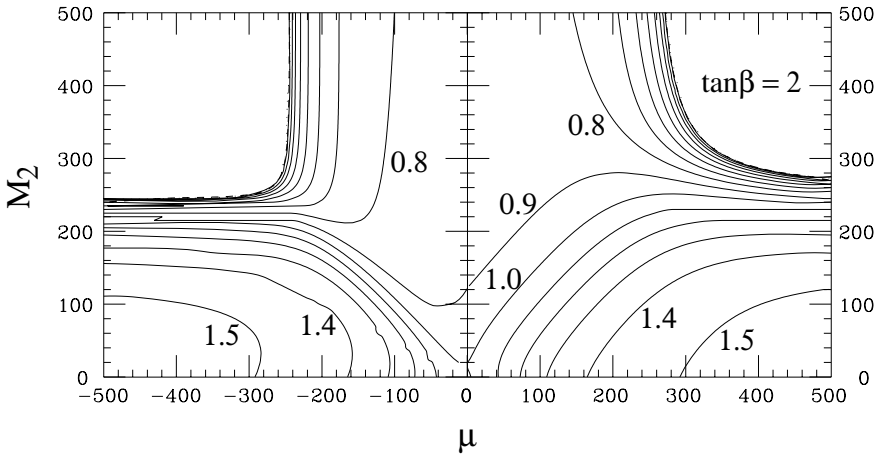

Figure 22: Contour of the total cross sections in pb of $\tilde{\chi}_1^\pm$ pair production from the left-handed electron beam at $\sqrt{s} = 500$ GeV, for $m_{\tilde{\nu}_e} = 1$ TeV. The kinematic limit is shown in dashed line, while the discovery reach at 20 fb^{-1} is shown in dotted line. They almost overlap with the contour of 0.1 fb.

The cross sections tell us whether the observed $\tilde{\tau}$ is either left- or right-handed (or their certain mixture). Also, the polarization of the final state tau leptons can, in principle, be measured with traditional methods: the easiest is the measurement of the energy distribution of the π from $\tau \to \pi\nu_\tau$. We might also use $\tau \to \rho\nu_\tau$ and $a_1\nu_\tau$ modes. Therefore, we can see whether the chirality of the final τ matches with the type (L or R) of the parent stau that was produced. If it does, the neutralino is dominantly gaugino-like; otherwise, it is higgsino-like. Indeed, the energy distribution of the π from $\tau \to \pi\nu_\tau$ is sensitive to the higgsino content of the $\tilde{\chi}_1^0$ [104].

8.2 $\tilde{\chi}_1^\pm$-pair production

Under the assumption that $\tilde{\chi}_1^\pm$ is the LVSP, it decays into $\tilde{\chi}_1^\pm \to \tilde{\chi}_1^0 f\bar{f}'$ where f, $\bar{f}'$ are light fermions in the standard model. The decay proceeds via (real or virtual) W-exchange, slepton- and squark-exchange. When W-exchange dominates, decays to various final states occur democratically, resulting in a branching fraction of 70% for hadronic modes and 10% for each of the leptonic modes. This is typical when the mass difference $\Delta m = m_{\tilde{\chi}_1^\pm} - m_{\tilde{\chi}_1^0}$ is larger than m_W where the decay into real W dominates. When the mass difference is smaller, the chargino decays directly into the three-body state. Branching ratios can vary as a function of slepton and squark masses just as the case at LEP-II. Both purely hadronic and mixed hadronic-leptonic mode of chargino pair can be used for the search.

The cross sections of the chargino pair are shown in Figs. 22,23,24. For the gaugino-dominant chargino, the cross section from the right-handed beam is very small. The t-channel $\tilde{\nu}_e$-exchange amplitude is destructive with the s-channel γ, Z-exchange amplitude, so that the cross section is reduced for lighter $\tilde{\nu}_e$. The

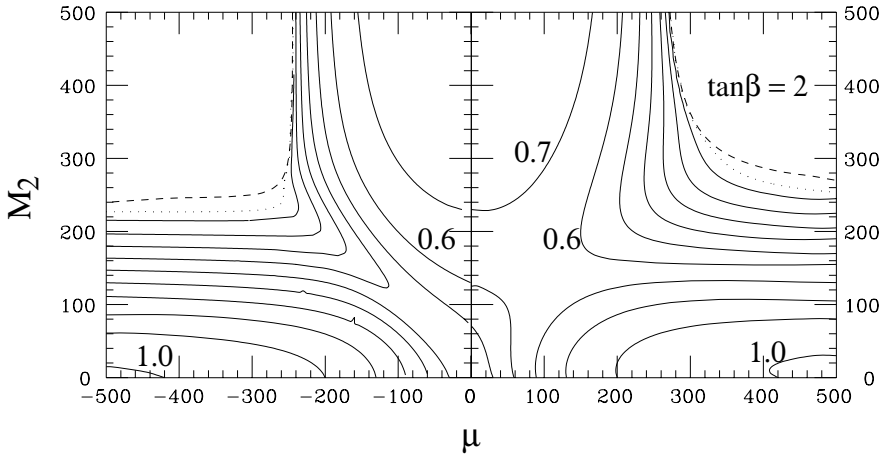

Figure 23: Contour of the total cross sections in pb of $\tilde{\chi}_1^{\pm}$ pair production from the left-handed electron beam at $\sqrt{s} = 500$ GeV, for $m_{\tilde{\nu}_e} = 250$ GeV. The kinematic limit is shown in dashed line, while the discovery reach at 20 fb^{-1} is shown in dotted line.

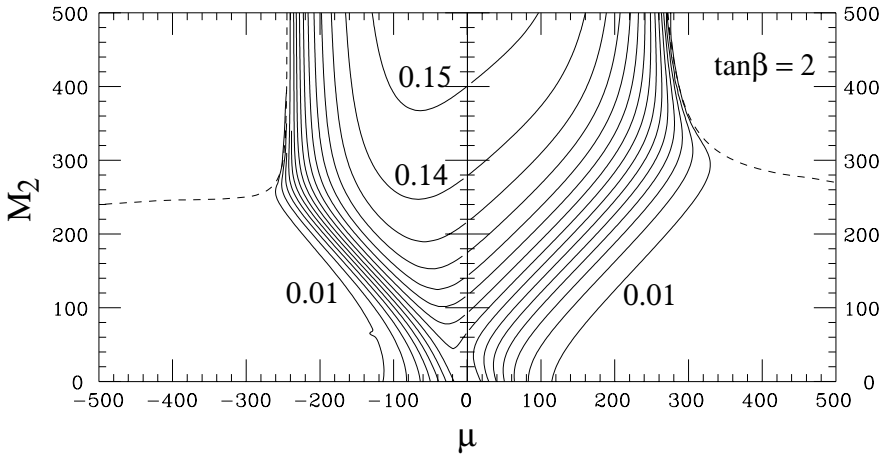

Figure 24: Contour of the total cross sections in pb of $\tilde{\chi}_1^{\pm}$ pair production from the right-handed electron beam at $\sqrt{s} = 500$ GeV. The kinematic limit is shown in dashed line.

higgsino-dominant chargino has reasonably large cross sections both from left- and right-handed beams.

The discovery is usually more efficient in purely hadronic mode because of the higher branching ratios. The W-pair background with one W decaying into quarks and the other into τ is much less severe at linear collider energies than at LEP-II because two W's are well separated in the phase space. One possible set of selection criteria for the purely hadronic mode at $\sqrt{s} = 500$ GeV is the following [105]:

1. number of tracks > 5.
2. The polar angle of the sphericity axis $> 45°$.
3. $\not{p}_T > 35$ GeV.
4. $\theta_{acop} > 30°$.
5. No one single charged particle which carries more than 70% of the total energy in the hemisphere.
6. 120 GeV $< m_{vis} <$ 220 GeV.
7. transverse missing mass > 200 GeV.

This set has an advantage that one can look for purely hadronic mode of chargino pair production when we do not know whether the decay is into a real W or three-body state. A conservative assumption is made on the detector capabilities: tracking resolution of $\Delta p_T/p_T = 1.5 \times 10^{-3} p_T/\text{GeV}$, ECAL (HCAL) resolutions of $0.17/\sqrt{E} + 0.03$ ($0.80/\sqrt{E}$) with E in GeV, and coverage of detectors to 18° (10°) for tracking detector (calorimeters).

A sample parameter $M_2 = 200$ GeV, $\mu = -325$ GeV, $\tan\beta = 4$, gives a signal cross section after cuts 63 fb (efficiency is 13%) while the background level is 7.5 fb. Assuming the integrated luminosity of $\int dt\mathcal{L} = 20$ fb^{-1}, 5σ signal can be obtained up to $m_{\tilde{\chi}_1^\pm} \simeq 248$ GeV, very close to the kinematic limit. The mixed hadronic-leptonic mode typically gives an efficiency of 2% and S/N $\simeq 1$, and not useful for discovery purpose.

Figs. 22,23 show the discovery reach of the chargino pair at $\sqrt{s} = 500$ GeV and $\int dt\mathcal{L} = 20$ fb^{-1}. The only region which is difficult to cover is the very pure higgsino region $M_2 \gg \mu$, where the mass of the chargino and LSP become nearly degenerate. In this region the decay $\tilde{\chi}_1^\pm \to \tilde{\chi}_1^0 f \bar{f}'$ has a small Q-value, and hence visible energy is small. There is no quantitative study so far on the discovery reach for small mass difference. It was estimated that, with an unpolarized beam, the charginos may evade discovery if the mass difference is smaller than $\Delta m < 20$ GeV [105].[15]

[15]However, one can use right-handed beam to reduce the background substantially while the signal cross section decreases only by a factor of three. Probably one can do a much better job. More study is necessary on this point. The higgsino LSP does not occur in the minimal supergravity, but may occur in extended scenarios [28].

Once one has found charginos, and seen whether the decay is into the real W or three-body state, one can find much more efficient cuts to reduce the background for a precision study. When the decay is into the real W and the LSP, then acoplanar W-pair with large missing energy is the signal. One can identify W's from di-jet invariant masses and requirement of large missing energy and acoplanarity reduces most of the backgrounds. Since the decay is two-body, the end points in the energy distribution of W (sum of two jet energies which form an invariant mass close to m_W) tell us the mass of both the chargino and the LSP. Therefore, this case is relatively easy.[16] When the decay is directly into the three-body state, the measurement is more complicated. We will discuss this case in detail below.

We now turn to the measurement of the chargino and LSP masses from the di-jet energy distribution. We assume three-body decay, and we do not want to use pure hadronic mode in order to avoid combination ambiguities of jets as the decay product of one chargino. We employ the mixed hadronic-leptonic mode below. For charginos with mixed hadronic-leptonic mode without real W, a possible set of selection criteria is:

1. number of tracks > 5, incl. isolated e or μ ($E_l > 5$ GeV, energy deposited within half-angle 30° cone less than 1 GeV).
2. 20 GeV $< E_{vis} < \sqrt{s} - 100$ GeV.
3. two jets with $y_{cut} > 5 \times 10^{-3}$, $m_{jj} < m_W - 12$ GeV, $E_{jj} < (\sqrt{s} - 100\ GeV)/2$.
4. $|\cos\theta_j| < 0.9$, $|\cos\theta_l| < 0.9$, $-Q_l \cos\theta_l < 0.75$, $Q_l \cos\theta_{jj} < 0.75$.
5. $|m_{l\nu} - m_W| > 10$ GeV for W-pair hypothesis.
6. $\theta_{acop} > 30°$ where acoplanarity angle is defined between the summed momentum of two jets and lepton momentum.

As an example, consider a sample parameter set $M_2 = 400$ GeV, $\mu = 250$ GeV, $\tan\beta = 2$, in the limit of heavy scalar masses. The chargino and LSP masses are 219 GeV and 169 GeV, respectively, and the final signal cross section is 234 fb (efficiency 10%) with the background from W-pair 37 fb and $e\nu W$ 6.6 fb. The efficiency and S/N ratio are at the comparable level we had for the purely hadronic mode above. The fit to the di-jet energy spectrum yields the mass determination at the 1% level (Fig. 25).[17]

[16] An exception is when the chargino is gaugino-like and $\tilde{\nu}_e$ is light so that the cross section is low. Then one needs relatively high luminosity of $\int dt\mathcal{L} \simeq 50$ fb^{-1} to achieve the 10% resolution in chargino and LSP masses. Fortunately, there are light sleptons in this case, so that one can measure LSP mass also from slepton study. Using constraint on the LSP mass, the resolution on the chargino mass can be still as good as 5%.

[17] The resolution of the jet energy measurements is crucial here. We tried to link tracks of the charged particles detected in the central drift chamber to energy clusters detected in the electromagnetic calorimeter or hadron calorimeter, and, when linked, we used the tracking information, since it has better resolution in general. To be realistic in this linking process, we generated calorimeter hits with a finite shower size and simulated the cluster overlapping [72, 24].

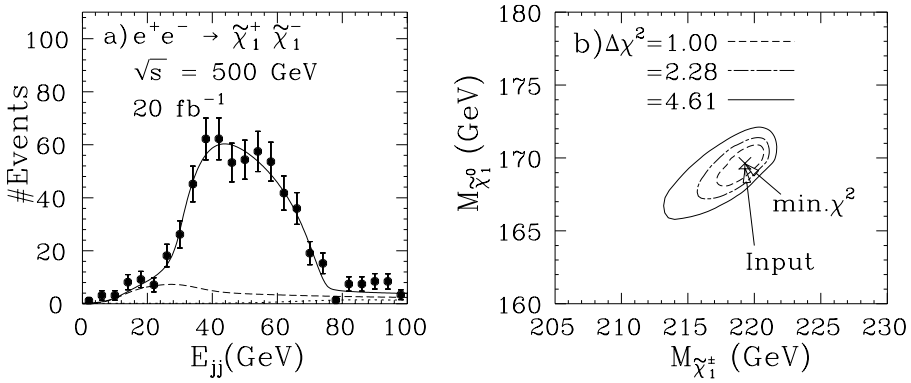

Figure 25: (a) Di-jet energy distribution from chargino pair production, (b) contour on the masses of chargino and LSP from a fit of the di-jet energy distribution.

8.3 Systematic Discoveries and Tests on GUT or Supergravity Models

A nice feature of the study of sparticles at an e^+e^- collider and measurement of masses is that one can place an upper bound on the next sparticle based on modest theoretical assumptions. Furthermore, having several sparticles at hand allows us to test various predictions of the GUT or SUGRA models at the several percent level.

Suppose the right-handed sleptons are the LVSPs. Knowing the masses of $\tilde{\mu}_R$ and $\tilde{e}_R$, one can test the universality of the scalar masses better than 1%, which is an assumption of minimal supergravity framework. The mass of the LSP is also measured better than 1%. If one assumes the GUT-relation for gaugino masses, one can put an upper bound on the mass of the chargino $m_{\tilde{\chi}_1^\pm} \lesssim 2m_{\tilde{\chi}_1^0}$ (Fig. 26) and similarly for the second neutralino. Therefore, we obtain an idea on the next target center-of-mass energy. If we will not discover chargino below that mass, at least a GUT with minimal particle content will be excluded.

If a chargino is the LVSP, we measure cross sections both from left-handed and right-handed beams, and the masses of the chargino and LSP. Using $m_{\tilde{\chi}_1^\pm}$, $m_{\tilde{\chi}_1^0}$ and the cross section from the right-handed beam, one can perform a three-dimensional fit on $(M_2, \mu, \tan\beta)$ space. Here, the GUT-relation of the gaugino masses is assumed. Then, we can predict the masses of other charginos and neutralinos. The obvious limitation of this fit is we effectively lose information on μ (M_2) when the chargino is gaugino-rich (higgsino-rich). However in the higgsino-rich case, we expect another neutralino nearby which should be discovered not too far above the chargino threshold. In the gaugino-rich case, one can extract the mass of the $\tilde{\nu}_e$ exchanged in the t-channel from the cross section from the left-handed beam. Since the mass of $\tilde{\nu}_e$ is related to the mass of $\tilde{e}_L$ by $m^2_{\tilde{e}_L} = m^2_{\tilde{\nu}_e} - m_Z^2 \cos^2\theta_W \cos 2\beta \leq m^2_{\tilde{\nu}_e} + 0.77 m_Z^2$, one can place an upper bound on the mass of $\tilde{e}_L$. Therefore, in both cases one obtains some information on the

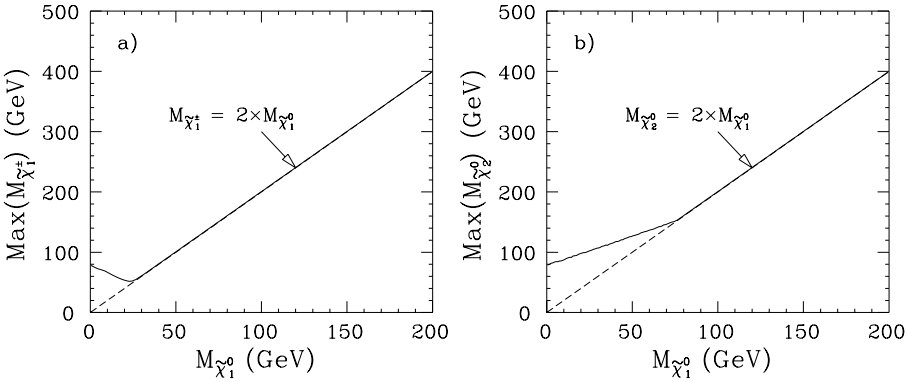

Figure 26: Upper bound on the chargino $\tilde{\chi}_1^\pm$ and second neutralino $\tilde{\chi}_2^0$ masses as a function of LSP mass $m_{\tilde{\chi}_1^0}$, assuming the GUT-relation for gaugino masses $M_2 \simeq 2.0 \times M_1$.

next sparticle mass.

If several sparticles are found, stringent tests on theoretical assumptions can be made. One sample case is the following [24]. Take the SUGRA parameters $m_0 = 70$ GeV, $M_2 = 250$ GeV, $\mu = 400$ GeV and $\tan\beta = 2$, which is in a cosmologically interesting region. The low-lying sparticle spectrum is:

$$\begin{aligned} \tilde{\chi}_1^0 &: \ 117.8 \text{ GeV}, \\ \tilde{l}_R &: \ 141.9 \text{ GeV}, \\ \tilde{\chi}_1^\pm &: \ 219.3 \text{ GeV}, \\ \tilde{\chi}_2^0 &: \ 221.5 \text{ GeV}, \\ \tilde{\nu}_L &: \ 227.2 \text{ GeV}, \\ \tilde{l}_L^\pm &: \ 235.5 \text{ GeV}. \end{aligned} \tag{16}$$

Then the right-handed sleptons are found first, and one can infer an upper bound on the chargino mass as discussed above. Once the chargino is found, one can use the following four physical observables to constrain the chargino and neutralino sectors:

The mass of LSP.
The mass of chargino.
The slepton production cross section from the right-handed beam.
The chargino production cross section from the right-handed beam.

Since there are four observables, a global fit on the four-dimensional space (M_1,M_2,μ,$\tan\beta$) is possible without assuming the GUT-relation $M_1/M_2 = (5/3)\tan^2\theta_W$. Then the result gives us an experimental test on the GUT-relation. For the above parameter set, the test is possible at 3% level, as seen in Fig. 27. Once the chargino and neutralino parameters are known, the chargino production cross section from the left-handed beam tells us the mass of $\tilde{\nu}_e$ (Fig. 28). Also the comparison between $\tilde{l}_R$ and $\tilde{l}_L$ masses allows us to extract the difference of their masses at the GUT-scale.

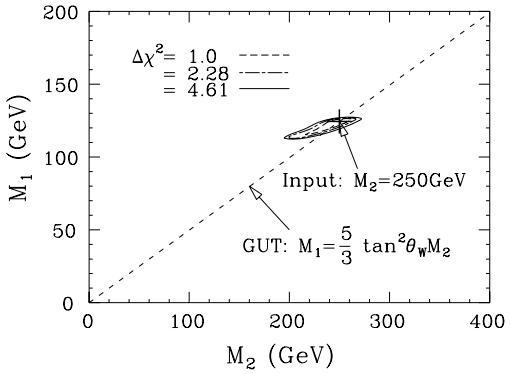

Figure 27: Test of the GUT-relation of the gaugino masses. The contours are obtained by a four-dimensional fit on $(M_1, M_2, \mu, \tan\beta)$.

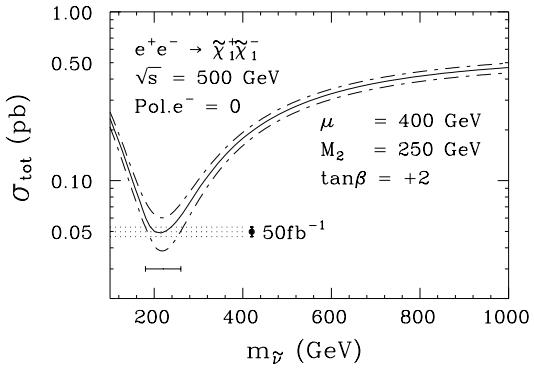

Figure 28: Extracting the mass of $\tilde{\nu}_e$ from the chargino production cross section, after measuring $(M_1, M_2, \mu, \tan\beta)$ from the global fit in the previous figure.

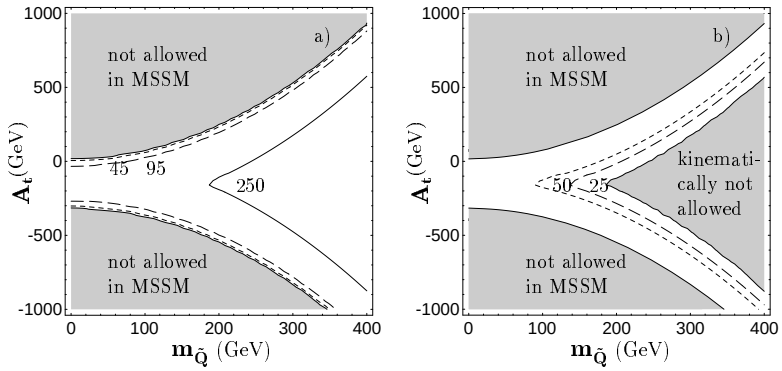

Figure 29: Contours of a) constant masses of the lightest stop (in GeV), and b) constant cross sections of $e^+e^- \to \tilde{t}_1\tilde{t}_1$ (in fb) as a function of $m_{\tilde{Q}}$ and A_t for $\tan\beta = 2$ and $\mu = -300$ GeV in the Minimal Supersymmetric Standard Model (MSSM). Masses of squark doublet and right-handed stop are assumed to be the same. In a), the kinematic production limits of $e^+e^- \to \tilde{t}_1\tilde{t}_1$ are given for LEP1, LEP2 (with $\sqrt{s} = 190$ GeV), and the future e^+e^- linear collider (with $\sqrt{s} = 500$ GeV). In b), the contours are given for 25 and 50 fb, which correspond approximately to the expected experimental sensitivity at $\sqrt{s} = 500$ GeV and $\int \mathcal{L}dt = 10$ fb^{-1}.

8.4 Other sparticles and higher order processes

The third generation squarks $\tilde{t}$, $\tilde{b}$ deserve a special attention, since they are probably the lightest among the squarks and hence the most likely candidate for the first signal of squarks at an e^+e^- collider. Also they have a mixing between left right states which is unique to the third generation squarks. They offer possibilities of measuring A-parameters, if μ and $\tan\beta$ are measured from neutrino, chargino or Higgs sectors. The dependence of masses and cross sections on A-parameters and m_Q are shown in Figs 29,30 for stop and sbottom production. For instance, knowing the masses of $\tilde{t}_1$, $\tilde{t}_2$ from the processes $\tilde{t}_1$-pair and $\tilde{t}_1\tilde{t}_2$ associated production, and their cross sections overdetermine the stop 2×2 mass matrix.

The search for and study of first- and second-generation squarks was discussed in [106], assuming degenerate masses for left-handed and right-handed squarks separately. It was shown that squark mass measurement at a few GeV level is possible even in the presence of cascade decays using the kinematic fits. Here again the beam polarization plays a crucial role to disentangle left- and right-handed squarks.

Higher order signal processes (three-body final states) have not been studied in enough detail for future linear e^+e^- colliders. One can look for final states like $\tilde{e}e\tilde{\chi}_1^0$, $\tilde{\nu}\tilde{\nu}^*\gamma$, $\tilde{\chi}_1^\pm\tilde{\nu}e^\mp$ to extend the discovery reach beyond that using the pair production processes. The main backgrounds are processes with t-channel exchange of the gauge bosons such as $ee\gamma$, $e\nu_e W$, $e\nu WZ$ and $eeWW$ final states with or without additional high p_T photons which become increasingly important at higher energies.

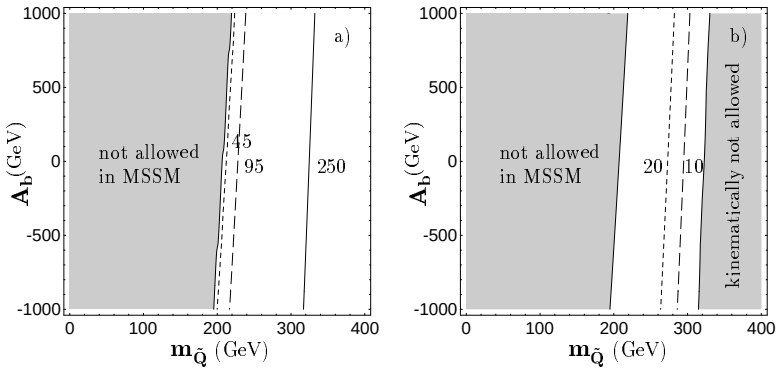

Figure 30: Contours of a) constant masses of the lightest sbottom (in GeV), and b) constant cross sections of $e^+e^- \to \tilde{b}_1\tilde{b}_1$ (in fb) as a function of $m_{\tilde{Q}}$ and A_b for $\tan\beta = 30$ and $\mu = -300$ GeV in the Minimal Supersymmetric Standard Model (MSSM). Masses of squark doublet and right-handed sbottom are assumed to be the same. In a), the kinematic production limits of $e^+e^- \to \tilde{b}_1\tilde{b}_1$ are given for LEP1, LEP2 (with $\sqrt{s} = 190$ GeV), and the future e^+e^- linear collider (with $\sqrt{s} = 500$ GeV). In b), the contours are given for 10 and 20 fb, which correspond approximately to the expected experimental sensitivity at $\sqrt{s} = 500$ GeV and $\int \mathcal{L}dt = 10$ fb^{-1}.

More work is necessary here. (See, however, [107]).

8.5 Quantitative verification of supersymmetry

In this subsection we discuss how one can test whether the new particles are indeed sparticles whose interactions are restricted by the supersymmetric Lagrangian. The measurements of parameters discussed above are based on the *assumption* that the newly discovered particles are sparticles, and we used supersymmetric Lagrangian to analyze the experimental data. Here we relax this assumption and try to test the supersymmetric invariance of the Lagrangian experimentally.

We assume that the chargino $\tilde{\chi}_1^\pm$ is the LVSP. Suppose the chargino is gaugino-rich, *i.e.*, almost a pure wino $\tilde{W}$. Then, assuming SUSY, its coupling g_χ to the electron and scalar neutrino is fixed to be the same as the $SU(2)_L$ gauge coupling g even if SUSY is spontaneously broken. We study whether this equality can be experimentally tested.

First of all, the chargino production cross section from the right-handed electron beam should nearly vanish in this limit. Therefore, we first learn, directly from experiment, that the hypercharge of the new particle is zero. Below we assume that it belongs to $SU(2)_L$ triplet as $\tilde{W}$ does. Then the s-channel amplitudes of γ- and Z-exchange are fixed completely by the gauge invariance. For the production of charginos from the left-handed electron beam, there is another diagram where

$\tilde{\nu}_e$ is exchanged in the t-channel, with a factor

$$\frac{g_\chi^2}{t - m_{\tilde{\nu}_e}^2} \tag{17}$$

in the amplitude. If $m_{\tilde{\nu}_e}$ is not too large, one can extract both g_χ and $m_{\tilde{\nu}_e}$ from the angular distribution of the charginos.

A sample case was studied in Ref. [108], with the following parameter set

$$(\mu, M_2, \tan\beta, M_1/M_2, m_{\tilde{\nu}_e}) = (-500, 170, 4, 0.5, 400). \tag{18}$$

In this case the MSSM gives

$$\begin{aligned} m_{\tilde{\chi}_1^\pm} &= 172 \text{ GeV}, \\ m_{\tilde{\chi}_1^0} &= 86 \text{ GeV}, \\ \sigma_R &= 0.15 \text{ fb}, \\ \sigma_L &= 612 \text{ fb}, \\ (\phi_+, \phi_-) &= (1.2^\circ, 12.8^\circ). \end{aligned}$$

Here σ_R, σ_L are the production cross sections from right-handed and left-handed electron beams, respectively. The angles (ϕ_+, ϕ_-) are the mixing angle for left- and right-handed charginos. Since the chargino $\tilde{\chi}_1^\pm$ decays into real W and LSP in this case, the branching ratios are known. Therefore the total cross section can be determined independently from the other SUSY parameters. The angular distribution of the chargino cannot be determined directly due to its decay. For the mixed hadronic-leptonic mode, one can use the forward-backward asymmetry of the W instead, where the charge of the W is determined by the lepton from the other chargino. The cuts are the same as the one used above for the chargino-pair decaying into the real W. Because of the asymmetric cut in the forward and backward region, the asymmetry is defined by

$$A^{had} = \frac{\sigma_L(0 < \cos\theta < 0.707) - \sigma_L(-1 < \cos\theta < 0)}{\sigma_L(-1 < \cos\theta < 0.707)}, \tag{19}$$

where the polar angle θ is that of the reconstructed W. This observable is strongly correlated with the corresponding asymmetry of the chargino polar angle A^χ. With an integrated luminosity of 100 fb^{-1} with the left-handed electron beam, one can measure the asymmetry as

$$A^\chi = 0.20 \pm 0.049, \tag{20}$$

and the cross section as

$$\frac{\Delta\sigma}{\sigma} = 5.6\%. \tag{21}$$

Given four experimental observables, the mass of the chargino $m_{\tilde{\chi}_1^\pm}$, the LSP mass $m_{\tilde{\chi}_1^0}$, the total cross section and the asymmetry, one can determine the region on the space $(m_{\tilde{\nu}_e}, g_\chi/g)$ which reproduce the data, as shown in Fig. 31. Since the measurements determine the parameters to lie in one of the two shaded regions of Fig. 31, we see that the equality of g_χ and g, and hence SUSY, may be tested to within 25%. For further details, and a test for SUSY when the chargino is a mixed gaugino-Higgsino state, we refer the reader to Ref.[108].

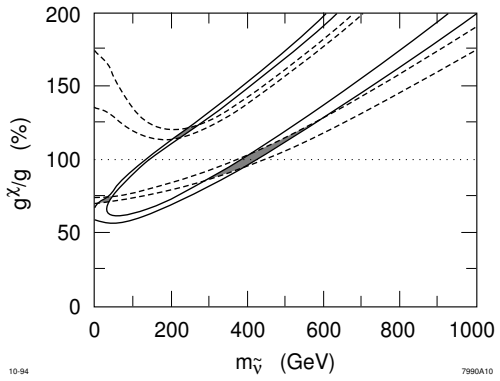

Figure 31: Allowed region (shaded) of the $(m_{\tilde{\nu}}, g^\chi)$ plane for the integrated luminosity 100 fb^{-1}. Solid (dashed) curves are contours of constant σ_L (A^χ) that bound the allowed regions. On the dotted lines, the SUSY relation $g^\chi = g$ is satisfied.

8.6 $\gamma\gamma$, $e\gamma$, e^-e^- options

The e^+e^- linear colliders have also options to operate as $\gamma\gamma$, $e\gamma$ or e^-e^- colliders. The discussion of each mode in this subsection is rather qualitative because full studies with realistic detectors have not been done. It is only meant to survey the advantages and disadvantages of each option.

There is a claim that $\gamma\gamma$ or $e\gamma$ colliders can achieve higher luminosity than e^+e^- colliders because of the absence of beam-beam interaction, *i.e.*, beamstrahlung [109]. Another advantage of $\gamma\gamma$ mode is that the scalar pair production occurs in S-wave, such that the threshold behavior of the cross section is $\propto \beta$ rather than β^3 at an e^+e^- collider. Also the production cross section is democratic, *i.e.*, it only depends on the electric charge of the sparticles. Disadvantages of $\gamma\gamma$ option is that the W-pair cross section is high $\simeq 100$ pb and stays constant above the threshold, and that the center-of-mass energy of $\gamma\gamma$ collision has a spread of $> O(10)\%$. The highest center-of-mass energy is 80% of the corresponding e^+e^- collider.

The search for sleptons has been discussed for $\gamma\gamma$ option, and is well possible even in the presence of large W-pair background [110]. For a case $m_{\tilde{l}} - m_{\tilde{\chi}^0_1} > 50$ GeV, one can even almost completely eliminate the W-pair background by requiring $p_T(l^\pm) > 50$ GeV and $\theta_{acop} > 90^\circ$, maintaining a reasonable efficiency $\sim 10\%$ for the signal. The measurement of the slepton mass is worse than e^+e^- case due to the energy spread of the backscattered γ-beam, but still possible at 5% level [111]. The discovery reach is more or less the same as the e^+e^- option, since it gains by S-wave production, but loses by the lower center of mass energy.

Chargino search at $\gamma\gamma$ colliders is more difficult than at e^+e^- colliders. For instance, when charginos decay into real $W + \tilde{\chi}^0_1$, acoplanar W-pair with large $\not{p}_T$ is the signature. However, given large W-pair cross section, there is still a long tail in missing p_T distribution from $WW\gamma$ production where γ escapes into the beam pipe [112]. More thorough study is necessary.

An interesting advantage of $e\gamma$ option is that it has higher reach than e^+e^-,

$\gamma\gamma$ modes on the search for a scalar electron.[18] One can produce $e\gamma \to \tilde{e}\tilde{\chi}_1^0$, and the kinematic reach is limited by $m_{\tilde{e}} + m_{\tilde{\chi}_1^0}$ rather than $2m_{\tilde{e}}$ [113]. The signature is a single lepton with a large angle and missing p_T. The most severe background is $e^-\gamma \to \nu_e W^-$, which can be suppressed by employing a right-handed electron beam. The kinematic suppression is only β, and a search is possible roughly up to the kinematic limit. Other sparticles are not easy to produce in this option, mainly only via effective $\gamma\gamma$ collision from t-channel γ-exchange, and hence the cross section is down by another factor of α.

At an e^-e^- collider, one can produce $\tilde{e}_{L,R}^-, \tilde{e}_{L,R}^-$ by t-channel neutralino exchange [114]. An advantage is the absence of W-pair background, and one can accumulate a very pure sample of selectron signals both with right- and left-handed beams. To avoid W-pair backgrounds at an e^+e^- collider, the use the right-handed electron beams was preferred for the precision studies. For the studies of the neutralino sector using selectron production, this choice of the right-handed electron beam drops the information on the wino component in the neutralino sector. At e^-e^- colliders, one can study $\tilde{e}_L^-\tilde{e}_L^-$ production with both the electron beams left-handed, and extract information on the wino component in the neutralino sector. Therefore this option could be used to study sleptons and neutralino sector further once discovered at the e^+e^- option [115].

9 Overview and complementarity of facilities

Here, we summarize our results for the SUSY reach of various hadron collider options (the reach of e^+e^- colliders is essentially the beam energy for most sparticles). Finally, we emphasize the complementarity of the hadron and e^+e^- collider options for a complete study of supersymmetry.

9.1 Comparison of Hadron Collider options

Our main results for the SUSY reach of various hadron collider options are summarized in Table 7. These have generally been obtained within the minimal supergravity framework, or using MSSM parameter values motivated by supergravity.

For the $\not{E}_T$ signal at the Tevatron and its upgrade options, we present two sets of numbers corresponding to the analysis of two different groups. The higher number is obtained from the study by Kamon *et. al.*[76], where it is assumed that the signal is observable using a "5σ" criterion; *i.e.* if the number of signal events (N_S) exceeds $5\sqrt{N_B}$, N_B being the number of background events. To extend the reach to large values of squark and gluino mass, these authors use a relatively hard cut $\not{E}_T \geq 150$ GeV. They argue that the background dominantly comes from $Z \to \nu\bar{\nu} + jet$ events and (conservatively) take the total background to be 5 times the Z background. Their analysis includes a detailed simulation of the CDF detector. The second number for the Tevatron $\not{E}_T$ reach in Table 7 is obtained

[18] However, the luminosity in this mode may be limited to avoid the beam-induced e^+e^- pair background.

Table 7: Estimates of the discovery reach of various options of future hadron colliders. The signals have mainly been computed for negative values of μ. We expect that the reach in especially the $all \to 3\ell$ channel will be sensitive to the sign of μ.

Signal	Tevatron II 0.1 fb^{-1} 1.8 TeV	Main Injector 1 fb^{-1} 2 TeV	Tevatron* 10 fb^{-1} 2 TeV	DiTevatron 1 fb^{-1} 4 TeV	LHC 10 fb^{-1} 14 TeV
$\not\!\!E_T(\tilde{q} \gg \tilde{g})$	$\tilde{g}(210)/\tilde{g}(185)$	$\tilde{g}(270)/\tilde{g}(200)$	$\tilde{g}(340)/\tilde{g}(200)$	$\tilde{g}(450)/\tilde{g}(300)$	$\tilde{g}(1300)$
$l^{\pm}l^{\pm}(\tilde{q} \gg \tilde{g})$	$\tilde{g}(160)$	$\tilde{g}(210)$	$\tilde{g}(270)$	$\tilde{g}(320)$	
$all \to 3l\ (\tilde{q} \gg \tilde{g})$	$\tilde{g}(180)$	$\tilde{g}(260)$	$\tilde{g}(430)$	$\tilde{g}(320)$	
$\not\!\!E_T(\tilde{q} \sim \tilde{g})$	$\tilde{g}(300)/\tilde{g}(245)$	$\tilde{g}(350)/\tilde{g}(265)$	$\tilde{g}(400)/\tilde{g}(265)$	$\tilde{g}(580)/\tilde{g}(470)$	$\tilde{g}(2000)$
$l^{\pm}l^{\pm}(\tilde{q} \sim \tilde{g})$	$\tilde{g}(180-230)$	$\tilde{g}(320-325)$	$\tilde{g}(385-405)$	$\tilde{g}(460)$	$\tilde{g}(1000)$
$all \to 3l\ (\tilde{q} \sim \tilde{g})$	$\tilde{g}(240-290)$	$\tilde{g}(425-440)$	$\tilde{g}(550^*)$	$\tilde{g}(550^*)$	$\gtrsim \tilde{g}(1000)$
$\tilde{t}_1 \to c\widetilde{\chi}_1^0$	$\tilde{t}_1$(80–100)	$\tilde{t}_1(120)$			
$\tilde{t}_1 \to b\widetilde{\chi}_1^{\pm}$	$\tilde{t}_1$(80–100)	$\tilde{t}_1(120)$			
$\Theta(\tilde{t}_1\tilde{t}_1^*) \to \gamma\gamma$	—	—	—	—	$\tilde{t}_1(250)$
$\tilde{\ell}\tilde{\ell}^*$	$\tilde{\ell}(50)$	$\tilde{\ell}(50)$	$\tilde{\ell}(50)$		$\tilde{\ell}$(250–300)

in Ref. [52] using ISAJET to simultaneously generate all sparticles, but with softer jet and $\not\!\!E_T$ ($\not\!\!E_T \geq 75$ GeV) requirements. These authors have estimated backgrounds from W, Z and $t\bar{t}$ production but have used a toy calorimeter for detector simulation.

A major difference from Ref.[76] is the criteria used to obtain the reach. Since there are systematic uncertainties, both theoretical (*e.g.* from higher order QCD corrections) as well as numerical (from simplifications in the simulations), in the computation of the backgrounds, Ref. [52] considers a signal to be observable if the signal satisfies $\sigma(signal) \geq 0.25\sigma(background)$ *in addition to* the 5σ criterion introduced above. Because we are considering very large integrated luminosities, this difference is important for signals with large SM backgrounds: for instance, a signal cross section of 200 fb (which yields 5K events with an integrated luminosity of 25 fb^{-1}), which would be observable over a background of 40 pb with just the 5σ criterion, but not with the additional (and somewhat arbitrary) requirement, $\frac{N_S}{N_B} \geq 0.25$. We should also mention that no attempt has been made to optimize the cuts in Ref.[52], and that it may be possible to further enhance the reach by using harder cuts as in Ref. [76].

For the reach in the SS dilepton and $all \to 3\ell$ channels, we have shown the numbers from the SUGRA analysis (with $\mu < 0$) of Ref. [52, 83]. For the high luminosity upgrades of the Tevatron, the reach in the trilepton channel is dominantly governed by the relatively clean event sample from $\widetilde{\chi}_1^{\pm}\widetilde{\chi}_2^0$ production since the production of squarks and gluinos is kinematically suppressed. For positive values of μ the reach will be governed by $\not\!\!E_T$ and SS dilepton events from gluino production and will, presumably, be somewhat smaller.

The following comments about Table 7 are worth noting:

- Given 10pb^{-1} of integrated luminosity (Tevatron run IA), the highest reach

in $m_{\tilde{g}}$ is attained via the multi-jet+$\not\!\!E_T$ channel. The rate limited SS and multilepton signals, which will have a significant reach by the end of Tevatron run IB, yield the maximum reach at the Main Injector and TeV^* upgrades of the Tevatron. Within the assumed framework, the reach in the clean trilepton channel from $\widetilde{\chi}_1^{\pm}\widetilde{\chi}_2^0$ production is comparable to that of multileptons if $\mu < 0$. For positive values of μ the branching fraction for the leptonic decay of $\widetilde{\chi}_2^0$, and consequently, the trilepton signal may be strongly suppressed.

- For the proposed DiTevatron $p\bar{p}$ collider, the reach in $m_{\tilde{g}}$ via the multi-jet+$\not\!\!E_T$ channel may be superior to the reach via multi-lepton channels. We quote DiTevatron reach values for only one value of integrated luminosity. If substantially higher luminosities can be achieved, then the reach in many of the channels can be significantly increased.

- At the TeV^* and at the DiTevatron, the hadronically quiet trilepton events may be observable all the way up to the spoiler, but only for some ranges of parameters — in particular, this is sensitive to the sign of μ because the leptonic branching fractions of $\widetilde{\chi}_2^0$ are considerably larger for $\mu < 0$ as compared to $\mu > 0$. The SS dilepton signal from gluinos and squarks is also somewhat suppressed for positive values of μ because $m_{\widetilde{\chi}_1^{\pm}} - m_{\widetilde{\chi}_1^0}$ tends to be smaller than in the $\mu < 0$ case, reducing the efficiency for passing the experimental cuts.

- The analysis of the LHC working group[91] has shown that the LHC can detect gluinos and squarks well beyond 1 TeV in the $\not\!\!E_T$ channel, and up to ~ 2 TeV if $m_{\tilde{q}} = m_{\tilde{g}}$. The SS and trilepton channels also have a reach of about 1 TeV, so that such events,which should be detected simultaneously with $\not\!\!E_T$ events should provide spectacular evidence for gluino and squark production.

- At the LHC, the reach of the clean trilepton signal from $\widetilde{\chi}_1^{\pm}\widetilde{\chi}_2^0$ production extends up to where the spoiler decay modes of $\widetilde{\chi}_2^0$ become accessible for negative values of μ. If $\mu > 0$, the signals are readily observable for rather small and very large values of the SUGRA parameter m_0; there are, however, significant regions ($m_0 = 400-100$ GeV) where this signal may be suppressed. It is also worth emphasizing that because it is possible to obtain a very clean sample of $\widetilde{\chi}_1^{\pm}\widetilde{\chi}_2^0$ events, it should be possible to reliably reconstruct $m_{\widetilde{\chi}_2^0} - m_{\widetilde{\chi}_1^0}$ (and, perhaps, also some other combinations of masses)[93] at the LHC. This may also be possible at the TeV^*, but will require the machine and detectors to perform at their limits.

- The Tevatron and its Main Injector upgrade should be able to search for $\tilde{t}_1$ up to, or just beyond about 100 GeV, regardless of whether these decay via the tree-level chargino mode or via the loop decay $\tilde{t}_1 \to c\widetilde{\chi}_1^0$[20]. Signals for yet heavier stops ($m_{\tilde{t}_1} \geq 150$ GeV) which could have other kinematically allowed decays are under investigation. It has also been pointed out, assuming that

$\tilde{t}_1 \to c\tilde{\chi}_1^0$ is the dominant decay mode of $\tilde{t}_1$, that it should be possible[116] to search for it at the LHC via two photon decays of its scalar bound state in much the same way that Higgs bosons are searched for. With an integrated luminosity of 100 fb^{-1}, the reach in this channel has been estimated to be $m_{\tilde{t}_1} \lesssim 250$ GeV.

- Finally, it appears that even the TeV^* will not probe sleptons significantly beyond the reach of LEP. The corresponding reach for the LHC is about 250 GeV[84]. The analysis for slepton signals at the DiTevatron has not been performed, but expectations are pessimistic.

9.2 Complementarity between e^+e^- and hadron colliders

At the LHC, supersymmetric events will, in general, manifest themselves via complicated cascades of heavy sparticles, resulting in relatively spectacular $\not{E}_T$ and multilepton signatures for SUSY. A number of complementary signals ought to be detectable. While the observation of such events will unequivocally signal the existence of New Physics, it will probably be difficult to unravel the complicated cascades in the rather messy environment of the hadron collider. Especially, it will not be easy (except in some cases such as $\widetilde{\chi}_1^{\pm}\widetilde{\chi}_2^0$ trilepton signal) to sort out the sources of various signals or do sparticle spectroscopy. In contrast, at a 500 GeV e^+e^- collider, where only relatively light sparticles will be kinematically accessible, the decay cascades will likely be less complicated or even absent. Note, however, that if gaugino masses have a common origin as in a GUT, a reach of about 250 GeV in the chargino mass is equivalent to a reach of $\sim 700 - 800$ GeV in $m_{\tilde{g}}$. We have also seen that these machines offer the prospects of precision measurements of masses, spins and, in some cases, also couplings of sparticles. Such measurements, which are generally difficult at hadron colliders, not only serve as the most direct tests of supersymmetry, but may also yield information about physics at very high energy scales.

It is also interesting to ask how the information about, say, chargino couplings and masses learned from e^+e^- experiments can be used to sort out the cascade decays seen at the LHC. If the turn-on of the future e^+e^- linear collider occurs significantly after the LHC becomes operational, it will be important to appropriately archive the raw data from LHC experiments for subsequent reanalysis in light of new knowledge from the future e^+e^- linear collider . This interplay between e^+e^- and pp collider analyses highlights yet another sense in which these two facilities are complementary.

10 Conclusions

We have seen that if low energy supersymmetry is the physics that stabilizes the electroweak scale, the supersymmetric partners of ordinary particles will, in many cases, almost certainly be detectable at the LHC or the future e^+e^- linear colliders,

but only if we are lucky, at the Tevatron or at LEP II. Although this is not the subject of this report, it is worth stressing that supercolliders are also capable of searching for a variety of other New Physics that Nature may have chosen to adopt. While the Tevatron upgrades that we have considered probe substantial ranges of SUSY parameters, they do not yield observable signals over what is generally accepted as the complete range of these parameters. Supercolliders appear to be essential both for a complete exploration of the parameter space as well as for the elucidation of any New Physics that might be discovered. Finally, we cannot overstress the complementary nature of e^+e^- and hadron supercollider if supersymmetry is indeed present at the weak scale. Experiments at these facilities will together not only lead to unambiguous discovery of sparticles, but will allow a comprehensive study of their properties, which in turn, may yield information about physics at ultra-high energy scales.

11 Acknowledgements

We thank Manuel Drees and Howie Haber for a critical reading of the manuscript, and for valuable comments. This work was supported in part by the U.S. Department of Energy under contract number DE-FG05-87ER40319, DE-AC03-76SF00098 and DE-FG-03-94ER40833.

References

[1] See chapter by M. Drees and S. Martin on *Supersymmetry: Model Building* (this volume).

[2] Y. Golfand and E Likhtman, JETP Lett. **13**, 323 (1971); D. Volkov and V. Akulov, Phys. Lett. **46B**, 109 (1973); J. Wess and B. Zumino, Nucl. Phys. **B70**, 39 (1974).

[3] R. Haag, J. Lopuszanski and M. Sohnius, Nucl. Phys. **B88**, 61 (1975).

[4] D. Freedman, S. Ferrara and P. van Nieuwenhuizen, Phys. Rev. **D13**, 3214 (1976); S. Deser and B. Zumino, Phys. Lett. **B62**, 335 (1976); D. Freedman and P. van Nieuwenhuizen, Phys. Rev. **D14**, 912 (1976)

[5] *Superstring Theory*, M. Green, J. Schwarz and E. Witten, Cambridge University Press (1987).

[6] E. Witten, Nucl. Phys. **B188**, 513 (1981); S. Dimopoulos and H. Georgi, Nucl. Phys. **B193**, 150 (1981); N. Sakai, Z. Phys. **C11**, 153 (1981); R. Kaul, Phys. Lett. **B109**, 19 (1982).

[7] S. Olsen, *Plenary talk at the 8th DPF meeting, Albuquerque, NM, August 1994.*

[8] U. Amaldi, W. de Boer and H. Fürstenau, Phys. Lett. **B260**, 447 (1991); J. Ellis, S. Kelley and D. Nanopoulos, Phys. Lett. **B260**, 131 (1991); P. Langacker and M. Luo, Phys. Rev. **D44**, 817 (1991).

[9] For phenomenological reviews of SUSY, see H. P. Nilles, Phys. Rep. **110**, 1 (1984); H. Haber and G. Kane, Phys. Rep. **117**, 75 (1985); X. Tata, in *The Standard Model and Beyond*, p. 304, edited by J. E. Kim, World Scientific (1991); R. Arnowitt and P. Nath, *Lectures presented at the VII J. A. Swieca Summer School, Campos do Jordao, Brazil, 1993* CTP-TAMU-52/93; *Properties of SUSY Particles*, L. Cifarelli and V. Khoze, Editors, World Scientific (1993).

[10] S. Wolfram, Phys. Lett. **B82**, 65 (1979); C. B. Dover, T. Gaisser and G. Steigman, Phys. Rev. Lett. **42**, 1117 (1979).

[11] P. F. Smith *et. al.* Nucl. Phys. **B149**, 525 (1979) and **B206**, 333 (1982); E. Norman *et. al.* Phys. Rev. Lett. **58**, 1403 (1987).

[12] L. Girardello and M. Grisaru, Nucl. Phys. **B194**, 65 (1982).

[13] K. Inoue, A. Kakuto, H. Komatsu and H. Takeshita, Prog. Theor. Phys. **68**, 927 (1982) and **71**, 413 (1984).

[14] L. Ibañez and G. Ross, Phys. Lett. **B110**, 215 (1982); L. Ibañez, Phys. Lett. **B118**, 73 (1982); J. Ellis, D. Nanopoulos and K. Tamvakis, Phys. Lett. **B121**, 123 (1983); L. Alvarez-Gaumé, J. Polchinski and M. Wise, Nucl. Phys. **B221**, 495 (1983).

[15] The assumption of minimal kinetic energy terms is crucial for obtaining universal scalar masses. Since the Lagrangian for supergravity is non-renormalizable, this really is an additional assumption. See *e.g.* S. K. Soni and H. A. Weldon Phys. Lett. **B126**, 215 (1983).

[16] B. Campbell, Phys. Rev. **D28**, 209 (1983); F. Gabbiani and A. Masiero, Nucl. Phys. **B322**, 235 (1989).

[17] We mention that while degenerate squarks are sufficient to suppress flavour changing neutral currents to acceptable levels, there are other means of doing so. For instance, if squark and quark matrices are essentially aligned due to an assumed symmetry at the scale M_X, flavour changing neutral currents are also sufficiently suppressed. See Y. Nir and N. Seiberg, Phys. Lett. **309B**, 337 (1993).

[18] J. Ellis and S. Rudaz, Phys. Lett. **B128**, 248 (1983).

[19] H. Baer, M. Drees, R. Godbole, J. Gunion and X. Tata, Phys. Rev. **D44**, 725 (1991); T. Kon and T. Nonaka, Phys. Lett. **B319**, 355 (1993) and Phys. Rev. **D50**, 6005 (1994); J. Wells, C. Kolda and G. Kane, Phys. Lett. **338B**, 219

(1994); J. Lopez, D. Nanopoulos and A. Zichichi, CERN preprint CERN-TH 7296/94 (1994) (hep-ph/9406254); see also Ref. [20].

[20] H. Baer, J. Sender and X. Tata, Phys. Rev. **D50**, 4517 (1994).

[21] H. Baer and X. Tata, Phys. Rev. **D47**, 2739 (1993); H. Baer, C. Kao and X. Tata, Phys. Rev. **D48**, 5175 (1993).

[22] H. Goldberg, Phys. Rev. Lett. **50**, 1419 (1983); J. Ellis, K. Olive, D. Nanopoulos, J. Hagelin and M. Srednicki, Nucl. Phys. **B328**, 453 (1984). For a more recent discussion in the context of minimal supergravity, see *e.g* M. Drees and M. Nojiri, Phys. Rev. **D47**, 376 (1993).

[23] Some recent analyses of supergravity mass patterns include, G. Ross and R. G. Roberts, Nucl. Phys. **B377**, 571 (1992); R. Arnowitt and P. Nath, Phys. Rev. Lett. **69**, 725 (1992); M. Drees and M. M. Nojiri, Nucl. Phys. **B369**, 54 (1993); S. Kelley, J. Lopez, D. Nanopoulos, H. Pois and K. Yuan, Nucl. Phys. **B398**, 3 (1993); M. Olechowski and S. Pokorski, Nucl. Phys. **B404**, 590 (1993); V. Barger, M. Berger and P. Ohmann, *ibid.* **49**, 4908 (1994); G. Kane, C. Kolda, L. Roszkowski and J. Wells, Phys. Rev. **D49**, 6173 (1994); D. J. Castaño, E. Piard and P. Ramond, Phys. Rev. **D49**, 4882 (1994); W. de Boer, R. Ehret and D. Kazakov, Karlsruhe preprint, IEKP-KA/94-05 (1994); H. Baer, C. H. Chen, R. Munroe, F. Paige and X.Tata, Phys. Rev. **D51**, 1046 (1995).

[24] T. Tsukamoto, K. Fujii, H. Murayama, M. Yamaguchi and Y. Okada, KEK preprint 93-146 (1993), to appear in Phys. Rev. **D**.

[25] J. Lopez, D. Nanopoulos, G. Park, X. Wang and A. Zichichi, Phys. Rev. **D50**, 2164 (1994); H. Baer, M. Drees, C. Kao, M. Nojiri and X. Tata, Phys. Rev. **D50**, 2148 (1994).

[26] See H. Baer, C-H. Chen, R. Munroe, F. Paige and X. Tata, Ref. [23].

[27] V. Kaplunovsky and J. Louis, Phys. Lett. **B306**, 269 (1993); A. Brignole, L. Ibanez and C. Muñoz, Nucl. Phys. **B422**, 125 (1994).

[28] Y. Kawamura, H. Murayama, and M. Yamaguchi, *Phys. Rev.* **D51**, 1337 (1995); M. Olechowski and S. Pokorski, Phys. Lett. **B344**, 201 (1995).

[29] See *e.g.*, J. Lopez, D. Nanopoulos and A. Zichichi, Phys. Lett. **B319**, 451 (1993) and Phys. Rev. **D49**, 343 (1994).

[30] See *e.g.* J. Ellis, J. Gunion, H. Haber, L. Roszkowski and F. Zwirner, Phys. Rev. **D39**, 844 (1989) and J. Hewett and T. Rizzo, Phys. Rep. **183**, 193 (1989).

[31] C. S. Aulakh and R. N. Mohapatra, Phys. Lett. **B119**, 316 (1982); L. J. Hall and M. Suzuki, Nucl. Phys. **B231**, 419 (1984); S. Dawson, Nucl. Phys. **B261**, 297 (1985); S. Dimopoulos and L. Hall, Phys. Lett. **B207**, 210 (1987); L. Hall, Mod. Phys. Lett. **A5**, 467 (1990).

[32] H. Baer, X. Tata and J. Woodside, Phys. Rev. **D45**, 142 (1992); H. Baer, M. Bisset, X. Tata and J. Woodside, Phys. Rev. **D46**, 303 (1992); The Solenoidal Detector Collaboration Technical Design Report; GEM Collaboration, Technical Design Report; Report of the Supersymmetry Working Group in Proceedings of the *Large Hadron Collider Workshop*, Aachen, October 1990, CERN90-10; F. Pauss, *ibid*; H. Baer *et. al.* in *Research Directions for the Decade*, E. Berger, Editor (World Scientific, 1992).

[33] S. Martin and M. Vaughn, Phys. Lett. **B318**, 331 (1993).

[34] See JLC Group Report, "JLC-1", KEK Report 92-16 (1992); C. Ahn *et. al.* SLAC Report SLAC-329 (1988).

[35] D. Amedei *et. al*, *Plenary talk at the 8th DPF meeting, Albuquerque, NM, August 1994*, Fermilab-Conf-94/249 (1994).

[36] See *e.g.* H. Baer, M. Drees and X. Tata, Phys. Rev. **D41**, 3414 (1990).

[37] H. Baer *et. al.*, Phys. Lett. **B161**,175 (1985); G. Gamberini. Z. Phys. **C30**, 605 (1986); H. Baer, V. Barger, D. Karatas and X. Tata, Phys. Rev. **D36**, 96 (1987); G. Gamberini, G. Giudice, B. Mele and G. Ridolfi, Phys. Lett. **203B**, 453 (1988); R. M. Barnett, J. Gunion and H. Haber, Phys. Rev. **D37**, 1892 (1988); A. Bartl, W. Majerotto, B. Mosslacher and N. Oshimo, Z. Phys. **C52**, 477 (1991).

[38] F. Paige and S. Protopopescu, in *Supercollider Physics*, p. 41, ed. D. Soper (World Scientific, 1986); H. Baer, F. Paige, S. Protopopescu and X. Tata, in *Proceedings of the Workshop on Physics at Current Accelerators and Supercolliders*, ed. J. Hewett, A. White and D. Zeppenfeld, (Argonne National Laboratory, 1993).

[39] J. Botts *et. al.*, Phys. Lett. **B304**, 159 (1993)

[40] H. Baer, A. Bartl, D. Karatas, W. Majerotto and X. Tata, Int. J. Mod. Phys. **A4**, 4111 (1989).

[41] S. Katsanevas and S. Melachroinos, SUSYGEN.

[42] A. Bartl, H. Fraas and W. Majerotto, Z.Phys. **C30**, 411 (1986), Z.Phys. **C41**, 475 (1988) and Nucl. Phys. **B278**, 1 (1986); A. Bartl, H. Fraas, W. Majerotto and B. Mosslacher, Z. Phys. **C55**, 257 (1992).

[43] See, for example, J.L. Feng and M.J. Strassler, SLAC-PUB-6497, hep-ph/9408359; see also Ref.[24].

[44] HELAS: HELicity Amplitude Subroutines for Feynman Diagram Evaluations, H. Murayama, I. Watanabe, K. Hagiwara, KEK-91-11, Jan 1992. 184pp.

[45] Particle Data Group, Phys. Rev. **D50**, 1173 (1994).

[46] J. Ellis, G. Ridolfi and F. Zwirner, Phys. Lett. **B237**, 423 (1990); A. Sopczak, CERN-PPE-94-188, Nov. (1994).

[47] D. Decamp *et.al.* (ALEPH Collaboration), Phys. Rep. **216**, 253 (1992); P. Abreu *et.al.* (DELPHI Collaboration), Phys. Lett. **B247**, 157 (1990); O. Adriani *et.al.* (L3 Collaboration), Phys. Rep. **236**,1 (1993); M. Akrawy *et.al.* (OPAL Collaboration), Phys. Lett **B240**, 261 (1990); for a review, see G. Giacomelli and P. Giacomelli, Riv. Nuovo Cim. **16**, 1 (1993).

[48] D. Decamp *et.al.* (ALEPH Collaboration) Ref.[47] and Phys. Lett. **B244**, 541 (1990); P. Abreu *et. al.* (DELPHI Collaboration) Phys. Lett. **B247**, 157 (1990); M. Akrawy *et.al.* (OPAL Collaboration) Phys. Lett. **B248**, 211 (1990).

[49] M. Paterno, Ph.D. thesis; D. Claes (D0 Collaboration), *presented at the 8th DPF meeting, Albuquerque, NM, Aug. 1994.*

[50] F. Abe *et. al.* (CDF Collaboration), Phys. Rev. Lett. **69**, 3439 (1992).

[51] H. Baer, X. Tata and J. Woodside, Phys. Rev. **D41**, 906 (1990); H. Baer, C. Kao and X. Tata, Phys. Rev. **D48**, R2978 (1993).

[52] H. Baer, C. Kao and X. Tata, Phys. Rev. **D51**, 2180 (1995).

[53] R. Arnowitt and P. Nath, Phys. Rev. Lett. **69**, 725 (1992); J. Hisano, H. Murayama and T. Yanagida, Nucl. Phys. **B402**, 46 (1993); J. Lopez, D. Nanopoulos and H. Pois, Phys. Rev. **D47**, 2468 (1993).

[54] The literature on this is vast. See *e.g.* M. Dugan, B. Grinstein and L. Hall, Nucl. Phys. **B255**, 413 (1985).

[55] Y. Kizukuri and N. Oshimo, Phys. Rev. **D46**, 3025 (1992), and references therein.

[56] S. Dimopoulos and L. Hall, Phys. Lett. **B344**, 185 (1995).

[57] R. Barbieri, C. Bouchiat, A. Georges, P. Le Doussal, *Nucl. Phys.* **B269**, 253 (1986).

[58] For instance, contribution of the squark-gluino vertex correction to the total hadronic width was discussed in K. Hagiwara and H. Murayama, Phys. Lett. **B246**, 533 (1990).

[59] See for example, M. Drees, K. Hagiwara and A. Yamada, Phys. Rev. **D45**, 1725 (1992).

[60] M. Boulware and D. Finnell, Phys. Rev. **D44**, 2054 (1991).

[61] J. Wells, C. Kolda and G. Kane, Phys. Lett. **B338**, 219 (1994).

[62] G. Altarelli, CERN-TH.7464/94.

[63] B. Barish, *et al.*, Presented at the *Int. Conf. on High Energy Physics, Glasgow, Scotland, Jul 20-26, 1994* CLEO-CONF-94-1 (1994)

[64] S. Bertolini, F. Borzumati, A. Masiero and G. Ridolfi, Nucl. Phys. **B353**, 591 (1991). For a recent studies, see M. Diaz, Phys. Lett. **B304**, 278 (1993); F. Borzumati, M. Drees and M. Nojiri, Phys. Rev. **D51**, 341 (1995); J. Lopez *et. al.* Phys. Rev. **D51**, 147 (1995); V. Barger *et. al.*, Phys. Rev. **D51**, 2438 (1995); R. Arnowitt and P. Nath, Phys. Lett. **B336**, 395 (1994).

[65] N. Deshpande *et. al.*, Phys. Rev. Lett. **59**, 183 (1987); S. Bertolini *et. al.*, Phys. Rev. Lett. **59**, 180 (1987); B. Grinstein *et. al.* Nucl. Phys. **B339**, 269 (1989); R. Grigjanis *et. al.* Phys. Lett. **B224**, 209 (1989); G. Cella *et. al.* Phys. Lett. **B325**, 227 (1994); M. Ciucini *et. al.* Phys. Lett. **334B**, 137 (1994).

[66] H. Anlauf, Nucl. Phys. **B340**, 245 (1994).

[67] A. J. Buras, M. Misiak, M. Münz and S. Pokorski, Nucl. Phys. **B424**, 374 (1994).

[68] C. Dionisi *et al.*, in ECFA Workshop on LEP 200 (Aachen, 1987), CERN 87-08, Vol. II, p. 380.

[69] M. Chen, C. Dionisi, M. Martinez, and X. Tata, *Phys. Rep.* **159**, 201 (1988).

[70] J. L. Feng and M. J. Strassler, Ref.[43]; N. Oshimo and Y. Kizukuri, *Phys. Lett.* **186B**, 217 (1987).

[71] J.-F. Grivaz, in Proceedings of the 23rd Workshop of the INFN Eloisatron Project, *eds.* L. Cifarelli and V.A. Khoze, World Scientific, 1993, p. 131.

[72] A. Miyamoto, in Proceedings of the Second Workshop on Japan Linear Collider (JLC), KEK, Nov. 6–8, 1990, edited by S. Kawabata, KEK Proceedings 91-10, Nov. 1991, p. 256.

[73] H. Baer, M. Brhlik, R. Munroe and X. Tata, FSU-HEP-950401 (in preparation).

[74] K. Hikasa and M. Kobayashi, Phys. Rev. **D36**, 724 (1987).

[75] A. Datta, A. Datta, and S. Raychaudhuri, DO-TH 94/25, hep-ph/9411435.

[76] T. Kamon, J. Lopez, P. McIntyre and J. T. White, Phys. Rev. **D50**, 5676 (1994).

[77] D. Dicus, S. Nandi and X. Tata, Phys. Lett. **B129**, 451 (1983); A. Chamseddine, P. Nath and R. Arnowitt, Phys. Lett. **B129**, 445 (1983).

[78] H. Baer and X. Tata, Phys. Lett. **B155**, 278 (1985); H. Baer, K. Hagiwara and X. Tata, Phys. Rev. Lett. **57**, 294 (1986) and Phys. Rev. **D35**, 1598 (1987).

[79] R. Arnowitt and P. Nath, Mod. Phys. Lett. **A2**, 331 (1987).

[80] R. Barbieri, F. Caravaglios, M. Frigeni and M. Mangano, Nucl. Phys. **B367**, 28 (1993).

[81] J. Lopez, D. Nanopoulos, X. Wang and A. Zichichi, Phys. Rev. **D48**, 2062 (1993) and CERN-TH.7535/94; J. Lopez, D. Nanopoulos, G. Park, X. Wang and A. Zichichi, Phys. Rev.**D50**, 2164 (1994)

[82] J. Wells, in *SUSY 94*, p. 553, edited by C. Kolda and J. Wells (U. of Michigan press UM-TH-94-35), 1994; see also talks by G. Kane at *Workshop on Future Facilities at FNAL*, Ann Arbor, October 1994 and talk at *Beyond the Standard Model IV* meeting, Lake Tahoe, 1994.

[83] H. Baer, C-H. Chen, C. Kao and X. Tata, FSU-HEP-950301 (1995).

[84] H. Baer, C-H. Chen, F. Paige and X. Tata, Phys. Rev. **D49**, 3283 (1994).

[85] I. Antoniadis, J. Ellis, S. Kelley and D. Nanopoulos, Phys. Lett. **B272**, 31 (1991); S. Kelly, J. Lopez and D. Nanopoulos, Phys. Lett. **B278**, 140 (1992); S. Kelly, J. Lopez, D. Nanopoulos, H. Pois and K. Yuan, Nucl. Phys. **B398**, 3 (1993).

[86] H. Baer, J. Gunion, C. Kao and H. Pois, Phys. Rev. **D51**, 2159 (1995).

[87] V. Barger, M. Berger, P. Ohmann and R. J. N. Phillips, Phys. Rev. **D50**, 4299 (1994).

[88] H. Baer, X. Tata and J. Woodside, Ref.[32].

[89] H. Baer, C-H. Chen, F. Paige and X. Tata, FSU-HEP-950204 (1995).

[90] See the Technical Design Reports of the GEM and SDC Collaborations.

[91] ATLAS Collaboration, Letter of Intent, CERN/LHCC/92-4 (1992). The values of the reach shown in Table 5 are in agreement with the updated numbers in the ATLAS Technical proposal, CERN/LHCC 94-3.

[92] R. M. Barnett, J. Gunion and H. Haber, Phys. Lett. **B315**, 349 (1993).

[93] H. Baer, C-H. Chen, F. Paige and X. Tata, Phys. Rev. **D50**, 4508 (1994).

[94] H. Baer, C-H. Chen, F. Paige and X. Tata, work in progress.

[95] F. del Aguila and Ll. Ametller, Phys. Lett. **B261**, 326 (1991).

[96] P. Chen, T.L. Barklow, and M.E. Peskin, Phys. Rev. **D49**, 3209 (1994).

[97] See also the earlier studies in *Proceedings of Workshop on Physics at Future Accelerators*, La Thuile, Italy and Geneva, Switzerland, Jan 7-13, 1987, Edited by J.H. Mulvey, CERN-87-07, 1987;
C. Ahn *et al*, "Opportunities and Requirements for Experimentation at a Very High-Energy e^+e^- Collider", SLAC-0329 (1988);
H. Baer, A. Bartl, D. Karatas, W. Majerotto, and X. Tata, *Int. J. Mod. Phys.* **A4**, 4111 (1989);
Report of the Supersymmetry Working Group in Proc. of the Workshop on e+ e- Collisions at 500 GeV: The Physics Potential, DESY 92-123B, p. 601, DESY 93-123C, p. 437, ed. P.M. Zerwas.

[98] Y. Okada, M. Yamaguchi, T. Yanagida, *Prog. Theor. Phys.* **85**, 1 (1991);
J. Ellis, G. Ridolfi, and F. Zwirner, *Phys. Lett.* **B257**, 83 (1991);
H.E. Haber, R. Hempfling, *Phys. Rev. Lett.* **66**, 1815 (1991).
See also, J. Rosiek and A. Sopczak, Phys. Lett. **B341**, 419 (1995).

[99] T. Moroi, Y. Okada, *Phys. Lett.* **B295**, 73 (1992);
T. Moroi, Y. Okada, *Mod. Phys. Lett.* **A7**, 187 (1992);
G.L. Kane, C. Kolda, J.D. Wells, *Phys. Rev. Lett.* **70**, 2686 (1993).

[100] J. Kamoshita, Y. Okada, M. Tanaka, *Phys. Lett.* **B328**, 67 (1994).

[101] P. Janot in *Proceedings of Workshop on Physics and Experiments with Linear e^+e^- Colliders*, Waikoloa, Hawaii, Apr 26–30, 1993, ed. by F.A. Harris, S.L. Olsen, S. Pakvasa, and X. Tata, World Scientific, Singapore, 1993.

[102] Howard Haber, talk given at 4th International Conference on Physics Beyond the Standard Model, Lake Tahoe, California, Dec 13–18, 1994.

[103] R. Becker and C. Van der Velde, in proceedings of *European Meeting of the Working Groups on Physics and Experiments at Linear e^+e^- Colliders*, ed. by P.M. Zerwas, DESY-93-123C.

[104] M.M. Nojiri, KEK-TH-425, hep-ph/9412374.

[105] J.-F. Grivaz, in *Proceedings of Physics and Experiments with Linear Colliders*, Saariselkä, Finland, Sep 9–14, 1991, ed. by R. Orava, P. Eerola, and M. Nordberg, World Scientific, Singapore, 1992.

[106] J. L. Feng and D. E. Finnell, *Phys. Rev.* **D49** 2369 (1994).

[107] M. Jimbo, T. Kon, T. Ochiai, *Phys. Rev.* **D37** 441 (1988); M. Jimbo and M. Katuya, *Europhys. Lett.* **16**, 243 (1991); M. Jimbo, *Europhys. Lett.* **11**, 701 (1990); T. Kon, H. Fujisaki, *Europhys. Lett.* **7**, 101 (1988); T. Kon, *Prog. Theor. Phys.* **79**, 1006 (1988); T. Kon, *Prog. Theor. Phys.* **79**, 159 (1988).

[108] J.L. Feng, M.E. Peskin, H. Murayama and X. Tata, SLAC-PUB-6654.

[109] V. Telnov, in *Proceedings of Workshop on Physics and Experiments with Linear e^+e^- Colliders*, Waikoloa, Hawaii, Apr 26–30, 1993, ed. by F.A. Harris, S.L. Olsen, S. Pakvasa, and X. Tata, World Scientific, Singapore, 1993.

[110] T. Kon, *Phys. Lett.* **B316**, 181 (1993);
Frank Cuypers, Geert Jan van Oldenborgh, and Reinhold Rückl, *Nucl. Phys.* **B409**, 144 (1993);
Akihiro Goto and Tadashi Kon, *Europhys. Lett.* **13**, 211 (1990); Erratum *ibid.*, **14** 281 (1991).

[111] W. Kilgore and H. Murayama, in preparation.

[112] O. Eboli, private communication.

[113] H. König and K.A. Peterson, *Phys. Lett.* **B294**, 110 (1992);
Akihiro Goto and Tadashi Kon, *Europhys. Lett.* **19**, 575 (1992);
Akihiro Goto and Tadashi Kon, *Phys. Lett.* **B295**, 324 (1992);
Frank Cuypers, Geert Jan van Oldenborgh, and Reinhold Rückl, "Supersymmetric Signals in electron-photon collisions", *Nucl. Phys.* **B383**, 45 (1992).

[114] Frank Cuypers, Geert Jan van Oldenborgh, and Reinhold Rückl, *Nucl. Phys.* **B409**, 128 (1993).

[115] H. Murayama and M. Strassler, work in progress.

[116] M. Drees and M. Nojiri, Phys. Rev. **D49**, 4595 (1994).